

**Production and Characterization of Bio-based Polyols and Polyurethanes  
from Biodiesel-derived Crude Glycerol and Lignocellulosic Biomass**

Dissertation

Presented in Partial Fulfillment of the Requirements for the Degree Doctor of  
Philosophy in the Graduate School of The Ohio State University

By

Shengjun Hu, M.S.

Graduate Program in Food, Agricultural and Biological Engineering

The Ohio State University

2013

Dissertation Committee:

Dr. Yebo Li, Advisor

Dr. Rudolph Buchheit

Dr. Katrina Cornish

Dr. Qian Chen

Copyright by

Shengjun Hu

2013

## Abstract

Polyurethanes (PU) are one of the most versatile polymer families and have been used in a broad range of commercial applications. Currently, polyols used for PU production are mainly petroleum-derived. This study focused on the development of bio-based polyols and PU from crude glycerol and lignocellulosic biomass. Crude glycerol is a low-cost byproduct from biodiesel production. Lignocellulosic biomass is the most abundant biomass on earth and is readily available at low cost. Crude glycerol and lignocellulosic biomass have the potential to produce low-cost bio-based polyols and PU.

Polyols were produced via the liquefaction of soybean straw using biodiesel-derived crude glycerol as a liquefaction solvent. The effects of liquefaction parameters on the properties of polyol and PU foams were investigated. Under optimal liquefaction conditions (240 °C, 180-360 min, 3 % sulfuric acid loading, and 10-15 % biomass loading), the polyols produced had hydroxyl numbers ranging from 440 to 490 mg KOH/g, acid numbers below 5 mg KOH/g, and viscosities from 16 to 45 Pa·s. PU foams were produced directly from the produced polyols and had densities ranging from 0.033 to 0.037g/cm<sup>3</sup> and compressive strength from 148 to 203 kPa. Certain impurities in crude glycerol improved the properties of the polyols and PU produced. The composition of five representative biodiesel-derived crude glycerol samples was determined to identify their components. All crude glycerol samples contained glycerol, soap, methanol, FAMES

(methyl esters of fatty acids), water, glycerides, FFAs (free fatty acids), and ash, but their proportions varied widely with the origins of crude glycerol.

The effects of crude glycerol impurities on the properties of polyols and PU foams derived from base- and acid-catalyzed biomass liquefaction processes were studied. For both liquefaction processes, increasing levels of organic impurities, including FFA, FAMES, and glycerides, in crude glycerol decreased biomass conversion and polyol hydroxyl numbers and increased polyol molecular weight ( $M_w$ ). The presence of suitable amounts of organic impurities, especially FFA and FAMES, in crude glycerol improved the properties of polyols and PU foams produced. For both processes, valid regression models ( $R^2=0.99$ ) were developed to predict the hydroxyl numbers of polyol from the contents of organic impurities in crude glycerol. Compared to the base-catalyzed process, the acid-catalyzed process featured faster biomass liquefaction and produced polyols with lower viscosities but higher acid numbers. However, the acid-catalyzed process needed crude glycerol with high glycerol content ( $\geq 50\%$ ) to prevent early occurrence of detrimental condensations, whereas no detrimental condensations were observed in the base-catalyzed process. Moreover, in contrast to their negligible effects on the base-catalyzed process, inorganic salts, including NaCl and Na<sub>2</sub>SO<sub>4</sub>, negatively affected the properties of polyols produced from the acid-catalyzed process.

A two-step sequential biomass liquefaction process was developed to combine the advantages of the acid- and base-catalyzed liquefaction processes. The first, acid-catalyzed, step rapidly liquefied biomass and promoted the esterification reactions between glycerol and FFA, while the second, base-catalyzed, step facilitated extensive

condensation reactions such as transesterification and etherification that occurred among liquefaction components. The polyols produced from three different crude glycerol samples had hydroxyl numbers ranging from 536 to 936 mg KOH/g, viscosities from 20.6 to 28.0 Pa.s, and  $M_w$  from 444 to 769 g/mol. The PU foams produced had densities ranging from 0.04 to 0.05 g/cm<sup>3</sup>, compressive strength from 223 to 420 kPa, and thermal conductivity from 32.2 to 38.9 mW/m.k.

A crude glycerol sample was used as a sole feedstock to produce polyol via a thermochemical conversion process. Under optimized reaction conditions, the polyol produced had a hydroxyl number of 378 mg KOH/g, functionality of 4.7, acid number of less than 5 mg KOH/g, and  $M_w$  of 702 g/mol. The produced polyol was used to prepare waterborne PU dispersions for coating applications. PU films cast from the prepared dispersions had relatively high glass transition temperatures ( $T_g$ , 63-81 °C) that increased with increasing hard segment contents in PU (41-63.2 %), and good thermal stability up to approximately 240 °C. PU coatings prepared from the produced PU dispersions had excellent adhesion and hardness properties, but relatively low flexibility on steel panels.

In summary, the properties of polyols and PU produced in this study compare well in many aspects to their analogs derived from conventional petrochemical-solvent based biomass liquefaction process. This suggests biodiesel-derived crude glycerol can be effectively used as an alternative biomass liquefaction solvent for polyol production. Furthermore, crude glycerol alone also has the potential to produce bio-based polyol and PU. The control and optimization of crude glycerol composition and polyol production processes are crucial to the success of crude glycerol-based polyol production.

## Dedication

This document is dedicated to my family

## **Acknowledgement**

I would like to express my heartfelt gratitude to my advisor, Dr. Yebo Li, for his extraordinary guidance and support throughout my Ph.D. study. Dr. Li has always been generous, kind, and supportive not only for my academic pursuits but also for my personal and professional development. Without his support, I would not have been able to make all the accomplishments I am proud of today.

I also would like to thank my committee members, Dr. Rudolph Buchheit, Dr. Katrina Cornish and Dr. Qian Chen, for their invaluable support and suggestions on my research as well as dissertation-writing.

My special thanks go to Mrs. Mary Wicks for being always helpful in proofreading my manuscripts and dissertation, and to Mike Klingman for his technical support on my research. Mrs. Peggy Christman and Mrs. Candy McBride are acknowledged for their administrative support.

All my colleagues in BBRL are amazing, and I cannot thank them enough for their supporting roles in my research. Particularly, Dr. Caixia Wan, Dr. Xiaolan Luo and Dr. Cong Li are acknowledged for their suggestions, advice, and collaborations on my research projects.

I feel greatly indebted to my parents, uncle and aunt, and the whole family for

their unfailing support and care throughout my life. Last but most importantly, I would like to present this dissertation as a special gift to my wife, Yi Guo, whose endless love, care, and encouragement have always been the inspiration and driving force of my life. Without her, I would not have been able to accomplish what I have accomplished today.

## Vita

November 11, 1982.....Born, Zhongjiang, China

2006.....B.S., Environmental Science,  
Huazhong Agricultural University, China

2010.....M.S. Forest Products, University of Idaho

2010 to present.....Graduate Research Associate, Department  
of Food, Agricultural and Biological  
Engineering, The Ohio State University

## Publications

Luo, X. L., Hu, S., Zhang, X., Li, Y. 2013. Thermochemical conversion of crude glycerol to biopolyols for the production of polyurethane foams. *Bioresource Technology* 139: 323-329.

Hu, S., Luo, X. L., Wan, C.X., and Li, Y. 2012. Characterization of crude glycerol from biodiesel plants. *Journal of Agricultural and Food Chemistry* 60: 5915-5921.

Hu, S., Wan, C. X., and Li, Y. 2012. Production and characterization of biopolyols and polyurethane foams from crude glycerol based liquefaction of soybean straw. *Bioresouce Technology* 107: 227-233.

## Field of Study

Major Field: Food, Agricultural and Biological Engineering

Study in: Biological Engineering

## Table of Contents

Abstract .....	ii
Dedication .....	v
Acknowledgement .....	vi
Vita.....	viii
List of Tables .....	xiv
List of Figures .....	xvi
Chapter 1 Introduction .....	1
1.1 Background .....	1
1.2 Research hypothesis .....	5
1.3 Research Objectives .....	6
1.4 Contribution of the dissertation.....	6
Chapter 2 Literature Review .....	8
2.1 Introduction .....	8
2.2 Liquefaction mechanism of lignocellulosic biomass by polyhydric alcohols.....	11
2.3 Factors affecting the efficiency of liquefaction process.....	14
2.3.1 Lignocellulosic biomass .....	14
2.3.2 Liquefaction solvent .....	15
2.3.3 Catalysts.....	18
2.3.4 Liquefaction temperature and time.....	19
2.4 Biomass liquefaction-derived polyols .....	21
2.5 PU from liquefaction-derived polyols.....	22
2.6 Summary and outlook .....	26
Chapter 3 Polyols and PU Foams from Crude Glycerol-based Liquefaction of Soybean Straw .....	29
3.1 Introduction .....	29

3.2 Materials and Methods .....	30
3.2.1 Materials .....	30
3.2.2 Liquefaction process for polyol production.....	31
3.2.3 Determination of biomass conversion .....	31
3.2.4 Determination of acid and hydroxyl numbers of polyols .....	32
3.2.5 Determination of polyol viscosity .....	33
3.2.6 Preparation of PU Foams.....	33
3.2.7 Characterization of PU Foams.....	34
3.2.8 Data analysis.....	34
3.3. Results and Discussion.....	34
3.3.1 Effects of reaction temperature.....	34
3.3.2 Effects of reaction time.....	37
3.3.3 Effects of sulfuric acid loading.....	38
3.3.4 Effects of biomass loading .....	40
3.3.5 Comparison to pure glycerol .....	41
3.4 Conclusions .....	43
Chapter 4 Characterization of Crude Glycerol from Biodiesel Plants.....	58
4.1 Introduction .....	58
4.2 Materials and Methods .....	60
4.2.1 Materials .....	60
4.2.2 Physical properties.....	61
4.2.3 Soap content determination .....	62
4.2.4 Water and ash content determination .....	62
4.2.5 Elemental analysis .....	63
4.2.6 Glycerol content determination by iodometric-periodic acid method.....	63
4.2.7 Fractionation of crude glycerol.....	63
4.2.8 HPLC analysis of glycerol and methanol .....	64
4.2.9 GC analysis of glycerides, glycerol, FAMES, and FFAs.....	65
4.2.10 Titrimetric determination of FFA content .....	66
4.2.11 Statistical analysis.....	67

4.3 Results and Discussion.....	67
4.3.1 Physical properties of crude glycerol .....	67
4.3.2 Comparative glycerol determination in crude glycerol .....	67
4.3.3 Glycerol and methanol in crude glycerol .....	68
4.3.4 FFAs, FAMEs, and glycerides in organic fractions .....	69
4.3.5 Elemental analysis .....	71
4.3.6 Soap, water, and ash in crude glycerol .....	71
4.3.7 Composition of crude glycerol .....	72
4.4 Conclusions .....	72
Chapter 5 Effects of Crude Glycerol Impurities on the Properties of Base-catalyzed Liquefaction-derived Polyols and PU Foams .....	86
5.1 Introduction .....	86
5.2 Materials and Methods .....	87
5.2.1 Materials .....	87
5.2.2 Experimental design and statistical analysis .....	88
5.2.3 Preparation of liquefaction solvents .....	89
5.2.4 Liquefaction process for polyol production.....	90
5.2.5 Determination of biomass conversion .....	90
5.2.6 Characterization of liquefaction-derived polyols .....	90
5.2.7 Preparation and characterization of PU Foams .....	91
5.3 Results and Discussion.....	91
5.3.1 Effects of inorganic salts on biomass conversion and hydroxyl numbers of polyols .....	91
5.3.2 Effects of organic impurities on acid and hydroxyl numbers of polyols.....	92
5.3.3 Effects of organic impurities on biomass conversion, molecular weights and functionalities of polyols .....	95
5.3.4 Effects of organic impurities on PU foam properties .....	96
5.4. Conclusions .....	98
Chapter 6 Effects of Crude Glycerol Impurities on the Properties of Acid-catalyzed Liquefaction-derived Polyols and PU Foams .....	111
6.1 Introduction .....	111

6.2 Materials and Methods .....	112
6.2.1 Materials .....	112
6.2.2 Experimental design and statistical analysis .....	112
6.2.3 Preparation of liquefaction solvents .....	113
6.2.4. Liquefaction process for polyol production.....	113
6.2.5. Determination of biomass conversion .....	113
6.2.6. Characterization of liquefaction-derived polyols .....	113
6.2.7. Preparation and characterization of PU Foams .....	114
6.3 Results and Discussion.....	114
6.3.1 Effects of inorganic salts on polyol properties .....	114
6.3.2 Effects of organic impurities on biomass conversion.....	115
6.3.3 Effects of organic impurities on hydroxyl numbers of polyols .....	117
6.3.4 Effects of organic impurities on acid numbers and viscosities of polyols .....	119
6.3.5 Effects of organic impurities on molecular weights of polyols.....	120
6.3.6 Effects of organic impurities on PU foam properties .....	120
6.3.7 Comparison between the acid- and base-catalyzed biomass liquefaction processes.....	121
6.4 Conclusions .....	122
Chapter 7 Polyols and PU Foams from a Two-step Sequential Liquefaction of Lignocellulosic Biomass by Crude Glycerol .....	137
7.1 Introduction .....	137
7.2 Materials and Methods .....	138
7.2.1 Materials .....	138
7.2.2 Two-step sequential liquefaction process for polyol production.....	138
7.2.3 Determination of biomass conversion .....	139
7.2.4 Characterization of liquefaction-derived polyols .....	139
7.2.5 Preparation and characterization of PU Foams .....	139
7.3 Results and Discussion.....	140
7.3.1. First step: acid-catalyzed biomass liquefaction process .....	140
7.3.2 Second step: base-catalyzed biomass liquefaction process .....	142

7.3.3 Properties of polyols produced from two-step liquefaction process .....	143
7.3.4 Properties of PU foams derived from the two-step liquefaction process .....	144
7.4 Conclusions .....	146
Chapter 8 Polyols and Waterborne PU Dispersions from Crude Glycerol.....	155
8.1. Introduction .....	155
8.2. Materials and Methods .....	158
8.2.1. Materials .....	158
8.2.2. Thermochemical conversion of crude glycerol to polyol .....	158
8.2.3 Characterization of crude glycerol-based polyols .....	159
8.2.4 Preparation of crude glycerol-based waterborne PU dispersions (CG-WPUDs) .....	159
8.2.5 Preparation and characterization of CG-WPUDs-derived PU films .....	160
8.2.6 Characterization of the coating performance of CG-WPUDs .....	161
8.3 Results and Discussion.....	161
8.3.1 Thermochemical conversion of crude glycerol to polyol.....	161
8.3.2 Production of crude glycerol-based waterborne PU dispersions (CG-WPUDs) .....	164
8.3.3 Properties of PU films cast from CG-WPUDs .....	166
8.3.4 Coating performance of CG-WPUDs.....	169
8.4 Conclusions .....	169
Chapter 9 Conclusions and Suggestions for Future Research .....	183
9.1 Conclusions .....	183
9.2 Suggestions for future research .....	186
References .....	189

## List of Tables

Table 2.1: General properties of polyols produced from lignocellulosic biomass liquefaction process .....	27
Table 3.1: PU foam production formula .....	44
Table 3.2: Comparison of pure and crude glycerol in polyol and PU foam production ...	45
Table 4.1: Physical properties of crude glycerol.....	74
Table 4.2: Comparative determination of the free glycerol content of CG-WV.....	75
Table 4.3: Glycerol, methanol, and organic fraction contents of crude glycerol .....	76
Table 4.4: Composition of organic fractions obtained without saponification .....	77
Table 4.5: Composition of organic fractions obtained with saponification .....	78
Table 4.6: Elemental analysis of crude glycerol .....	79
Table 4.7: Composition of crude glycerol.....	80
Table 5.1: Box-Behnken design with three variables and general properties of polyols	100
Table 5.2: Coding of the independent variables.....	101
Table 5.3: ANOVA of the fitted second-order model for polyol hydroxyl numbers .....	102
Table 5.4: ANOVA of the fitted first-order model for polyol hydroxyl numbers .....	103
Table 5.5: Verification of the developed linear model for predicting polyol hydroxyl numbers.....	104
Table 5.6: Effects of FFA and FAMES on molecular weights and functionalities of polyols	

.....	105
Table 6.1: Central composite design and general properties of polyols .....	123
Table 6.2: Coding of the independent variables.....	124
Table 6.3: ANOVA of the first-order model for biomass conversion .....	125
Table 6.4: ANOVA of the second-order model for polyol hydroxyl numbers.....	126
Table 6.5: Verification of the developed models for predicting biomass conversion and polyol hydroxyl numbers .....	127
Table 6.6: Effects of organic impurities on polyol molecular weights and functionalities .....	128
Table 6.7: Comparison between the properties of polyols and PU foams derived from acid- and base-catalyzed liquefaction processes.....	129
Table 7.1: Composition of crude glycerol used in the two-step liquefaction process ....	147
Table 7.2: The properties of polyols produced the two-step liquefaction process.....	148
Table 7.3: The properties of PU foams produced the two-step liquefaction process.....	149
Table 8.1: Formulation of crude glycerol based waterborne polyurethane dispersions (CG-WPUDs) prepared from crude glycerol-based polyol (CG-POL) .....	171
Table 8.2: Composition of crude glycerol and CG-POL .....	172
Table 8.3: Thermal properties of CG-WPUDs-derived PU films and coating performance of CG-WPUDs.....	173

## List of Figures

Figure 2.1: Reaction between polyols and isocyanates to form PU .....	28
Figure 2.2: Schematic representation of the liquefaction mechanism of acid-catalyzed cellulose liquefaction in polyhydric alcohols .....	28
Figure 3.1: Effects of reaction temperature on biomass conversion and polyol viscosity (Note: missing data with viscosity > 1,000 Pa·s; reaction time: 90 min; sulfuric acid loading: 3 %; biomass loading: 10 %; each data point represents the mean of duplicate liquefaction) .....	46
Figure 3.2: Effects of reaction temperature on polyol acid and hydroxyl numbers (Note: reaction time: 90 min; sulfuric acid loading: 3 %; biomass loading: 10 %; each data point represents the mean of duplicate liquefaction) .....	47
Figure 3.3: Effects of reaction temperature on compressive strength and density of PU foams (Note: reaction time: 90 min; sulfuric acid loading: 3 %; biomass loading: 10 %; each data point represents the mean of duplicate liquefaction) .....	48
Figure 3.4: Effects of reaction time on biomass conversion and polyol viscosity (Note: missing data with viscosity > 1,000 Pa·s; reaction temperature: 240 °C; sulfuric acid loading: 3 %; biomass loading: 10 %; each data point represents the mean of duplicate liquefaction) .....	49
Figure 3.5: Effects of reaction time on polyol acid and hydroxyl numbers (Note: reaction	

temperature: 240 °C; sulfuric acid loading: 3 %; biomass loading: 10 %; each data point represents the mean of duplicate liquefaction) .....	50
Figure 3.6: Effects of reaction time on compressive strength and density of PU foams (Note: reaction temperature: 240 °C; sulfuric acid loading: 3%; biomass loading: 10%; each data point represents the mean of duplicate liquefaction) .....	51
Figure 3.7: Effects of sulfuric acid loading on biomass conversion and polyol viscosity (Note: missing data with viscosity>1,000 Pa·s; reaction temperature: 240 °C; reaction time: 90 min; biomass loading: 10 %; each data point represents the mean of duplicate liquefaction) .....	52
Figure 3.8: Effects of sulfuric acid loading on polyol acid and hydroxyl numbers (Note: reaction temperature: 240 °C; reaction time: 90 min; biomass loading: 10 %; each data point represents the mean of duplicate liquefaction) .....	53
Figure 3.9: Effects of sulfuric acid loading on compressive strength and density of PU foams (Note: reaction temperature: 240 °C; reaction time: 90 min; biomass loading: 10 %; each data point represents the mean of duplicate liquefaction).....	54
Figure 3.10: Effects of biomass loading on biomass conversion and polyol viscosity (Note: missing data with viscosity>1,000 Pa·s; reaction temperature: 240 °C; reaction time: 180 min; sulfuric acid loading: 3 %; each data point represents the mean of duplicate liquefaction) .....	55
Figure 3.11: Effects of biomass loading on polyol acid and hydroxyl numbers (Note: reaction temperature: 240 °C; reaction time: 180 min; sulfuric acid loading: 3%; each data point represents the mean of duplicate liquefaction) .....	56
Figure 3.12: Effects of biomass loading on compressive strength and density of PU foams	

(Note: reaction temperature: 240 °C; reaction time: 180 min; sulfuric acid loading: 3 %; each data point represents the mean of duplicate liquefaction) .....	57
Figure 4.1: Scheme of crude glycerol fractionation and characterization .....	81
Figure 4.2: Representative HPLC chromatogram for the determination of glycerol and methanol in crude glycerol.....	82
Figure 4.3: Chemical reactions occurring in crude glycerol fractionation processes: (a): $R_1$ : aliphatic tails; (b): $R_1$ : aliphatic tails; $R_2$ and $R_3$ : -H or -COR ( $R$ : aliphatic tails); (c): $R_1$ : Na or K; $R_2$ : aliphatic tails .....	83
Figure 4.4: Representative GC chromatogram for the determination of FAMEs in organic fractions obtained without saponification.....	84
Figure 4.5: Representative GC chromatogram for the determination of glycerides in organic fractions obtained without saponification .....	85
Figure 5.1: Effects of inorganic salts (NaCl and Na <sub>2</sub> SO <sub>4</sub> ) on biomass conversion and the hydroxyl numbers of polyols .....	106
Figure 5.2: Response surface plots and its corresponding contour plots of the dependence of the hydroxyl number of polyols on: (a) FFA and FAME (at glyceride: 5 %); (b) FFA and glyceride (at FAME: 20 %); (c) FAME and glyceride (at FFA: 20 %) .....	107
Figure 5.3: Effects of organic impurities on compressive strength and density of PU foams (Note: FA: FFA; FM: FAMEs; GD: glycerides) .....	109
Figure 5.4: SEM images of PU foams produced from crude glycerol containing: (a) 5 % glycerides; (b) 20 % FFA, 20 % FAMEs and 5 % glycerides.....	110
Figure 6.1: Effects of NaCl and Na <sub>2</sub> SO <sub>4</sub> on biomass conversion and viscosities of polyols .....	130

Figure 6.2: Effects of NaCl and Na <sub>2</sub> SO <sub>4</sub> on hydroxyl and acid numbers of polyols .....	131
Figure 6.3: Chemical reactions occurring between salts and sulfuric acid during acid-catalyzed biomass liquefaction process .....	131
Figure 6.4: Response surface plots and its corresponding contour plots of the dependence of polyol hydroxyl numbers on: (a) FFA and FAME (at glyceride: 2.5 %); (b) FFA and glycerides (at FAMES: 10 %); (c) FAMES and glycerides (at FFA: 10 %).....	132
Figure 6.5: Effects of organic impurities on acid numbers and viscosities of polyols (Note: FA: FFA; FM: FAMES; GD: glycerides) .....	134
Figure 6.6: Effects of organic impurities on compressive strength and density of PU foams (Note: FA: FFA; FM: FAMES; GD: glycerides) .....	135
Figure 6.7: SEM images of PU foams produced from crude glycerol containing: (a) 0 % impurities; (b) 20 % FFA, 20 % FAMES and 5 % glycerides .....	136
Figure 7.1: The change (s) of FFA and FAMES contents in polyols and of biomass conversion during acid-catalyzed liquefaction process .....	150
Figure 7.2: The changes of hydroxyl and acid numbers of polyols during acid-catalyzed liquefaction process .....	151
Figure 7.3: The changes of biomass conversions and polyol hydroxyl numbers during base-catalyzed liquefaction (data points at 0 min represent the properties of polyol obtained from acid-catalyzed liquefaction (150 °C, 90 min)) .....	152
Figure 7.4: The changes of glycerol and monoglyceride contents in polyols during base-catalyzed liquefaction (data points at 0 min represent the values of polyol obtained from acid-catalyzed liquefaction (150 °C, 90 min)).....	153
Figure 7.5: TGA curves of PU foams derived from two-step biomass liquefaction process	

.....	154
Figure 8.1: Time-dependent changes of FFA contents in polyols at different soap levels (3.3 to 20 %, reaction temperature: 180 °C).....	174
Figure 8.2: Time-dependent changes of FAMEs contents in polyols at different soap levels (3.3 to 20 %, reaction temperature: 180 °C).....	175
Figure 8.3: Time-dependent changes of FFA contents in polyols at different reaction temperatures (160-190 °C, soap content: 6.6 %).....	176
Figure 8.4: Time-dependent changes of FAMEs contents in polyols at different reaction temperatures (160-190 °C, soap content: 6.6 %).....	177
Figure 8.5: FT-IR spectra of CGPU-63.2 at different reaction time: a: 5 h; b: 10 h; c: 24 h; d: 45 h.....	178
Figure 8.6: FT-IR spectra of CG-WPUDs-derived PU films: (a): CGPU-63.2, (b) CGPU-58.2, (c) PCGPU-51.5, (d) PCGPU-41.....	179
Figure 8.7: DSC thermograms of CG-WPUDs-derived PU films: (a): CGPU-63.2, (b) CGPU-58.2, (c) PCGPU-51.5, (d) PCGPU-41.....	180
Figure 8.8: TGA curves of CG-WPUDs-derived PU films.....	181
Figure 8.9: Derivative TGA curves of CG-WPUDs-derived PU films.....	182

## Chapter 1 Introduction

### 1.1 Background

With increasing concerns over the depletion of fossil fuels, there has been much interest and effort to search for renewable and sustainable energy alternatives. Biodiesel is a promising renewable fuel that is commonly produced through transesterification of vegetable oils or animal fats (Ma and Hanna, 1999; Chien et al., 2009); it is a proven fuel and has great potential in the compensation and/or replacement of traditional petroleum diesel fuels (Chisti, 2007; Chouhan and Sarma, 2011). Crude glycerol is a major by-product generated during biodiesel production. It is estimated that approximately 1 kg crude glycerol is generated for every 10 kg of biodiesel produced (Thompson and He, 2006; Johnson and Taconi, 2007). With the rapid growth of the world's biodiesel production in recent years, a large surplus of glycerol has been created (Johnson and Taconi, 2007; Pagliaro et al., 2007), leading to the closure of several traditional glycerol plants (McCoy, 2006). At present, biodiesel-derived crude glycerol is of little economic value, i.e., approximately \$0.1/kg (Johnson and Taconi, 2007) and contains various impurities such as methanol, FFAs /soap, FAMES, and alkaline catalyst residues (Santibanez et al., 2011; Hu et al., 2012b). Upgrading or refining crude glycerol to technical grade glycerol (>98%) makes its composition more consistent, but currently this is not economically viable for most biodiesel plants, especially for small and/or medium

size plants (Manosak et al., 2011). Currently, crude glycerol has become a financial and environmental liability for the biodiesel industry (Johnson and Taconi, 2007).

Considerable research has been conducted to develop both chemical and biological processes for value-added conversion of crude glycerol. Several reviews are available on this topic (Pachauri and He, 2006; Johnson and Taconi, 2007; Behr et al., 2008; Zhou et al., 2008; Santibanez et al., 2011). Some examples of glycerol-derived products are acrolein (Ott et al., 2006; Chai et al., 2007; Corma et al., 2008), 1, 3-propanediol (Mu et al., 2006; Asad-ur-Rehman et al., 2008), docosahexaenoic acid (DHA) (Chi et al., 2007; Pyle et al., 2008), hydrogen (Sabourin-Provost and Hallenbeck, 2009; Fountoulakis and Manios, 2009), polyols and PU foams (Hu et al., 2012b), and polyhydroxylalkanoates (Mothes et al., 2007; Dobroth et al., 2011). However, most of these processes are still at research and development stage. In addition, the composition of biodiesel-derived crude glycerol varies widely with different feedstocks, processes, and post-treatments used in different biodiesel plants. This creates further challenges in the quality-control of crude glycerol conversion processes. To maintain process consistency, the effects of crude glycerol impurities on process efficiency as well as on product properties need to be investigated.

The effects of crude glycerol impurities on certain biological conversion processes have been previously investigated. Impurities such as soap, FFAs, FAMES, methanol, and salts have been found to inhibit the growth of microorganisms and consequently decrease conversion efficiency (Chi et al., 2007; Pyle et al., 2008; Athalye et al., 2009; Chatzifragkou et al., 2010; Liang et al., 2010; Moon et al., 2010; Santibanez

et al., 2011; Anand and Saxena, 2012; Venkataramanan et al., 2012). Recently, a review that discusses the effects of crude glycerol impurities on biological conversions of crude glycerol has been published (Chatzifragkou and Papanikolaou, 2012). In addition to their effects on biological conversions, crude glycerol impurities also have been reported to affect thermochemical conversions of crude glycerol (Lehnert and Claus, 2008; Wolfson et al., 2009; Dou et al., 2010; Xiu et al., 2010; da Silva and Mota, 2011; Ramachandran et al., 2011). The detrimental effects of impurities such as salts, methanol, water, FAMEs, and glycerides on thermochemical conversion of crude glycerol have been previously reported (Lehnert and Claus, 2008; da Silva and Mota, 2011; Ramachandran et al., 2011). Compared to the extensive reports on the negative effects of crude glycerol impurities, reports on the positive effects of crude glycerol impurities have been few. Xu et al. (2012) reported certain crude glycerol impurities (FFAs, soap, FAMEs, and glycerides) improved the efficiency of microbial conversion of crude glycerol to triacylglycerols. In a different study, Xiu et al. (2010) reported that FFAs in crude glycerol increased bio-oil yield of the hydrothermal pyrolysis of crude glycerol.

PU have been widely used in a wide range of commercial applications. Flexible and rigid foams are two predominant application forms of PU, with coatings, sealants, elastomers, and adhesives being some other common applications (Petrovic, 2008). Currently, the PU industry is heavily petroleum-dependent because its two major feedstocks, i.e. polyols and isocyanates, are largely petroleum-derived. Due to concerns over the depletion of petroleum resources, extensive research has concentrated on developing polyols and PU products from renewable sources. Vegetable oils and

lignocellulosic biomass are two major types of biomass that have attracted extensive attention for the production of bio-based polyols and PU. Epoxidation-oxirane opening, hydroformylation, ozonolysis, and transesterification/amidation are four major techniques used to convert vegetable oils to polyols. Depending on the specific conversion technique and vegetable oil used, oil-derived polyols have different structures and properties that are suitable for various PU applications. In recent years, several reviews on this topic have been published (Petrovic, 2008; Lligadas et al., 2010; Pfister et al., 2011).

As another major feedstock for the production of bio-based polyols, lignocellulosic biomass is considered to be the world's most abundant renewable material. Some examples of lignocellulosic biomass are wood, soybean straw, corn stover, and wheat straw. The conversion of lignocellulosic biomass to polyols is typically achieved by a liquefaction process, during which polyols are produced from a series of solvolysis and hydroxyalkylation reactions (Yao et al., 1996). A wide variety of lignocellulosic biomasses, such as wood (Kurimoto et al., 1999; Kurimoto et al., 2001a), wheat straw (Wang and Chen, 2007; Chen and Lu, 2009), corn bran (Lee et al., 2000) and corn stalk (Yan et al., 2008), have been studied for polyol production. Generally, the polyols produced showed promising properties suitable for the production of rigid or semi-rigid PU foams. However, liquefaction of lignocellulosic biomass generally requires a high-volume of petroleum-based liquefaction solvents, i.e. approximately 100 g of solvent is needed to liquefy 25 g of lignocellulosic biomass for optimal polyol production (Yao et al., 1996; Hassan and Shukry, 2008). The extensive use of petroleum-based solvents increases not only the cost of polyol production but also the reliance of biomass

liquefaction on petrochemical derivatives.

As a polyhydric alcohol, glycerol is capable of liquefying biomass via solvolysis. In fact, glycerol has been commonly used as a co-solvent (usually 10- 20 wt. % in liquefaction solvent) for biomass liquefaction in previous reports. This study aimed to investigate the feasibility of producing bio-based polyols and PU from biodiesel-derived crude glycerol and lignocellulosic biomass. The feasibility of using crude glycerol as a low-cost and renewable biomass liquefaction solvent for polyol and PU production was investigated and demonstrated for the first time. To study the effects of crude glycerol impurities on the properties of liquefaction-derived polyols and PU foams, industrially-obtained crude glycerol samples were characterized to identify their major impurities. Subsequently, the effects of crude glycerol impurities on base- and acid-catalyzed biomass liquefaction processes were investigated, from which the knowledge obtained helped identify the optimal crude glycerol composition for biomass liquefaction and the respective advantages of base- and acid-catalyzed processes. To improve the properties of liquefaction-derived polyols and PU foams, a two-step sequential biomass liquefaction process was developed to combine the advantages of base- and acid-catalyzed biomass liquefaction. Last, crude glycerol, as a sole feedstock, also was evaluated for its potential to produce polyols and PU. Polyol production was achieved via an optimized thermochemical process, and the polyol produced was evaluated for its potential to produce waterborne PU dispersions (WPUDs).

## **1.2 Research hypothesis**

The central hypothesis of this study is that crude glycerol and lignocellulosic

biomass can be effectively utilized for the production of polyols and PU products with commercially-acceptable properties.

### **1.3 Research Objectives**

The overall goal of this research was to use crude glycerol and lignocellulosic biomass as major feedstocks to produce bio-based polyols and PU with properties comparable to their commercial analogs. Specific objectives in support of this goal were to:

- 1) Demonstrate the feasibility of producing high-quality polyols and PU foams from a crude glycerol-based biomass liquefaction process (Chapter 3).
- 2) Identify and quantify the major impurities in biodiesel-derived crude glycerol (Chapter 4).
- 3) Investigate the effects of crude glycerol impurities on the properties of polyols and PU foams derived from base- and acid-catalyzed biomass liquefaction processes (Chapters 5 and 6).
- 4) Develop a novel two-step biomass liquefaction process capable of producing polyols and PU with improved properties (Chapter 7).
- 5) Produce crude glycerol-based polyol using crude glycerol as a sole feedstock and evaluate its application in producing waterborne PU dispersions (WPUDs) (Chapter 8).

### **1.4 Contribution of the dissertation**

Two papers (from Chapters 3 and 4) have been published in peer-reviewed

journals. Four additional papers are expected to be published in peer-reviewed journals in the near future based on Chapters 5 to 8.

Papers published:

- 1) Hu, S., Luo, X. L., Wan, C.X., and Li, Y. 2012. Characterization of crude glycerol from biodiesel plants. *Journal of Agricultural and Food Chemistry* 60: 5915-5921.
- 2) Hu. S., Wan, C. X., and Li, Y. 2012. Production and characterization of biopolyols and polyurethane foams from crude glycerol based liquefaction of soybean straw. *Bioresouce Technology* 107: 227-233.

## Chapter 2 Literature Review

### 2.1 Introduction

In general, polyols refer to compounds that contain two or more hydroxyl groups in one molecule. Depending on their  $M_w$ , polyols can be divided into monomeric and polymeric polyols. Monomeric polyols, such as glycerol and ethylene glycol, are useful starting materials for the production of a broad spectrum of valuable chemicals via chemical reactions such as esterification (Hilditch and Rigg, 1935; Diaz et al., 2000; Behr et al., 2008), dehydration (Akiyama et al., 2009; Alhanash et al., 2010; ten Dam and Hanefeld, 2011), and hydrogenation (Amada et al., 2010; Chia et al., 2011; Gandarias et al., 2012). Polymeric polyols, which mainly consist of polyether and polyester polyols, are almost exclusively used to produce PU products, such as foams, coatings, and elastomers, via condensation polymerization reactions with isocyanates (Figure 2.1). To meet different PU application needs, polyols with a wide range of chemical structures and properties have been produced commercially; for example, polyols commonly used for PU production have functionalities varying widely from two to eight and  $M_w$  from 200 to 8,000 g/mol (Randall and Lee, 2002b). The broad window of polyol properties allows the tunable design of PU structures, making them one of the most versatile families of polymeric materials (Randall and Lee, 2002b). A large number of PU products, such as foams, coatings, and adhesives, have been commercially produced and used in many

aspects of our daily lives. For example, flexible PU foams are widely used as cushion materials in car seats, mattress, and upholstery, while rigid PU foams are common thermal insulation materials used by the refrigerator and construction industries.

Currently, commercial polyols and PU are mainly produced from petroleum derivatives. Recently, concerns over the depletion of fossil resources have spurred extensive interest in developing bio-based polyols and PU from renewable resources (Petrovic, 2008). Lignocellulosic biomass, such as wood and agricultural crop residues, is considered to be the world's most abundant renewable material. Their main structural units are cellulose (30-35 %), hemicellulose (15-35 %), and lignin (20-35 %) (Behrendt et al., 2008), all of which are highly functionalized materials rich in hydroxyl groups, making them promising materials for bio-based polyols production. However, lignocellulosic biomasses are solid materials and need to be converted into liquid polyols before they can be used to produce PU. Currently, two major technologies exist for this conversion: oxypropylation and liquefaction. The oxypropylation of biomass is a polymerization process that grafts oligo (propylene oxide) or propylene oxide homopolymer onto biomass macromolecular structures (Evtiouguina et al., 2000). Usually, this process is conducted under high pressure and high temperature (ca. 100-200 °C) in the presence of KOH as a catalyst, during which biomass is first activated and functionalized, followed by oxypropylation reactions with propylene oxide (Evtiouguina et al., 2002; Aniceto et al., 2012). Oxypropylation-derived polyols are mixtures of various compounds, including oxypropylated biomass, polypropylene oxide, and some unreacted or partially oxypropylated biomass, which can be used directly for the

preparation of PU (Aniceto et al., 2012). Presently, there have been reports on the preparation of polyols via the oxypropylation of sugar beet pulp (Pavier and Gandini, 2000), cork (Evtiouguina et al., 2000; Evtiouguina et al., 2002), and lignin (Cateto et al., 2009; Ahvazi et al., 2011; Xue et al., 2013). Recently, a review on this topic was published (Aniceto et al., 2012).

Alternatively, lignocellulosic biomass can be converted into liquid polyols via a liquefaction process. The liquefaction process is usually conducted at elevated temperatures (150-250 °C) under atmospheric pressure and uses polyhydric alcohols, such as polyethylene glycol (PEG) and/or glycerol, as liquefaction agents (Lee et al., 2000; Yan et al., 2008; Yu et al., 2008; Chen and Lu, 2009; Hu et al., 2012b). The liquefaction can be either acid- or base-catalyzed, with the former being much more commonly used. During the liquefaction process, biomass is degraded and decomposed into smaller molecules by polyhydric alcohols via solvolytic reactions. The produced polyols are largely a mixture of different compounds rich in hydroxyl groups and can be used directly to prepare various PU such as foams (Yao et al., 1995; Yan et al., 2008; Gao et al., 2010; Hu et al., 2012b), adhesives (Lee and Lin, 2008; Juhaida et al., 2010), and films (Kurimoto et al., 2000; Kurimoto et al., 2001a; Kurimoto et al., 2001b). A large number of lignocellulosic biomasses, such as wood (Yao et al., 1993; Yao et al., 1995; Kurimoto et al., 1999; Yamada and Ono, 1999; Kunaver et al., 2010), and agricultural residues (Lee et al., 2000; Liang et al., 2006; Yu et al., 2006; Wang and Chen, 2007; Hassan and Shukry, 2008; Yan et al., 2008; Chen and Lu, 2009; Yan et al., 2010; Briones et al., 2012; Hu et al., 2012b; Zhang et al., 2012a), lignin (Jin et al., 2011), and industrial

and bio-refinery byproducts ( Lee et al., 2002; Yu et al., 2008; Briones et al., 2011; Briones et al., 2012), have been liquefied for the production of polyols and PU. The following section focusses on the mechanism of biomass liquefaction process, followed by a discussion on factors that affect the efficiency of the liquefaction process and a discussion of the general properties of liquefaction-derived polyols and PU. Finally, we conclude with a summary and outlook section.

## **2.2 Liquefaction mechanism of lignocellulosic biomass by polyhydric alcohols**

The liquefaction of lignocellulosic biomass by polyhydric alcohols proceeds mainly via solvolytic reactions, which cleave various chemical bonds (e.g. glycoside bonds) existing in biomass structures and produce smaller biomass-derived molecules or fragments (Yamada and Ono, 2001; Yamada et al., 2007). These small biomass derivatives are fairly reactive and can further react with either themselves or liquefaction solvent, forming a large number of biomass and/or liquefaction solvent-derived compounds. Because of their different structures and morphologies, biomass components are usually liquefied at different stages of the liquefaction process. Usually, the liquefaction of hemicellulose, lignin, and amorphous cellulose occurs rapidly during the early stages of the liquefaction process because they have amorphous structures that are easily accessible to liquefaction solvents. In contrast, the liquefaction of crystalline cellulose is slower and continues until the later stages of the liquefaction process because it has a well-packed structure that is less accessible to the solvents (Yao et al., 1993; Lee et al., 2002; Chen and Lu, 2009; Zhang et al., 2012a). For this reason, cellulose

liquefaction is commonly considered to be the rate-limiting step in biomass liquefaction (Kobayashi et al., 2004; Zhang et al., 2012b).

Previous research has suggested that the acid-catalyzed liquefaction of cellulose by different liquefaction solvents, including ethylene glycol (EG), PEG, and ethylene carbonate (EC), proceed via similar reaction pathways (Figure 2.2) (Yamada and Ono, 2001; Yamada et al., 2007) as follows: (a) cellulose is first decomposed by solvolysis into glucose or other small cellulose derivatives that can react with liquefaction solvent to form glycoside derivatives; (b) the produced glycoside derivatives can undergo further reactions to form levulinic acid and/or levulinates. The formation of glycoside and levulinic derivatives in acid-catalyzed cellulose liquefaction process also has been confirmed by other studies (Kobayashi et al., 2004; Jasiukaityte et al., 2009). In a later effort, Zhang et al. (2007) conducted a qualitative analysis of the products formed during the acid-catalyzed liquefaction of bagasse in ethylene glycol (EG). The obtained liquefaction products were fractionated into water-soluble, acetone-soluble, and insoluble residue fractions. Fractional analyses showed that the insoluble residue fraction mainly consisted of insoluble derivatives from cellulose and lignin, the acetone-soluble fraction was rich in high molecular weight derivatives from lignin, and the water-soluble fraction mainly contained a mixture of EG, EG derivatives, diethylene glycol (DEG), saccharides, alcohols, aldehydes, ketones, phenols, and organic acids (Zhang et al., 2007). The presence of such a wide spectrum of different compounds in liquefaction-derived polyols indicates the complex nature of the biomass liquefaction process: various reactions occur and compete against each other simultaneously. The reaction mechanism shown in Figure

2.2 represents one of the major reactions occurring during the cellulose liquefaction process. Although there have been studies on the mechanism of lignin liquefaction by phenol (Lin et al., 1997a; Lin et al., 1997b; Lin et al., 1997c; Lin et al., 2001b; Lin et al., 2001a), the mechanism/reaction pathway of lignin liquefaction by polyhydric alcohols has not been reported.

Recondensation reactions among biomass derivatives and/or liquefaction solvents occur and compete against degradation reactions during biomass liquefaction process. When dominant, these recondensation reactions can decrease liquefaction efficiency by increasing percent insoluble residues in the liquefaction-derived polyols. In fact, this phenomenon has been commonly observed in acid-catalyzed liquefaction processes, particularly under high acid loadings, extended liquefaction time, and high biomass/liquefaction solvent ratios (Yao et al., 1993; Kurimoto et al., 1999; Yan et al., 2008; Chen and Lu, 2009). Usually, liquefaction parameters, such as liquefaction temperature and time, catalyst loading, and biomass/solvent ratio, are optimized to minimize the negative effects of recondensation reactions. The mechanism of recondensation reactions in acid-catalyzed biomass liquefaction processes has been studied previously by liquefying cellulose, steamed lignin, alkali lignin, and their mixtures under identical liquefaction conditions (Kobayashi et al., 2004). No recondensation occurred when cellulose or lignin were liquefied alone, even at a prolonged liquefaction time of 480 min. In contrast, when cellulose and lignin were liquefied together, significant recondensations were observed: for a liquefaction time of 480 min, the percent insoluble residue reached 50 and 76 % for cellulose/steamed lignin

and cellulose/alkali lignin mixtures, respectively (Kobayashi et al., 2004). Based on these observations, the authors suggested that recondensation reactions occurring during acid-catalyzed liquefaction process were largely caused by reactions among depolymerized cellulose and degraded aromatic derivatives from lignin and/or by the nucleophilic displacement reaction of cellulose by phenoxide ions (Kobayashi et al., 2004).

## **2.3 Factors affecting the efficiency of liquefaction process**

### *2.3.1 Lignocellulosic biomass*

Biomass liquefaction efficiency varies with the compositions, structures and morphologies of lignocellulosic biomasses. A study on the liquefaction of seven different species of wood (hardwood and softwood) suggested that, although three hardwood species shared similar liquefaction behaviors, significantly different liquefaction behaviors were observed for four softwood species (Kurimoto et al., 1999). Compared to hardwood, softwood exhibited faster liquefaction rates but an earlier occurrence of unfavorable recondensation reactions. This has been explained by the existence of a large number of guaiacyl propane units in softwood that are more reactive than the syringyl propane units existing in hardwood (Kurimoto et al., 1999). Lee et al. (2002) studied the liquefaction of three types of waste paper (box paper, newspaper, and business paper) and wood. The order of liquefaction rates were found to be: wood > newspaper > business paper > box paper. The higher liquefaction rates of wood and newspaper were explained by their higher contents of lignin and hemicellulose, which can be liquefied rapidly at the early stages of liquefaction process (Lee et al., 2002). Different liquefaction behaviors of agricultural crop residues have been observed through side by side comparisons: cotton

stalks and bagasse (Hassan and Shukry, 2008), and corn stover, rice straw, and wheat straw (Liang et al., 2006). More recently, Briones et al. (2012) investigated the liquefaction behaviors of five types of agro-industrial residues, including rapeseed cake, date seeds, olive stone, corncob, and apple pomace, and liquefaction yields ranging from 84 to 97 % were obtained.

### 2.3.2 Liquefaction solvent

Liquefaction solvent plays a paramount role in biomass liquefaction. To produce polyols with suitable properties for PU applications, liquefaction solvent needs not only to promote rapid and effective biomass liquefaction but also to possess suitable polyol properties for desired PU applications. This is because most liquefaction processes are conducted at large liquefaction solvent/biomass ratios (approximately 3/1 to 5/1) in order to achieve high biomass liquefaction efficiency. After liquefaction, liquefaction solvent or its derivatives constitute a major part of liquefaction-derived polyols and has significant effects on polyol properties. Usually, the choice of liquefaction solvent depends on not only its liquefaction capability but also its polyol properties (i.e. polyhydric alcohols also, as liquefaction solvents, are polyols). For example, a binary mixture of PEG 400 ( $M_w$ : 400 g/mol)/glycerol (w/w: 4/1) is the liquefaction solvent most commonly used to produce polyols with properties suited to rigid or semi-rigid PU foam applications (Lee et al., 2000; Lee et al., 2002; Chen and Lu, 2009; Gao et al., 2010). In contrast, PEG 4000 ( $M_w$ : 4000 g/mol) is used a liquefaction solvent to produce polyols suitable for highly resilient PU foam applications (Ge et al., 2000).

Various polyhydric alcohols such as PEG, EG, glycerol, and EC have been used for biomass liquefaction (Yao et al., 1993; Yao et al., 1995; Yamada and Ono, 1999). The binary mixture of PEG 400 and glycerol (4/1, w/w) is most frequently used due to its combination of high liquefaction efficiency and ability to dampen detrimental recondensation reactions (Yao et al., 1993; Yao et al., 1995; Lee et al., 2000; Lee et al., 2002; Yan et al., 2008; Chen and Lu, 2009). However, since lignocellulosic biomass is structurally heterogeneous, a 4:1 mixed PEG/glycerol is not optimal for all types of biomass. Indeed, studies have suggested different optimal PEG/glycerol ratios for different biomasses, such as 9/1 for some wood species, bagasse, and cotton stalks (Kurimoto et al., 1999; Hassan and Shukry, 2008) and 2/3 for acid hydrolysis residues of corn cobs (Zhang et al., 2012a).

Cyclic carbonates, including EC and PC, are capable of rapidly liquefying cellulose and hardwood. Almost-complete liquefaction was achieved within 40 min at 150 °C for EC and PC, while incomplete liquefaction was observed even after 120 min for PEG 400/glycerol (4/1) (Yamada and Ono, 1999). The high liquefaction efficiency of cyclic carbonates was explained by their high permittivity that leads to the high acid potential of liquefaction system (Yamada and Ono, 1999). However, in a later study, Wang et al. (2008) liquefied corn stover (CS) using EC at different CS/EC ratios (0.2-0.4): incomplete liquefaction (i.e. percent solid residue ranging from 2.0 to 11.6 %) was observed even after 90 min of liquefaction at 170 °C. These different observations might be caused by the different compositions and morphologies of the specific biomass feedstocks liquefied.

The liquefaction of lignocellulosic biomass usually requires large solvent/biomass ratios (i.e. 3/1-5/1) to obtain high liquefaction efficiency and minimize the detrimental effects of recondensation reactions (Yao et al., 1993; Yao et al., 1995; Hassan and Shukry, 2008). For wood, high liquefaction efficiency (i.e. percent biomass residue less than 10 %) can be obtained at a solvent/biomass ratio as low as 3/1, while agricultural crop residues generally need a minimum solvent/biomass ratio of 5/1 to obtain comparable liquefaction efficiency (Yao et al., 1993; Yao et al., 1995; Lee et al., 2000; Hassan and Shukry, 2008). Yao et al. (1993) studied the acid-catalyzed liquefaction of birch wood at different solvent/wood ratios (3/1 to 11/9), and significant decreases in liquefaction efficiency were observed for ratios below 3/2. In a later study, Lee et al. (2000) studied the liquefaction of corn bran at solvent/biomass ratios of 5/1, 3/1, and 2/1 and decreases in biomass liquefaction efficiency were observed at solvent/biomass ratios below 5/1. Similarly, Hassan and Shukry (2008) studied the liquefaction of agricultural crop residues, i.e. bagasse and cotton stalks, and found high liquefaction efficiency was obtained at solvent/biomass ratios larger than or equal to 5/1.

Currently, almost all liquefaction solvents used are expensive petroleum-derived polyhydric alcohols. To reduce the high cost and increase the renewability of biomass liquefaction processes, our research group focuses on the use of crude glycerol, a byproduct from biodiesel production, as an alternative biomass liquefaction solvent for polyol production. Compared to conventional petroleum-derived solvents, crude glycerol is bio-based, renewable, and inexpensive, but contains impurities, such as FFA, soap, and FAMES (Hu et al., 2012a). For most crude glycerol conversion processes, these

impurities are unfavorable and detrimental and need to be removed beforehand. Recently, we investigated the feasibility of biomass liquefaction by 100 % unrefined crude glycerol (Hu et al., 2012b). Despite the relatively low biomass liquefaction efficiency, the polyols and PU foams produced exhibited properties comparable to those obtained from conventional petrochemical solvent-based liquefaction processes. More importantly, our study also indicated that certain impurities in crude glycerol, such as FFA, soap and FAMES, improved the properties of polyols and PU foams due to their synergistic interactions with glycerol and/or biomass components. This indicates that unrefined crude glycerol can be used directly as an effective biomass liquefaction solvent without expensive upgrading or refining treatments. This could potentially improve the economics and sustainability of lignocellulosic biomass liquefaction processes.

### *2.3.3 Catalysts*

The liquefaction of lignocellulosic biomass can be either acid- or base-catalyzed, although the former is more commonly used. Among all acids investigated so far, concentrated (98 %) sulfuric acid has the highest catalytic ability in biomass liquefaction (Wang and Chen, 2007). The effect of different sulfuric acid loadings on the liquefaction of lignocellulosic biomass has been extensively studied (Lee et al., 2000; Wang and Chen, 2007; Hassan and Shukry, 2008; Zhang et al., 2012a). Generally, significant improvements on biomass liquefaction efficiency were obtained by increasing sulfuric acid loadings from 1 to 3 % (wt. basis on liquefaction solvent). For example, increasing acid loadings from 1 to 3 % decreased percent biomass residue from approximately 45 % to less than 20 % for the liquefaction of cotton stalks, wheat straw and corncob-derived

acid hydrolysis residue (AHR) (Wang and Chen, 2007; Hassan and Shukry, 2008; Zhang et al., 2012a). Further increasing sulfuric acid loadings to over 3 % provides little improvement in biomass liquefaction efficiency and risks accelerating recondensation reactions (Hassan and Shukry, 2008; Zhang et al., 2012a; Zhang et al., 2012b). Unnecessarily high sulfuric acid loadings may even decrease biomass liquefaction efficiency, by accelerating detrimental recondensation reactions (Lee et al., 2000; Zhang et al., 2012a; Zhang et al., 2012b). For most lignocellulosic biomasses, sulfuric acid loadings between 3 and 4 % provide a good balance between high liquefaction efficiency and effective retardation of detrimental recondensation reactions.

Compared to the extensive studies on acid-catalyzed liquefaction processes, reports on base-catalyzed liquefaction processes are few. Generally, base-catalyzed liquefaction processes require higher liquefaction temperatures (approximately 250 °C) to achieve liquefaction efficiency comparable to those obtained from acid-catalyzed processes (Maldas and Shiraishi, 1996; Alma and Shiraishi, 1998). However, base-catalyzed liquefaction processes have the advantage of causing less corrosion to metal equipment used in liquefaction process.

#### *2.3.4 Liquefaction temperature and time*

The temperature effect on the liquefaction of different types of lignocellulosic biomasses, such as corn bran (Lee et al., 2000), wheat straw (Wang and Chen, 2007; Chen and Lu, 2009), bagasse and cotton stalks (Hassan and Shukry, 2008), corn stalk (Yan et al., 2008), rapeseed cake residue (Briones et al., 2011), and acid hydrolysis residue (AHR) of corncob (Zhang et al., 2012a), has been studied. Among these studies,

the liquefaction processes were all acid-catalyzed and conducted at temperatures ranging from 130-170 °C using binary mixtures of PEG/glycerin as liquefaction solvents. Significant improvements on biomass liquefaction efficiency were observed for temperatures increasing from 130 to 150 °C, beyond which little improvement was observed.

Lignocellulosic biomass usually features a rapid liquefaction stage in the first 15-30 min of acid-catalyzed biomass liquefaction process, after which the liquefaction proceeds at a much slower rate (Lee et al., 2000; Chen and Lu, 2009; Zhang et al., 2012a). As discussed before (Section 2.2), the first rapid liquefaction stage is largely due to the degradation of more accessible biomass components such as lignin, hemicellulose, and amorphous cellulose, while the slow liquefaction process stage mainly features the degradation of well-packed and less solvent-accessible crystalline cellulose (Lee et al., 2002; Chen and Lu, 2009; Zhang et al., 2012a). In addition, recondensation reactions among derivatives from biomass and/or liquefaction solvents always accompany and compete against biomass liquefaction reactions. Under high liquefaction temperature and prolonged liquefaction time, these reactions may become significant enough to decrease biomass liquefaction efficiency. For most lignocellulosic biomass, a liquefaction process at 150 °C for 90 min provides high biomass liquefaction efficiency (Yao et al., 1993; Lee et al., 2000; Lee et al., 2002; Wang and Chen, 2007; Hassan and Shukry, 2008; Yan et al., 2008; Chen and Lu, 2009).

## 2.4 Biomass liquefaction-derived polyols

To assess their suitability in PU applications, polyols produced from the liquefaction of lignocellulosic biomass are typically characterized in terms of hydroxyl number, acid number, viscosity, and  $M_w$ , all of which change dynamically during biomass liquefaction. For example, the  $M_w$  of polyols usually increase at the early stages of liquefaction process, due to the release of a large amount of macromolecules from biomass. As these macromolecules get gradually degraded, the  $M_w$  of polyols decrease accordingly but may increase again if significant recondensation reactions occur at the late stages of liquefaction process (Kobayashi et al., 2004; Yan et al., 2008). The hydroxyl numbers of polyols decrease, while the acid numbers of polyols increase, with the progression of biomass liquefaction. The decreasing polyol hydroxyl numbers can be ascribed to the consumption of hydroxyl moieties by reactions such as oxidation and dehydration, while the increasing polyol acid numbers can be explained by the formation of organic acids from the decomposition of lignocellulosic biomass and/or the oxidation of polyhydric solvents (Lee et al., 2000; Yamada and Ono, 2001; Yamada et al., 2007). Polyol viscosities usually decrease with the gradual liquefaction of biomass (Hassan and Shukry, 2008; Chen and Lu, 2009; Hu et al., 2012b).

In summary, for almost all biomass liquefaction processes using polyhydric alcohols as liquefaction solvents, the hydroxyl number and viscosities of polyols decrease, while their acid number increase, with the increasing liquefaction extent of the lignocellulosic biomass (Chen and Lu, 2009; Lee et al., 2000). However, when crude glycerol is used as liquefaction solvent, the acid numbers and viscosities of polyols

decreased and increased, respectively, with increasing liquefaction temperatures (120 to 240 °C). This contradictory observation can be explained by the extensive condensation reactions occurred among crude glycerol components such as glycerol and fatty acids (Hu et al., 2012b). When liquefaction was conducted at 240 °C for prolonged reaction times, biomass liquefaction became dominant and the changes of polyol properties (hydroxyl and acid numbers, viscosity) with liquefaction time showed similar trends to those observed in conventional polyhydric alcohol-based liquefaction processes (Hu et al., 2012b).

The properties of polyols produced from the liquefaction of various lignocellulosic biomasses (including woody and herbaceous plant biomass) have been reported, and a summary of them is shown in Table 2.1. As shown in Table 2.1, depending on the specific liquefaction parameters and biomass type, biomass liquefaction-derived polyols show hydroxyl numbers ranging from approximately 100 to 600 mg KOH/g, acid numbers from 0 to 40 mg KOH/g, viscosities from 0.3 to 45 Pa.s, and  $M_w$  from 250 to over 7000 g/mol. Generally, liquefaction-derived polyols are suitable for the production of rigid or semi-rigid PU foams, but their uses in the preparation of PU adhesives (Lee and Lin, 2008; Juhaida et al., 2010) and films (Kurimoto et al., 2000; Kurimoto et al., 2001a; Kurimoto et al., 2001b) also have been reported.

## **2.5 PU from liquefaction-derived polyols**

Biomass liquefaction-derived polyols are most commonly used to produce rigid or semi-rigid PU foams. Acid-catalyzed liquefaction-derived polyols usually have high acid numbers (0-40 mg KOH/g) and need to be neutralized by bases such as NaOH or MgO

before being used to prepare PU foams (Yao et al., 1995; Chen and Lu, 2009; Liu et al., 2009). The neutralized polyols can be used alone or as partial substitutes for petroleum-derived polyols to produce PU foams. PU foams produced from mixtures of liquefaction- and petroleum-derived polyols can have improved compressive strength and thermal stability (Chen and Lu, 2009; Liu et al., 2009; Hakim et al., 2011). For example, in the studies of Chen and Lu (2009) and Abdel Hakim et al. (2011), the compressive strength and thermal stability of PU foams increased with increasing substitution levels up to 30 %. In the study of Liu et al. (2009), a similar trend was observed with substitution levels up to 60 %. These property improvements can be largely attributed to the increased hard segment contents and crosslinking densities in PU foams resulted from biomass liquefaction-derived polyols (Chen and Lu, 2009; Liu et al., 2009; Hakim et al., 2011) .

PU foams produced from 100 % liquefaction-derived polyols also have been prepared and characterized (Yao et al., 1995; Lee et al., 2000; Lee et al., 2002; Gao et al., 2010; Yan et al., 2010; Hu et al., 2012b). Mostly, their properties depend on both polyol properties and foaming formulations. In one example, Yao et al. (1995) prepared PU foams from high biomass content (50 %) polyols produced by the combined liquefaction of wood and starch. Polyols with different properties were produced when different wood/starch ratios were used in the liquefaction process, leading to the production of PU foams with different properties (density around  $0.03 \text{ g/cm}^3$ , compressive strength: 80-150 kPa, and elastic modulus: 3-10 MPa) (Yao et al., 1995). In another example, PU foams prepared from polyols derived from the liquefaction of different types of waste paper showed densities ranging from  $0.036$  to  $0.05 \text{ g/cm}^3$ , compressive strength from 68 to 195

kPa, and elastic moduli from 0.8 to 3.4 MPa (Lee et al., 2002). In our study of crude glycerol-based liquefaction of soybean straw (Hu et al., 2012b), liquefaction parameters significantly affected the properties of PU foams produced. Under optimal liquefaction conditions, the PU foams produced showed densities ranging from 0.033 to 0.037 g/cm<sup>3</sup> and compressive strength from 148 to 227 KPa. The effects of foaming formulations such as NCO/OH ratio and catalyst loading on the properties of PU foams also have been studied (Yan et al., 2008; Gao et al., 2010). Higher NCO/OH ratios resulted in PU foams with higher mechanical strength and higher thermal stability, due to the increased contents of hard segment and crosslinking density in polymer networks (Yan et al., 2008). However, excessive amounts of isocyanates in foaming formulations could be detrimental to foam properties due to the incomplete cure of isocyanates (Yan et al., 2008).

Compared to PU foams produced from petroleum-derived polyols, PU foams produced from liquefaction-derived polyols have shown better biodegradability (Lee et al., 2002; Wang and Chen, 2007). For example, PU foams derived from the liquefaction of waste paper showed a weight loss of around 20 % over a six-month buried period in leaf mold, while PU foam produced from petroleum-derived polyol showed negligible weight loss (Lee et al., 2002). Similarly, PU foams produced from the liquefaction of wheat straw also showed better biodegradability (around 16 % weight loss over a one-year buried period in soil) than their petroleum analog (negligible biodegradation) (Wang and Chen, 2007). To prepare flexible and highly resilient PU foams from liquefaction-derived polyols, petroleum-derived polyether polyols with high  $M_w$  were used to liquefy

tannin-containing bark and starch (Ge et al., 2000). The results showed that PEG 4000 achieved the optimal balance between high liquefaction efficiency and good foam resilience. Results from this study also showed that the compressive strength, density, and resilience of PU foam were affected by the tannin and starch contents in the liquefaction system: (a) the higher the tannin content, the higher the density and resilience values of PU foams; (b) the higher the starch content, the higher the density and compressive strength, but the lower the resilience value (Ge et al., 2000). The PU foams prepared in this study also showed better biodegradability than their petroleum analogs (Ge et al., 2000).

In addition to foams, liquefaction-derived polyols also have been used to prepare other forms of PU, such as adhesives (Lee and Lin, 2008; Juhaida et al., 2010), resins (Wei et al., 2007), and films (Kurimoto et al., 2000; Kurimoto et al., 2001a; Kurimoto et al., 2001b). Kurimoto et al. (2000; 2001b) studied the mechanical properties and network structures of PU films prepared from wood liquefaction-derived polyols. Their results showed that liquefied wood in polyols could act as crosslinkers in PU networks, leading to increased tensile strength, glass transition temperature, and thermal stability of PU films (Kurimoto et al., 2000; Kurimoto et al., 2001b). Polyols prepared from six different wood species exhibited similar hydroxyl values, moisture content, and amounts of dissolved woody components (DWC), but different viscosities, which led to the production of PU films with different properties (Kurimoto et al., 2001a). The properties of liquefaction-derived polyols and PU formulations, such as isocyanate types and

NCO/OH ratios, also affect the gel time and glue bonding strength of PU adhesives and resins (Wei et al., 2007; Lee and Lin, 2008; Juhaida et al., 2010).

## **2.6 Summary and outlook**

Lignocellulosic biomass has great potential as a renewable, abundant, and inexpensive feedstock to produce bio-based polyols and PU. Polyols produced from the liquefaction of lignocellulosic biomass have broad applications in preparing a wide range of PU products, such as foams, films, and adhesives. Among them, the preparation of semi-rigid and rigid PU foams is most commonly seen. Generally, liquefaction-derived PU foams have comparable mechanical properties, better thermal stability, and better biodegradability compared to their petroleum-derived analogs. However, with all their great promise, liquefaction of lignocellulosic biomass still faces certain challenges such as high production cost and low versatility. The high-volume use of petroleum-derived liquefaction solvents inevitably reduces the bio-content and renewability of liquefaction-derived polyols. Advances in liquefaction techniques, the use of bio-based liquefaction solvent and post-refining of liquefaction-derived polyols could contribute to solving or alleviating these issues. Last but not least, the inherent heterogeneities of lignocellulosic biomasses pose significant challenges for the production of polyols and PU with consistent structures and properties. The use of more homogenous biomass derivatives, such as cellulose and glucose, should help produce polyols and PU with more homogeneous structures and consistent qualities. Despite all these challenges, the inevitable depletion of the world's fossil resources demands continued efforts to advance the technologies and economics of lignocellulosic biomass-based polyols and PU.

Table 2.1: General properties of polyols produced from lignocellulosic biomass liquefaction process<sup>a</sup>

Lignocellulosic biomass	Polyol properties					Reference
	Biomass conversion (%)	Hydroxyl number (mg KOH/g)	Acid number (mg KOH/g)	Viscosity (Pa.s)	$M_w$ (g/mol)	
Acid-catalyzed liquefaction process						
Enzymatic hydrolysis lignin	98	249	-	-	-	(Jin et al., 2011)
Cellulose or waste paper	55-99	360-396	19-30	2.6-3.9	650-900	(Yamada and Ono, 1999; Lee et al., 2002)
Agricultural crop residues <sup>b</sup>	60-95 %	109-430	15-30	1.0-1.7	1050-1400	(Liang et al., 2006; Wang and Chen, 2007; Hassan and Shukry, 2008; Wang et al., 2008; Yan et al., 2008; Chen and Lu, 2009; Zhang et al., 2012a)
Industrial or bio-refinery residues <sup>c</sup>	84-98	137-586	28-34	0.4-3.0	250-2000	(Lee et al., 2000; Hassan and Shukry, 2008; Yu et al., 2008; Liu et al., 2009; Briones et al., 2011; Briones et al., 2012)
Wood <sup>d</sup>	80-98	200-435	12-38	0.3-31.6	583-667	(Kurimoto et al., 1999; Kurimoto et al., 2000; Kurimoto et al., 2001a; Lee and Lin, 2008)
Base-catalyzed liquefaction process						
Birch wood	>99	112-204	24-41	-	1500-7900	(Maldas and Shiraishi, 1996; Alma and Shiraishi, 1998)
Soybean straw <sup>e</sup>	65-75	440-540	<5	16-45	-	(Hu et al., 2012b)

Notes: a: unless otherwise stated, properties reported are for polyols produced using petrochemical-based polyhydric alcohols as liquefaction solvents; b: includes wheat straw, rice straw, corn stover, cotton stalk, cornstalk, corncob, etc; c: includes sugarcane bagasse, DDGS (dried distillers grains), corn bran, date seeds, rapeseed cake residue, apple pomace, olive stone, etc; d: include both softwood and hardwood species; e: crude glycerol from biodiesel plant used as liquefaction solvent.

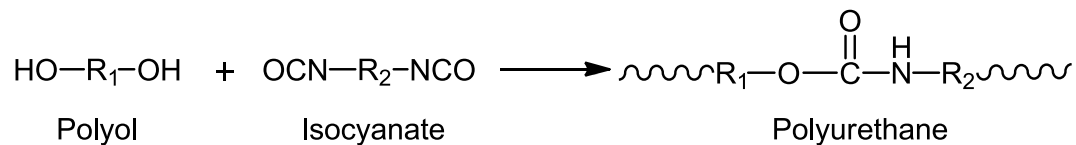


Figure 2.1: Reaction between polyols and isocyanates to form PU

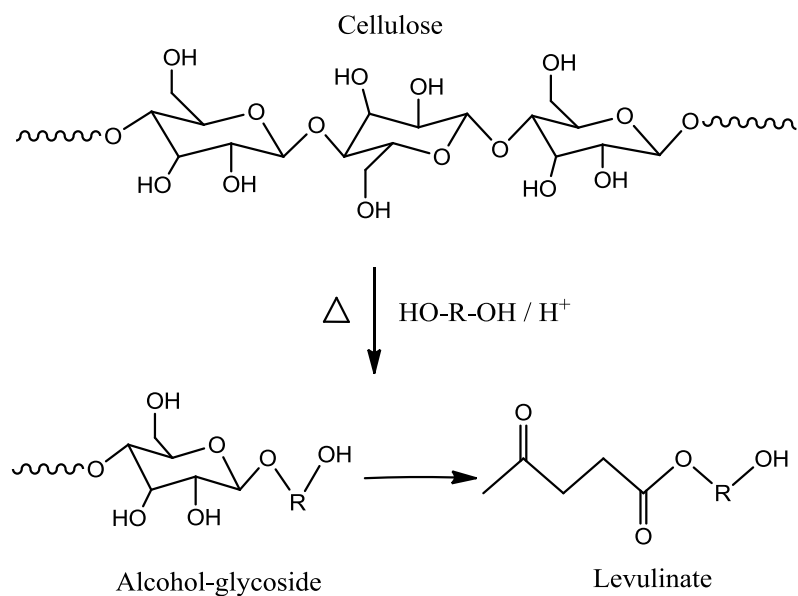


Figure 2.2: Schematic representation of the liquefaction mechanism of acid-catalyzed cellulose liquefaction in polyhydric alcohols

## **Chapter 3 Polyols and PU Foams from Crude Glycerol-based Liquefaction of Soybean Straw**

The feasibility of using crude glycerol to liquefy soybean straw for the production of polyols and polyurethane (PU) foams was investigated. Liquefaction conditions of 240 °C, 180-360 min, 3% sulfuric acid loading, and biomass loading of 10-15% were preferred for the production of polyols with promising properties. The polyols produced showed hydroxyl numbers from 440 to 490 mg KOH/g, acid numbers below 5 mg KOH/g, and viscosities from 16 to 45 Pa·s. The PU foams produced showed densities from 0.033 to 0.037g/cm<sup>3</sup> and compressive strength from 148 to 203 kPa. These results suggest that crude glycerol can be used as an effective solvent to liquefy lignocellulosic biomass for the production of polyols and PU foams. The PU foams produced showed density and compressive strength comparable to their analogs from petrochemical solvent-based liquefaction processes.

### **3.1 Introduction**

As the world's most abundant biomass, lignocellulosic biomass can be liquefied to produce polyols for PU applications. However, the biomass liquefaction process requires high volumes of petroleum-derived solvents to be used as liquefaction agents, which reduces the renewability of liquefaction-derived polyols. Crude glycerol, as a low-cost byproduct from biodiesel industry, has the potential to be used as biomass

liquefaction solvent for polyol production. The successful replacement of petroleum-derived liquefaction solvents by crude glycerol could contribute to reducing the production cost of and increasing the renewability of liquefaction-derived polyols and PU foams. In addition, the production of polyols from crude glycerol also contributes to alleviating the crude glycerol glut problem. Soybean straw, as an abundant agricultural crop residue, has not been studied for its potential in polyol and PU foam production. This study aimed to investigate the feasibility of using biodiesel-derived crude glycerol to liquefy soybean straw for the production of polyols and PU foams.

## **3.2 Materials and Methods**

### *3.2.1 Materials*

Unrefined crude glycerol was obtained from Bio100 Technologies, LLC. (Mansfield, OH) and contains approximately 37% total FFAs, 11% methanol, 39% glycerol, 6% water, 0.06% salt, and other impurities. Soybean straw was harvested from the farm at the Ohio Agricultural Research and Development Center (OARDC), Wooster, OH. Air-dried soybean straw was ground through a 60 mesh screen and oven-dried for 24 h before being used for liquefaction. Reagent grade pure glycerol, 98% sulfuric acid, ethanol, and standard NaOH solutions (0.1 N and 1 N) were purchased from Fisher Scientific (Pittsburgh, PA). Additives used in PU foaming were obtained from Air Products & Chemicals, Inc. (Allentown, PA). Polymeric MDI (methylene-4,4'-diphenyl diisocyanate) was obtained from Bayer Material Science (Pittsburgh, PA).

### *3.2.2 Liquefaction process for polyol production*

The liquefaction process for polyol production was carried out in a 500-ml three-neck flask under atmospheric pressure with constant stirring. The reactor was heated by a temperature-controlled heating mantle (Thermo Electron Corp., Madison, WI). After the solvents (crude glycerol and concentrated 98% sulfuric acid (at 0 to 5%)) reached the desired liquefaction temperature (120 to 240 °C,) pre-weighed soybean straw (loading from 10 to 25%) was added. Liquefaction was conducted at different but preset reaction times (45 to 360 min), after which the flask was removed and quenched in ambient tap water. Water, methanol, and other volatiles evaporated during the liquefaction process were recovered by a glass Graham condenser connected to the flask. Polyols were recovered from the flask. All liquefaction treatments were conducted in duplicates. The loadings of concentrated sulfuric acid and soybean straw applied in the liquefaction process were weight percentages based on the net weight of crude glycerol.

### *3.2.3 Determination of biomass conversion*

Approximately 2 g of polyol was weighed from thoroughly mixed polyol and well-dissolved in 30 ml of ethanol in a 250-ml Erlenmeyer flask. Solid residues were separated by centrifugation at 10,000 rpm for 10 min. The supernatant was decanted and the solid residues were rinsed with 30 ml ethanol and separated by centrifugation as described above. The solid residues were transferred from the centrifugation tubes into a 250-ml flask using 50 ml of de-ionized water. The flask was then shaken at 30 °C for 10 minutes to completely dissolve any sulfates formed between the added sulfuric acids and the residual alkaline catalysts existing in the crude glycerol. The dissolved mixture was

vacuum-filtered via a 50-ml pre-dried fritted glass filtering crucible with a layer of glass fiber filter paper (20 mm dia.) placed on the frit. De-ionized water was used to rinse residual solids in the crucible until the filtrate became colorless. Then the crucible was dried in an oven at 105 °C for 24 h to ensure complete drying. Biomass conversion ratio was calculated using the equation below:

Biomass conversion ratio (%) =  $100 - ((W_1 - W_2)/W_3 \times W_4 \times 100)/W_5$ , where

$W_1$ : total dry weight of filtering crucible with biomass residue;  $W_2$ : net weight of filtering crucible without soybean straw residue;  $W_3$ : weight of polyol weighed for biomass conversion analysis;  $W_4$ : total weight of polyol obtained from liquefaction process;  $W_5$ : weight of soybean straw added in liquefaction process.

#### *3.2.4 Determination of acid and hydroxyl numbers of polyols*

The acid number of polyol was determined in accordance with ASTM D4662-08. Approximately 2 g of polyols were dissolved in 50 ml of ethanol in a 250-ml Erlenmeyer flask. Titration was conducted using a 0.1 N standard NaOH solution, and the end point was indicated by a digital pH meter (Accumet AP110, Fisher Scientific, Pittsburgh, PA). The hydroxyl number of polyol was determined in accordance with ASTM D4274-05D, in which the esterification process is catalyzed by imidazole. Specifically, polyol was weighed into a 250-ml Erlenmeyer flask, followed by the addition of 25 ml of esterification reagent (phthalic anhydride and imidazole in pyridine). The flask was capped with aluminum foil and pre-warmed in a water bath and swirled to ensure complete dissolution of polyols. Then, the flask was placed in a water bath maintained at

98 ± 2 °C for 15 min. After that, the flask was removed from the water bath and cooled to ambient temperature before titration. Titration was conducted using a 0.5 N standard NaOH solution (diluted from 1N standard NaOH solution) and the end point determined by a digital pH meter. Both acid and hydroxyl numbers were calculated using formulas detailed in their respective ASTM standards.

### *3.2.5 Determination of polyol viscosity*

The viscosity of polyol was determined at 25 ± 0.5 °C according to ASTM D 4878-08 using a Brookfield DV II+Pro viscometer, equipped with a small sample adapter, temperature probe, and temperature control unit (Brookfield Engineering Laboratories, Inc., Middleboro, MA).

### *3.2.6 Preparation of PU Foams*

PU foams were prepared in 650-ml plastic cups at an isocyanate index of 100. Polyol, catalysts, and a blowing agent (water) were premixed vigorously by a high-speed stirrer for 10-15 s in a plastic container to achieve homogenous mixing. Pre-weighted polymeric MDI was then added, and the mixture was stirred vigorously for another 10-15 s. The mixture was then rapidly poured into a 650 ml plastic cup and left to grow foam at ambient temperature (23±2°C). All foam samples were allowed to cure overnight before removal from the plastic cups. Additives used in the PU foaming process were Polycat 5 and 8 and DABCO DC5357 obtained from Air Products & Chemicals, Inc. The formula used for the PU foam preparation is shown in Table 3.1.

### *3.2.7 Characterization of PU Foams*

The density and compressive strength of PU foam were measured in accordance with ASTM D 1622-08 and ASTM D 1621-10, respectively. Compressive strength tests were conducted using a TA-XT2 texture analyzer (Stable Micro System Texture technology, Godalming, UK) with a crosshead displacement rate of 2.5 mm/min.

### *3.2.8 Data analysis*

The data analysis in this study was performed using IBM SPSS Statistics 19 (Armonk, NY). The ANOVA (analysis of variance) was performed to test the significance of factors at  $\alpha=0.05$ .

## **3.3. Results and Discussion**

### *3.3.1 Effects of reaction temperature*

Biomass conversion ratio increased from 15 to 50% as the reaction temperature increased from 120 to 240 °C, indicating the acceleration of liquefaction reactions with increasing temperatures (Figure 3.1). Polyol viscosity increased from 36 to 75 Pa·s when reaction temperature increased from 120 to 180 °C (Figure 3.1); a further increase in temperature to over 180 °C caused a dramatic increase in viscosity to much higher than 100 Pa·s (data not shown). Previous studies have suggested that an increase in biomass conversion/liquefaction ratio usually results in a decrease in polyol viscosity due to the liquefaction of biomass (Lee et al., 2000; Chen and Lu, 2009). Chen and Lu (2009) studied the liquefaction of wheat straw using PEG 400/glycerol as the liquefaction

solvent. It was shown that polyol viscosity decreased from approximately 1.8 to 0.8 Pa·s as reaction temperature increased from 130 to 160 °C. This is inconsistent with our finding that polyol viscosity increased with increasing reaction temperature. This disagreement is probably caused by the use of different liquefaction solvents (Yamada and Ono, 1999; Wang and Chen, 2007; Yu et al., 2008): when a mixture of PEG 400 and glycerol were used as the liquefaction solvent, polyol viscosity decreased with increasing temperature because more biomass was liquefied at higher reaction temperatures. However, when crude glycerol was used as a liquefaction solvent, its components such as glycerol, methanol, and fatty acids/soap can react with each other via reactions such as esterification, trans-esterification, and etherification (Biswas and Ganguly, 1960; Ruppert et al., 2008; Ionescu and Petrovic, 2010). Increases in reaction temperature enhance these reactions during the liquefaction process, producing compounds with higher  $M_w$  and higher viscosities. In addition, the intensified evaporation of volatile compounds at higher reaction temperatures also might contribute to the increase of viscosity with increasing temperatures.

Polyol hydroxyl and acid numbers decreased from 635 to 533 mg KOH/g and from 23 to 2.7 mg KOH/g, respectively, as liquefaction temperature increased from 120 to 240 °C (Figure 3.2). The decrease in hydroxyl number can be caused by dehydration/condensation reactions of liquefaction solvents and/or by thermal oxidative reactions that occurred between liquefaction components (i.e., liquefaction solvents and liquefied components of lignocellulosic biomass) (Yao et al., 1996; Lee et al., 2000). Previous studies have suggested that, during liquefaction, the acid numbers of polyols

tends to increase with increasing biomass conversion ratio due to the formation of acidic substances (Lee et al., 2000; Yamada and Ono, 2001). This disagrees with our observation of a decrease in polyol acid number (Figure 3.2). This inconsistency is likely due to the impurities existing in crude glycerol; for instance, fatty acid/soap residues can react with glycerol or other hydroxyl groups-containing compounds during the liquefaction process, which can cause consumption of acidic compounds. It is likely that these reactions became dominant compared to those that form acidic compounds at high reaction temperatures, leading to the decrease in the acid numbers of polyols. This agrees with the observed increase in polyol viscosities with increasing reaction temperatures (Figure 3.1), which may be due to reactions between crude glycerol impurities.

In this study, polyols produced from the liquefaction process were used directly to produce PU foams. The compressive strength and density of PU foams varied between 112 and 150 kPa and 0.031 and 0.035 g/cm<sup>3</sup>, respectively, for reaction temperatures between 180 and 240 °C (Figure 3.3). Linear correlations between compressive strength and density of PU foams were observed for temperatures ranging from 180 to 220 °C ( $R^2=0.95$ ) and for temperatures ranging from 200 to 240 °C ( $R^2=0.99$ ), indicating that more compact and denser structures contributed to the higher compressive strength of PU foams; however, the compressive strength PU foams at 240 °C were much higher than those from 180 °C, even though they showed similar density around 0.032 g/cm<sup>3</sup> (Figure 3.3). This suggests that, in addition to density, the compressive strength of PU foams might be affected by other factors, such as biomass residues or the chemical structure of different polyols. An ANOVA analysis indicated that the effect of liquefaction

temperature on the compressive strength and density of PU foams was significant ( $p < 0.05$ ).

### 3.3.2 *Effects of reaction time*

Biomass (i.e., soybean straw) conversion ratio increased from 46 to 75% with the increasing reaction time from 45 to 360 min (Figure 3.4). Previous studies on PEG 400/glycerol binary solvent-based liquefaction of corn bran (Lee et al., 2000), wheat straw (Wang and Chen, 2007; Chen and Lu, 2009), depithed bagasse and cotton stalk (Hassan and Shukry, 2008) showed that biomass conversion ratios  $\geq 90\%$  were achieved for a liquefaction time of  $\leq 180$  min. The relatively lower conversion ratio obtained in this study might be explained by the use of a different liquefaction solvent (i.e., crude glycerol versus PEG400/glycerol) and of different lignocellulosic biomass (Wang and Chen, 2007; Hassan and Shukry, 2008; Yu et al., 2008). The viscosities of polyols decreased sharply from over 100 to 35 Pa·s as liquefaction time increased from 135 to 180 min, after which they decreased gradually to 16 Pa·s at 360 min (Figure 3.4). Polyols obtained from the PEG400/glycerol-based liquefaction of lignocellulosic biomass showed viscosities generally less than 0.5 Pa·s (Lee et al., 2000; Wang and Chen, 2007; Chen and Lu, 2009). The higher polyol viscosity found in this study might be explained by the lower biomass conversion ratio. However, the viscosities of the polyols at 16 to 35 Pa·s is still comparable to those of some commercial polyols (Dow polyols, 2011) and are suitable for PU foam production.

The hydroxyl numbers of polyols decreased from 550 to 450 mg KOH/g as liquefaction time increased from 45 to 360 min (Figure 3.5). Various dehydration,

oxidation, and/or condensation reactions might contribute to the decrease in the hydroxyl numbers of polyols (Yao et al., 1996; Lee et al., 2002). The acid numbers of polyols were found to be relatively low, ranging from 2.7 to 3.6 mg KOH/g.

The compressive strength and density of PU foams varied between approximately 140 to 230 kPa and between 0.031 to 0.04 g/cm<sup>3</sup>, respectively, for reaction times from 45 to 360 min (Figure 3.6). The effects of reaction time on the density and compressive strength of PU foams were found to be significant (ANOVA,  $p < 0.05$ ). Lee et al. (2000) prepared PU foams from liquefied corn bran, which showed compressive strength between 70 and 142 kPa and density between 0.038 and 0.040 g/cm<sup>3</sup>. Similarly, PU foams prepared from liquefied wheat straw showed compressive strength and density varying from 169 to 212 kPa and from 0.030 to 0.056 g/cm<sup>3</sup>, respectively, depending on the isocyanate index and the content of liquefied wheat straw in PU foams (Chen and Lu, 2009). Thus, it can be seen that PU foams produced from crude glycerol-based liquefaction of soybean straw have properties (i.e., compressive strength and density) comparable to those prepared from petroleum solvent-based liquefaction processes.

### *3.3.3 Effects of sulfuric acid loading*

The decomposition of lignocellulosic biomass during liquefaction proceeds mainly via a series of hydrolysis and solvolysis reactions (Yao et al., 1996; Hassan and Shukry, 2008), which can be catalyzed by either acids or bases. Wang and Chen (2007) compared the catalytic effects of hydrochloric, phosphoric, and sulfuric acids on wheat straw liquefaction and found that sulfuric acid exhibited the highest catalytic efficiency. Typically, sulfuric acid loadings between 3 to 5% are suitable to improve liquefaction

efficiency and reduce the risk of significant condensation reactions that might occur between liquefied components (Yao et al., 1993; Hassan and Shukry, 2008).

Biomass conversion ratio decreased slightly from 55 to 51% as sulfuric acid loading increased from 0 to 4% and that a decrease in biomass conversion from 51 to 39% occurred when acid loading increased from 4 to 5% (Figure 3.7). This finding is contrary to the results reported by other studies, in which the addition of sulfuric acid generally improved biomass conversion (Lee et al., 2000; Hassan and Shukry, 2008). Mostly, these studies used petrochemical polyhydric alcohols as the liquefaction solvent, where the addition of sulfuric acid resulted in acid-catalyzed hydrolysis and/or solvolysis and thus higher biomass conversion ratios. In this study, it was found that the pH of crude glycerol (i.e., liquefaction solvent) decreased from alkalinity to neutrality as acid loading increased from 0 to 5% due to the neutralization of the alkaline catalyst residues (KOH or NaOH) in crude glycerol, which are left from biodiesel production process. Thus, the crude glycerol based-liquefaction process in this study was conducted in basic conditions and thus base-catalyzed. The increase in acid loading resulted in the decrease of the alkalinity of liquefaction solvents and thus lower biomass conversion ratios. Alma and Shiraishi (1998) studied the PEG400 based-liquefaction of birch wood meal catalyzed by NaOH and found that biomass conversions over 99% can be obtained within 1 h at 5% NaOH and 250 °C; the PU foams produced were found to have comparable physico-mechanical properties to those prepared from acid-catalyzed liquefaction processes. The viscosity of polyols decreased from over 100 to around 82 Pa·s when acid loading increased from 0 to 5% (Figure 3.7, data not shown for 0 to 2% acid loading due to their

extremely high viscosity). This is due to the fact that more acids resulted in more neutralization of soap (i.e. alkaline salts of fatty acids) existing in crude glycerol, leading to lower polyol viscosity. Thus, it can be seen that the addition of small amounts (i.e. 3-4%) of sulfuric acid contributes to decreasing the viscosity of biopolyols without significant loss of biomass conversion efficiency.

The acid numbers of polyols were less than 5 mg KOH/g at all acid loadings from 0 to 5% (Figure 3.8). The hydroxyl numbers of polyols decreased with increases in acid loadings due to the consumption of hydroxyl groups by protons (Figure 3.8). When acid loading increased from 3 to 5%, the compressive strength and density of PU foams increased from 144 to 213 kPa and from 0.031 g/cm<sup>3</sup> to 0.041 g/cm<sup>3</sup>, respectively (Figure 3.9). However, the variation of the compressive strength of PU foams increased with increasing acid loadings, indicating that the structure of PU foams at higher acid loadings was less uniform. An ANOVA analysis found that acid loading had no significant effect on compressive strength of PU foams ( $p > 0.05$ ), but significant effect on the density of PU foams ( $p < 0.05$ ), with higher acid loading resulting in higher density PU foams.

#### *3.3.4 Effects of biomass loading*

Polyols and PU foams properties can be substantially affected by the biomass content in the liquefaction solvent (Yao et al., 1996). Biomass conversion ratios at 10 and 15% soybean straw contents were similar at approximately 65% (Figure 3.10), but further increases in biomass loading to 20 and 25% resulted in sharp decreases in the biomass conversion ratio to approximately 54 and 51%, respectively. The viscosity of polyols was 35 and 45 Pa·s at 10 and 15% biomass loading, respectively, which are both acceptable

for the preparation of PU foams (Yao et al., 1996; Dow polyols, 2011). Polyols produced at 20 and 25% biomass loading showed high viscosities ( $>100 \text{ Pa}\cdot\text{s}$ ) and have limited uses in PU foam applications.

The acid numbers of polyols produced with biomass loading from 10 to 20% were less than  $5 \text{ mg KOH/g}$  (Figure 3.11). The hydroxyl numbers of polyols decreased from 480 to  $460 \text{ mg KOH/g}$  when biomass loading increased from 10 to 15%, and polyols produced from the 20% biomass loading showed a hydroxyl number of  $463 \text{ mg KOH/g}$ , very close to that from the 15% biomass loading. The density of PU foams increased from  $0.035$  to  $0.037 \text{ g/cm}^3$  when biomass loading increased from 10 to 20% (Figure 3.12), which was not significant (ANOVA,  $p>0.05$ ). The compressive strength of PU foams decreased from 159 to  $113 \text{ kPa}$  as biomass loading increased from 10 to 20% (Figure 3.12). An ANOVA test showed there was no significant difference ( $p>0.05$ ) between the compressive strength of PU foams with 10 and 15% biomass loading, while the compressive strength of PU foam with 20% biomass loading was significantly lower ( $p<0.05$ ) than that with 10 and 15% biomass loading. The decrease of compressive strength was probably due to the lower biomass conversion ratio at the higher biomass loading.

### *3.3.5 Comparison to pure glycerol*

To obtain high-quality polyols from the liquefaction of lignocellulosic biomass, polyhydric alcohols with appropriate  $M_w$  and hydroxyl numbers need to be used as liquefaction solvents (Yao et al., 1996). A majority of previous studies used a mixture of PEG 400/glycerol as the solvent to liquefy lignocellulosic biomass for the production of

polyols and PU foams. In this study, it was shown that polyols and PU foams with promising properties were produced from lignocellulosic biomass (i.e., soybean straw) by using crude glycerol as an alternative liquefaction solvent. Pure glycerol has not been used alone to liquefy lignocellulosic biomass for polyol production because of its low  $M_w$  and extremely high hydroxyl number (1800 mg KOH/g). It has been commonly used as a co-solvent, for example, PEG 400/glycerol mixture, in liquefaction processes since it helps suppress recondensation reactions of lignin (Lee et al., 2000). Therefore, considering the compositional differences and potentially distinct performance of pure and crude glycerol in liquefaction processes, a comparison between pure and crude glycerol as liquefaction solvent was performed.

Table 3.2 shows the properties of polyols and PU foams prepared from soybean straw with pure or crude glycerol as the liquefaction solvent. The polyol produced from the crude glycerol-based liquefaction process had a hydroxyl number of 573 mg KOH/g, which is suitable for the production of rigid PU foams (Yao et al., 1996). However, the polyol obtained from the pure glycerol-based liquefaction process had a much higher hydroxyl number of 1391 mg KOH/g, which appears to be too high for PU foam production. The lower hydroxyl number of the polyol produced from crude glycerol can be explained by the presence of various impurities that do not contain hydroxyl groups in crude glycerol.

In addition, it was found that the polyol produced from the crude glycerol liquefaction process showed good reactivity in the PU foaming process, and the PU foam produced exhibited density of 0.034 g/cm<sup>3</sup> and compressive strength of 150 kPa (Table

3.2). However, the PU foam produced from the pure glycerol-based polyol seemed incompletely cured even after 12 h. These results indicate that the performance of crude and pure glycerol in the liquefaction processes were markedly different. The polyol and PU foam prepared from the crude glycerol-based liquefaction process showed better material properties than their analogs from the pure glycerol-based liquefaction process.

### **3.4 Conclusions**

The properties of liquefaction-derived polyols and PU foams were affected by liquefaction parameters such as sulfuric acid loading, reaction temperature and time, and biomass loading. To produce polyols of suitable material properties for PU production, liquefaction conditions of 240 °C, 180-360 min, 3% sulfuric acid loading, and biomass loading of 10-15% are preferred. Crude glycerol performed remarkably better than pure glycerol in the production of polyols and PU foams, most likely due to the presence of impurities, such as soap/fatty acids. This study suggests that crude glycerol can be used as a liquefaction solvent for the production of high-quality polyols and PU foams from lignocellulosic biomass such as soybean straw.

Table 3.1: PU foam production formula

<b>Ingredients</b>	<b>Function</b>	<b>Parts by weight</b>
Polyol	Donation of hydroxyl groups	100
Polymer MDI	Donation of isocyanate groups	Equivalent weight for isocyanate index of 100
Polycat 5	Catalysis of water-isocyanate reaction	0.84
Polycat 8	Catalysis of polyol-isocyanate reaction	1.26
DABCO DC5357	Surfactant for cell structure stabilization	2.5
Water	Foaming agent	3

Table 3.2: Comparison of pure and crude glycerol in polyol and PU foam production<sup>a</sup>

	Liquefaction solvent	Pure glycerol	Crude glycerol
Polyols	Conversion (%)	34	40
	Acid number (mg KOH/g)	<5	<5
	Hydroxyl number (mg KOH/g)	1391	573
	Viscosity (Pa·s)	35.2	>100
PU foam <sup>b</sup>	Density (g/cm <sup>3</sup> )	- <sup>c</sup>	0.034
	Compressive strength (kPa)	- <sup>c</sup>	150

a: Liquefaction conducted at 220 °C, 90 min, and 10% biomass loading;

b: PU foam produced using the formula shown in Table 3.1;

c: No testable foam specimen was obtained.

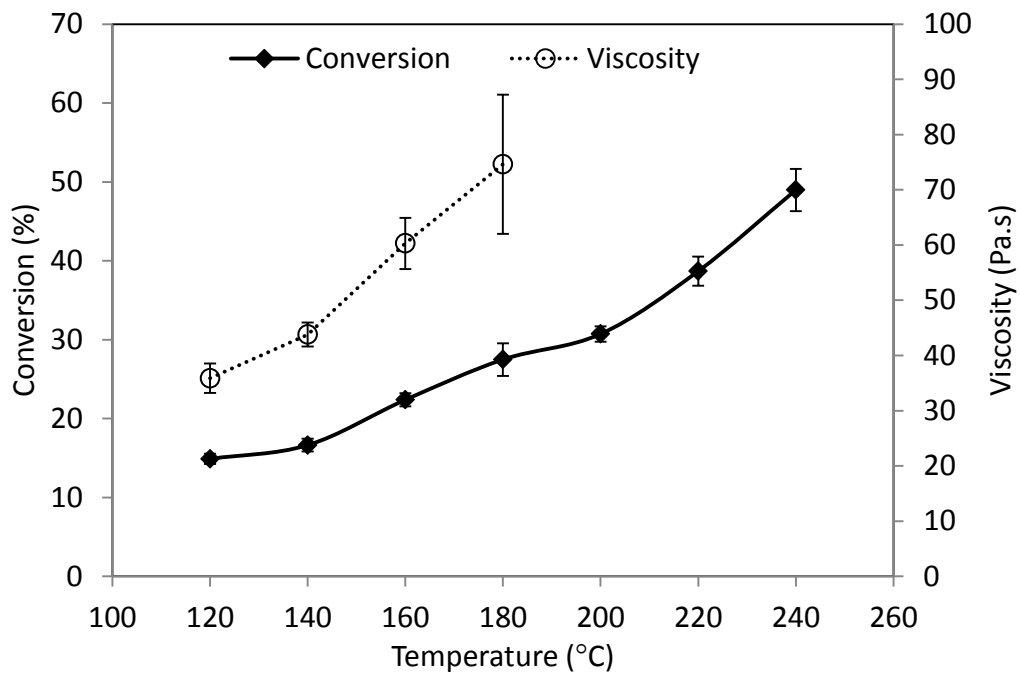


Figure 3.1: Effects of reaction temperature on biomass conversion and polyol viscosity (Note: missing data with viscosity > 1,000 Pa.s; reaction time: 90 min; sulfuric acid loading: 3 %; biomass loading: 10 %; each data point represents the mean of duplicate liquefaction)

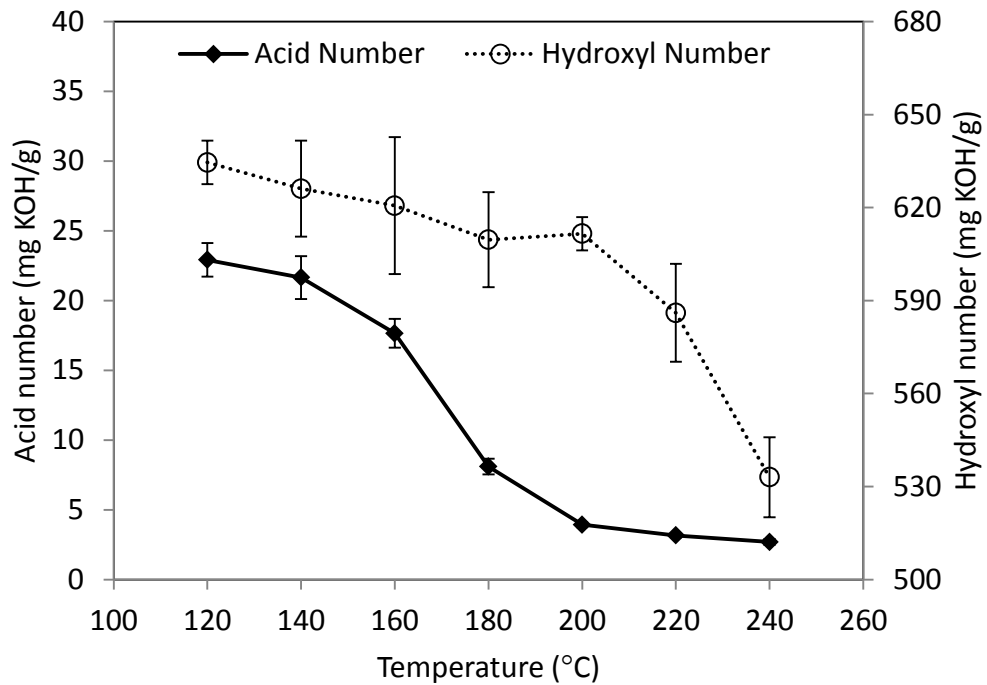


Figure 3.2: Effects of reaction temperature on polyol acid and hydroxyl numbers (Note: reaction time: 90 min; sulfuric acid loading: 3 %; biomass loading: 10 %; each data point represents the mean of duplicate liquefaction)

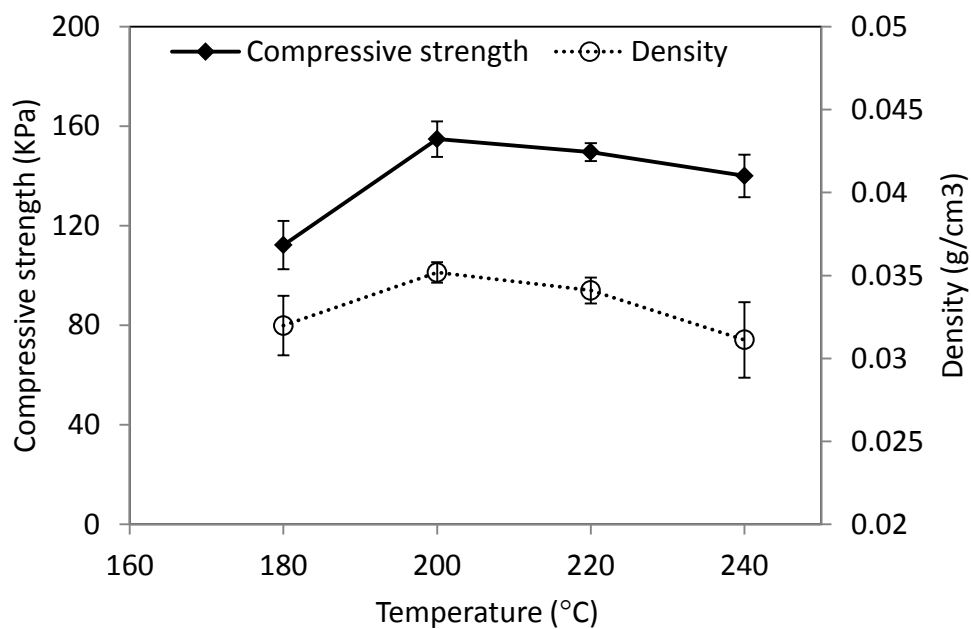


Figure 3.3: Effects of reaction temperature on compressive strength and density of PU foams (Note: reaction time: 90 min; sulfuric acid loading: 3 %; biomass loading: 10 %; each data point represents the mean of duplicate liquefaction)

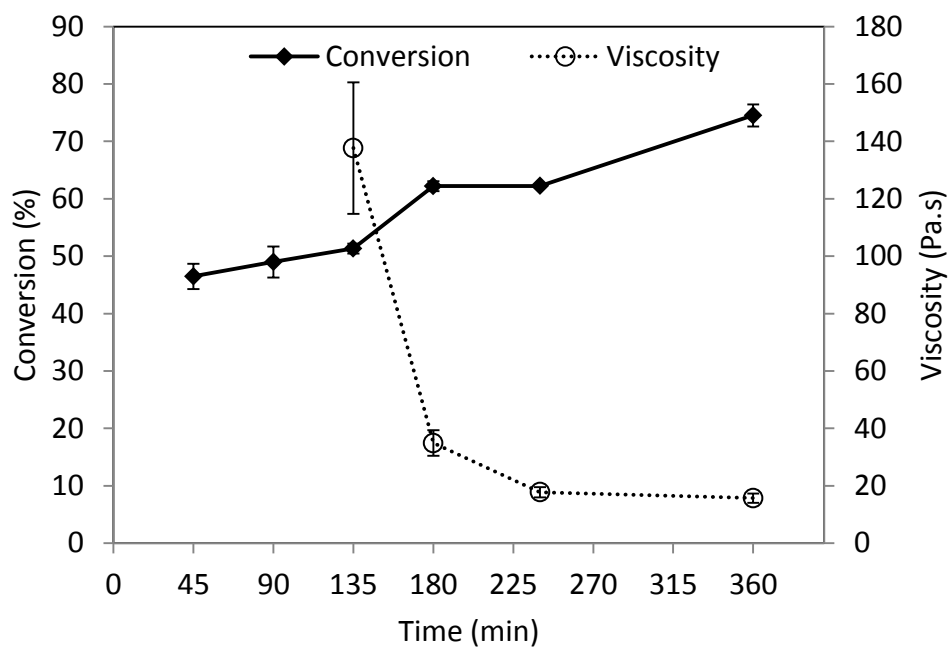


Figure 3.4: Effects of reaction time on biomass conversion and polyol viscosity (Note: missing data with viscosity > 1,000 Pa·s; reaction temperature: 240 °C; sulfuric acid loading: 3 %; biomass loading: 10 %; each data point represents the mean of duplicate liquefaction)

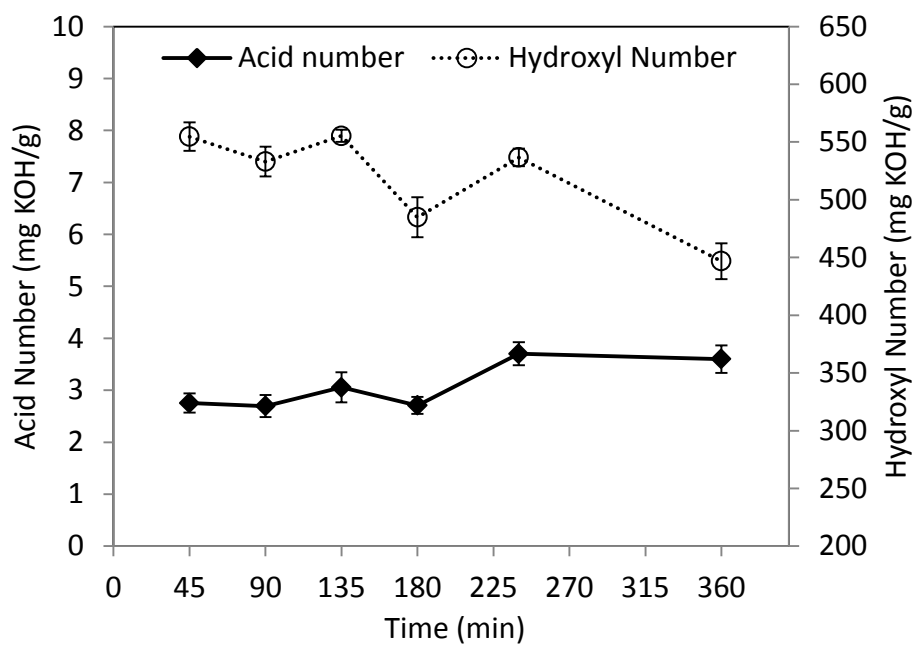


Figure 3.5: Effects of reaction time on polyol acid and hydroxyl numbers (Note: reaction temperature: 240 °C; sulfuric acid loading: 3 %; biomass loading: 10 %; each data point represents the mean of duplicate liquefaction)

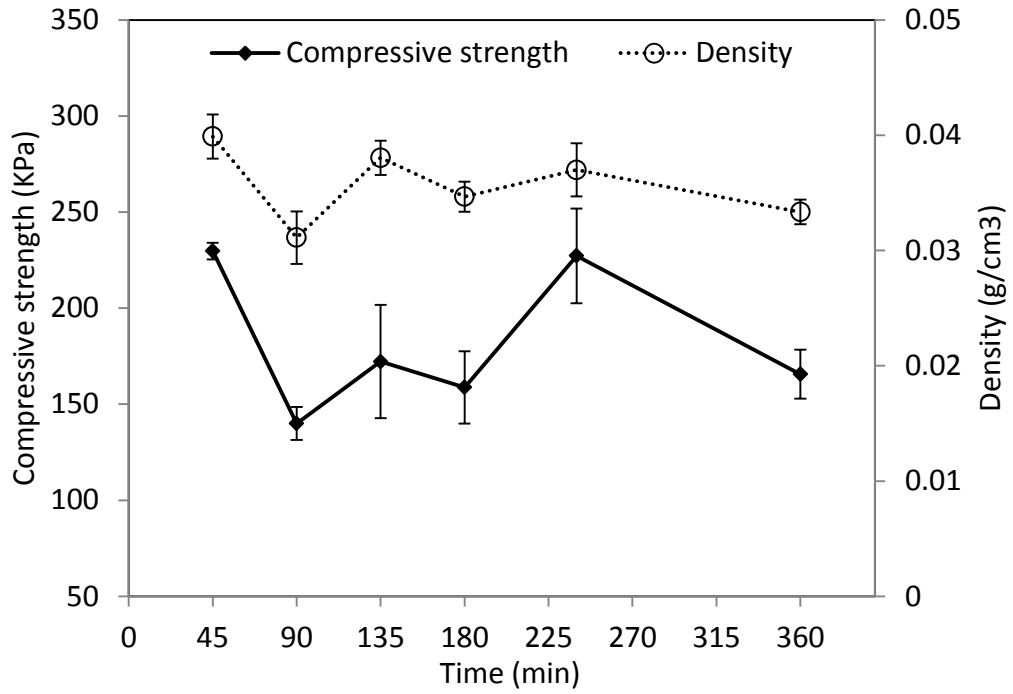


Figure 3.6: Effects of reaction time on compressive strength and density of PU foams (Note: reaction temperature: 240 °C; sulfuric acid loading: 3%; biomass loading: 10%; each data point represents the mean of duplicate liquefaction)

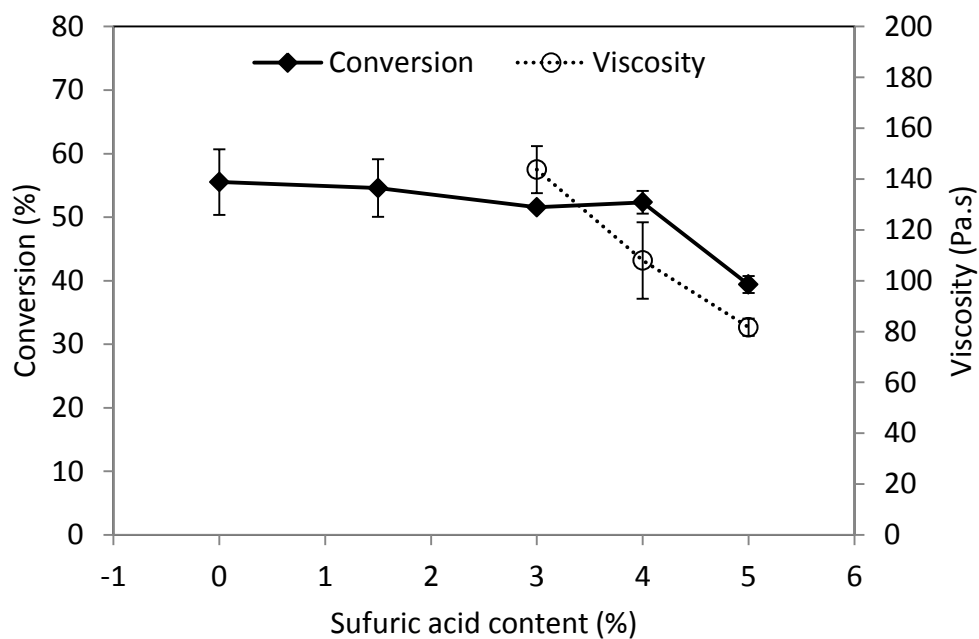


Figure 3.7: Effects of sulfuric acid loading on biomass conversion and polyol viscosity (Note: missing data with viscosity > 1,000 Pa.s; reaction temperature: 240 °C; reaction time: 90 min; biomass loading: 10 %; each data point represents the mean of duplicate liquefaction)

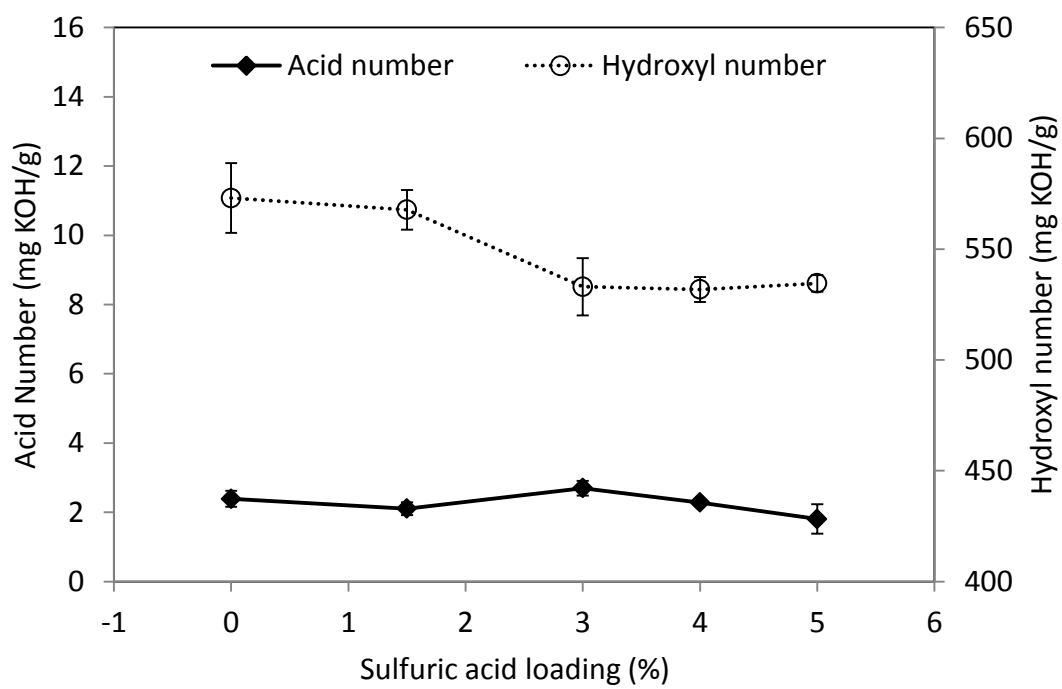


Figure 3.8: Effects of sulfuric acid loading on polyol acid and hydroxyl numbers (Note: reaction temperature: 240 °C; reaction time: 90 min; biomass loading: 10 %; each data point represents the mean of duplicate liquefaction)

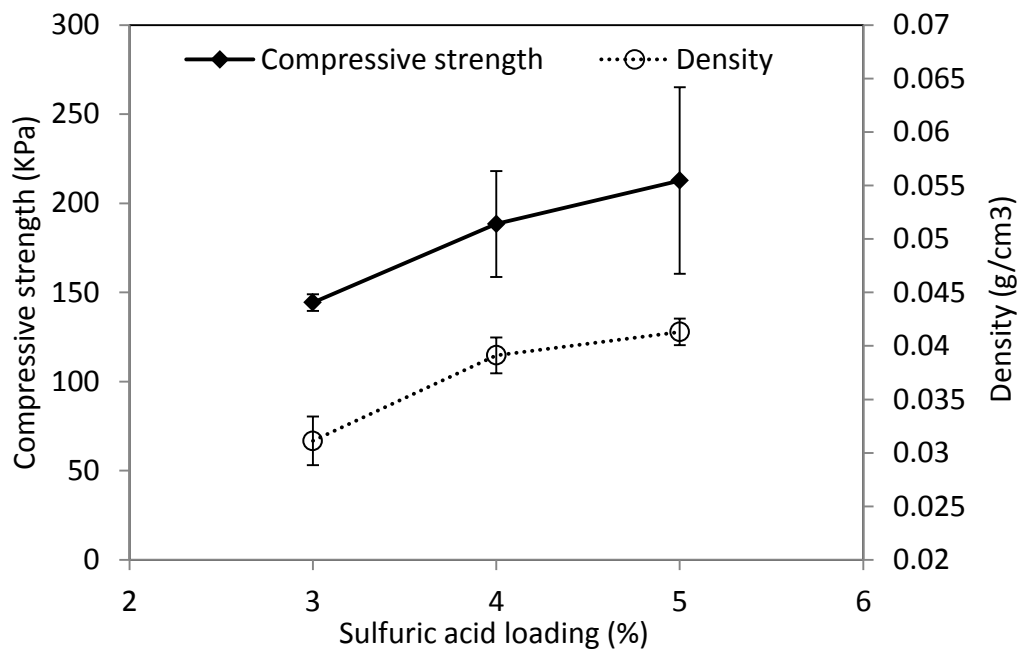


Figure 3.9: Effects of sulfuric acid loading on compressive strength and density of PU foams (Note: reaction temperature: 240 °C; reaction time: 90 min; biomass loading: 10 %; each data point represents the mean of duplicate liquefaction)

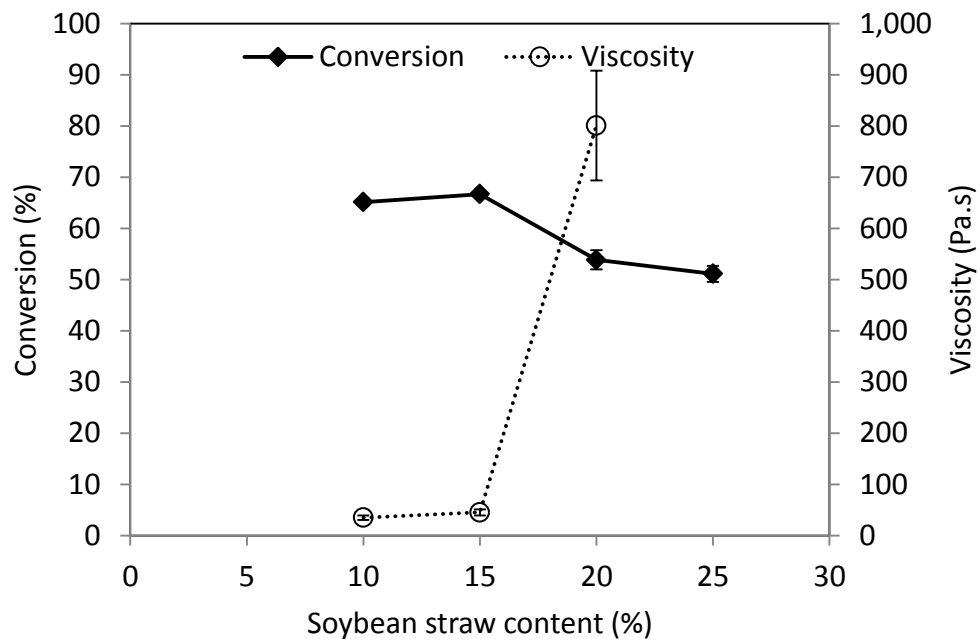


Figure 3.10: Effects of biomass loading on biomass conversion and polyol viscosity (Note: missing data with viscosity > 1,000 Pa·s; reaction temperature: 240 °C; reaction time: 180 min; sulfuric acid loading: 3 %; each data point represents the mean of duplicate liquefaction)

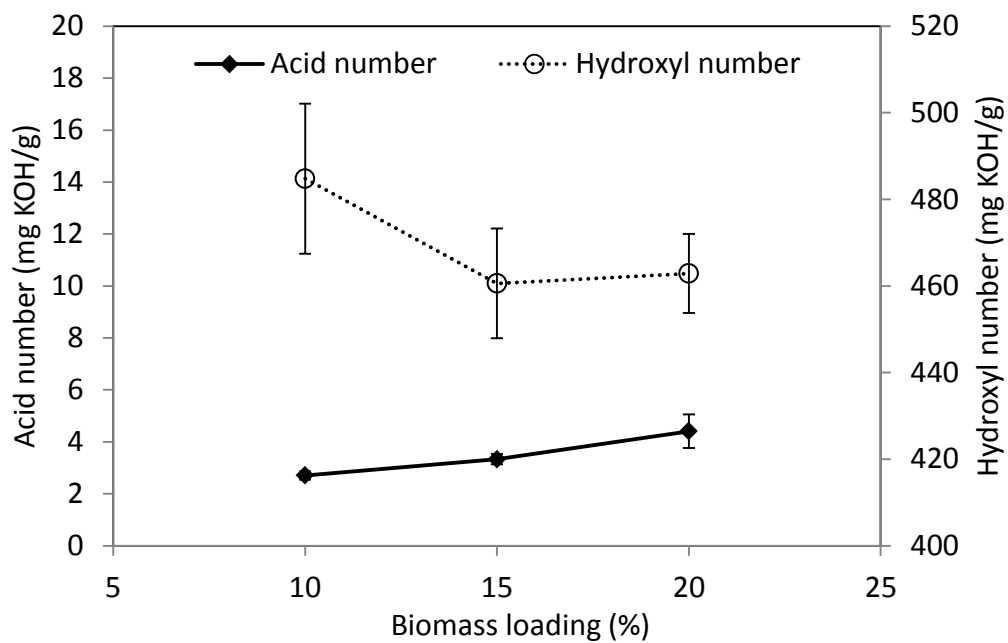


Figure 3.11: Effects of biomass loading on polyol acid and hydroxyl numbers (Note: reaction temperature: 240 °C; reaction time: 180 min; sulfuric acid loading: 3%; each data point represents the mean of duplicate liquefaction)

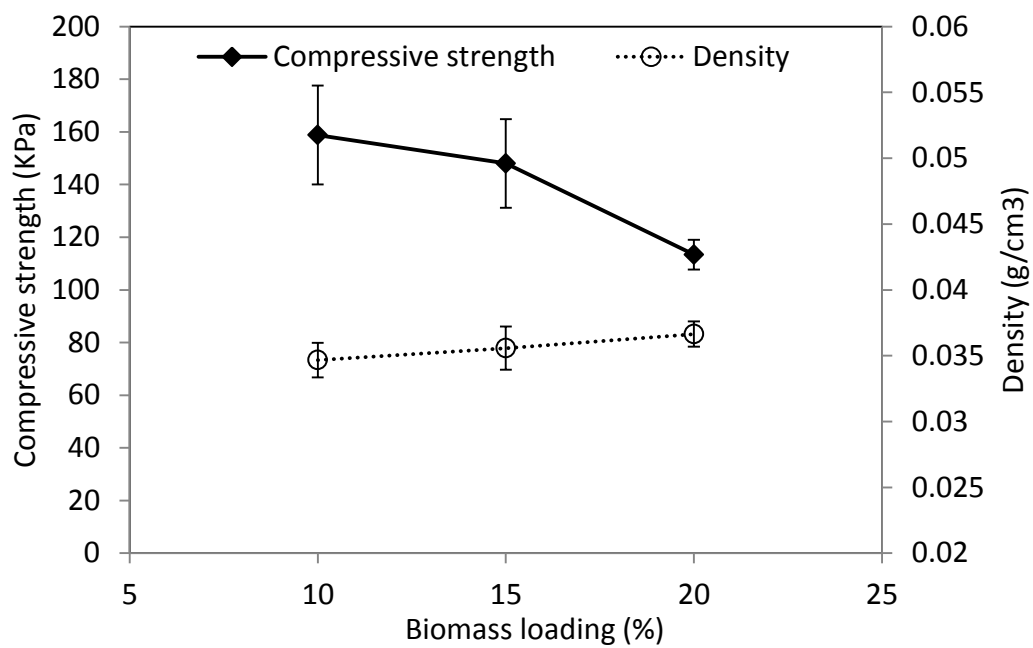


Figure 3.12: Effects of biomass loading on compressive strength and density of PU foams (Note: reaction temperature: 240 °C; reaction time: 180 min; sulfuric acid loading: 3 %; each data point represents the mean of duplicate liquefaction)

## **Chapter 4 Characterization of Crude Glycerol from Biodiesel Plants**

Characterization of crude glycerol is very important to its value-added conversion. In this study, the physical and chemical properties of five representative biodiesel-derived crude glycerol samples were determined. Three methods, including iodometric-periodic acid method, high performance liquid chromatography (HPLC), and gas chromatography (GC), were shown to be suitable for the determination of glycerol content in crude glycerol. The compositional analysis of crude glycerol was successfully achieved by crude glycerol fractionation and characterization of the obtained fractions (aqueous and organic) using titrimetric, HPLC, and GC analysis. The aqueous fraction consisted mainly of glycerol and methanol, while the organic fraction contained fatty acid methyl esters (FAMES), free fatty acids (FFAs), and glycerides. Despite the wide variations in the proportion of their components, all raw crude glycerol samples contained glycerol, soap, methanol, FAMES, water, glycerides, FFAs, and ash.

### **4.1 Introduction**

Currently, one of the major challenges for the utilization of crude glycerol is the inconsistency of its composition since it varies with the feedstocks, production processes, and post-processing treatments involved in biodiesel production. Upgrading or refining crude glycerol to technical grade glycerol (>98% glycerol content) makes its composition more consistent, but currently this is not economically-viable, especially for small- and/or

medium-size biodiesel plants (Manosak et al., 2011). Compared to the extensive research reports on the utilization of crude glycerol, there are few reports on the characterization of crude glycerol. Thompson and He (Thompson and He, 2006) characterized seven crude glycerol samples prepared, using the same production practices, from six different types of seed oil feedstocks and one waste cooking oil. Little variation existed, among the crude glycerol samples, in their physical and chemical properties, including viscosity, heat of combustion, glycerol, methanol, and elemental contents, and food nutrition values. Hansen et al. (2009) characterized eleven crude glycerol samples collected from different biodiesel plants in Australia. In contrast to the findings of Thompson and He, Hansen et al. showed that the properties of different crude glycerol samples, including pH and density, and chemical composition properties, including glycerol, moisture, ash, methanol and MONG, i.e. matter organic non-glycerol, contents of crude glycerol, varied significantly with each other, mostly likely caused by the different biodiesel production processes used.

In addition to the crude glycerol components determined in the above two studies, raw/unrefined crude glycerol from biodiesel plants also contains other components, such as soap, free fatty acids (FFAs), FAMES, and glycerides. The impurities present in crude glycerol significantly affect its properties and thus its value-added conversions. For example, soap and methanol have been found to negatively influence the algal production of DHA from crude glycerol (Pyle et al., 2008), and the high salinity (Na or K) of crude glycerol can inhibit microbial activity during anaerobic digestion (Santibanez et al., 2011). In addition, heavy metals in crude glycerol might be harmful and present safety

concerns especially in pharmaceutical and food applications (Pyle et al., 2008). In contrast, some studies indicated that certain crude glycerol impurities can improve the properties of crude glycerol-based products such as bio-oil (Xiu et al., 2010) and polyols and PU foams (Hu et al., 2012b). Therefore, when considering the significant effects of crude glycerol impurities on the value-added processing of crude glycerol, it is vital to first understand the chemical composition of crude glycerol.

To our knowledge, there has been no study dedicated to a comprehensive compositional analysis, i.e., identification of all chemical constituents, of biodiesel-derived crude glycerol. In this study, five representative crude glycerol samples were selected from a large number of crude glycerol samples obtained from different biodiesel plants. Crude glycerol was treated and fractionated into aqueous and organic fractions to better characterize its individual components. The main purposes of this study were to: (1) obtain a complete chemical compositional profile of biodiesel-derived crude glycerol; and (2) evaluate different analytical methods for the characterization of biodiesel-derived crude glycerol.

## **4.2 Materials and Methods**

### *4.2.1 Materials*

Five crude glycerol samples (soybean oil-based: CG-Soy1, CG-Soy2, and CG-Soy3; waste vegetable oil-based: CG-WV; soybean oil-waste vegetable oil mixture based: CG-SW) were provided by Bio100 Technologies, LLC. (Mansfield, OH). Chemicals purchased from Fisher Scientific (Pittsburgh, PA) included bromophenol blue (sodium

salt), potassium iodide, potassium hydroxide, phenolphthalein, periodic acid, pure glycerol, trace metal grade HNO<sub>3</sub>, concentrated HCl (35-38% wt.), standard HCl (0.1 N), NaOH (1 N), Na<sub>2</sub>S<sub>2</sub>O<sub>3</sub> (1 N), 0.1% w/v methyl orange, and 1% w/v starch indicator solution. Chemicals purchased from Sigma Aldrich (St. Louis, MO) included anhydrous hexane, anhydrous Na<sub>2</sub>SO<sub>4</sub>, methyl heptadecanoate, standard FAME mix (GLC-10), HPLC grade H<sub>2</sub>SO<sub>4</sub> (50% wt.), and 10% wt. BF<sub>3</sub>-methanol. Chloroform, glacial acetic acid, ethanol, methanol, and petroleum ether were purchased from Pharmco-AAPER (Shelbyville, KY). Standard stock solutions of monoolein, diolein, triolein, 1,2,4-butanetriol, tricaprins, and derivatization reagent N-methyl-N-trimethylsilyltrifluoroacetamide (MSTFA) were purchased from Restek (Bellefonte, PA). All chemicals used were of reagent grade or higher purity.

#### *4.2.2 Physical properties*

The density of crude glycerol was determined by measuring the volume and weight of crude glycerol at room temperature ( $23 \pm 0.5$  °C). For pH determination, crude glycerol ( $1.00 \pm 0.1$  g) was dissolved in 50 ml of deionized (DI) water and the pH of the solution was measured by a digital pH meter (Oakton pH 11 series, South Burlington, VT) at room temperature ( $23 \pm 0.5$  °C). The viscosity of crude glycerol was measured at  $25 \pm 0.5$  °C according to ASTM D 4878-08 using a Brookfield DV II+Pro viscometer equipped with a small sample adapter, a temperature probe, and a temperature control unit (Brookfield Engineering Laboratories, Inc., Middleboro, MA).

#### *4.2.3 Soap content determination*

The soap content of crude glycerol was determined with reference to AOCS Recommended Practice Cc 17-95 and ASTM D 4662-08. Briefly, the unadjusted soap content of crude glycerol was determined according to AOCS Recommended Practice Cc 17-95. The alkalinity of crude glycerol was determined according to ASTM D 4662-08 and used to adjust the soap content. The adjusted soap content of crude glycerol was calculated as:

Soap as sodium oleate, % =  $(V_s - V_a) \times N \times 30.44/W$ , where

$V_s$ : ml of titrant consumed, soap titration

$V_a$ : ml of titrant consumed, alkalinity titration

N: normality, HCl solution

W: mass (g) of crude glycerol weighed

#### *4.2.4 Water and ash content determination*

The water content of crude glycerol was determined by volumetric Karl Fischer titration using a T70 automatic titration system (Mettler Toledo, Columbus, OH) with reference to AOCS Official Method Ea 8-58. The ash content of crude glycerol was determined by burning approximately 1 g of sample in a furnace at 750 °C for 3 h (Manosak et al., 2011).

#### *4.2.5 Elemental analysis*

The carbon (C) and nitrogen (N) contents of crude glycerol were determined by VarioMax CNS analyzer (Mt. Laurel, NJ). Elements including Na, Mg, Al, P, K, Ca, Mn, Fe, Co, Cu, and Zn were determined by ICP-MS (Agilent Technologies ICP-MS 7500 series, Santa Clara, CA). Crude glycerol (0.2-0.5 g) was digested using 10 ml of trace metal grade HNO<sub>3</sub> in a microwave digester (MARSXpress<sup>TM</sup>, CEM Corporation, Matthews, NC). The digester temperature was ramped to 200 °C in 15 min, maintained at 200 °C for 15 min, and cooled down to 25 °C. The digested crude glycerol solution was transferred into a 500-ml volumetric flask and filled to mark using Mini-Q water (Synergy UV, Millipore Corp., Billerica, MA). The solution was mixed and analyzed using ICP-MS.

#### *4.2.6 Glycerol content determination by iodometric-periodic acid method*

The determination of free glycerol content by iodometric-periodic acid method was conducted with reference to AOCS Official Method Ca 14-56.

#### *4.2.7 Fractionation of crude glycerol*

Crude glycerol was fractionated into aqueous and organic fractions according to the procedures shown in Figure 4.1. For fractionation without saponification, a crude glycerol sample was weighed and well-dissolved in 50 ml of DI water in a 120-ml pressure tube (pressure rating: 1 MPa, ACE Glass Inc. Vineland, NJ). The solution was then acidified and fractionated with reference to AOCS Official Method G 3-53: briefly, complete conversion of soap in crude glycerol to FFAs was achieved by acidifying the

crude glycerol solution using 5 ml of 1:1 (v:v) HCl solution, and then the organic fraction was recovered by petroleum ether extraction. To ensure the complete recovery of organic fraction, petroleum ether extraction was repeated until the top petroleum ether layer became colorless. The organic fraction was obtained after the removal of petroleum ether by rotary-evaporation (Laborota efficient 4001, Heidolph, Schwabach, Germany) and vacuum-drying until constant weight (Isotemp 282A, Fish Scientific, Pittsburgh, PA). For fractionation with saponification, a crude glycerol sample was weighed into a 120-ml pressure tube (ACE Glass Inc. Vineland, NJ) and dissolved in 10 ml of 50 g/l KOH-ethanol solution. The tight-capped tube was heated in an oil bath at 90 °C for 1 h with constant magnetic stirring (200 rpm). Upon completion, the tube was removed from the bath and cooled to room temperature ( $23 \pm 0.5$  °C) in a fume hood, followed by the addition of 50 ml of DI water. The solution was then acidified and fractionated using the procedures as described above. All aqueous and organic fractions obtained from the fractionation of crude glycerol were kept for later analyses.

#### *4.2.8 HPLC analysis of glycerol and methanol*

The free glycerol and methanol contents of crude glycerol were determined by HPLC analysis using aqueous fractions obtained from crude glycerol fractionation without saponification. The total glycerol content of crude glycerol was determined by HPLC analysis using aqueous fractions obtained from crude glycerol fractionation with saponification. Each sample was filtered and analyzed using a LC-20 AB HPLC system (Shimadzu, Columbia, MD) equipped with a RID-10A refractive index detector and a RFQ-Fast Fruit H+ (8%) column (Phenomenex, Torrance, CA). The mobile phase used

was 0.005 N H<sub>2</sub>SO<sub>4</sub> at a flow rate of 0.6 ml/min. The column and RID temperatures were maintained at 60 °C and 55 °C, respectively. The injection volume was 10 µl. An external calibration curve was constructed by analyzing standard glycerol and methanol solutions at different concentration levels.

#### *4.2.9 GC analysis of glycerides, glycerol, FAMES, and FFAs*

The free glycerol in crude glycerol, the FAMES and glycerides in organic fractions obtained without saponification, and the fatty acid profiles of the free fatty acids (FFAs) in organic fractions obtained with saponification, were determined by gas chromatography (GC) using a Shimadzu GC-2010 plus GC system (Shimadzu, Columbia, MD) equipped with a flame ionization detector (FID). The GC analysis of glycerides was conducted according to ASTM D6584-10a.

The GC analysis of free glycerol content was conducted as follows: weighed crude glycerol (40-100 mg) was acidified by 100 µl 1:1 HCl (v/v) and then dissolved in 10 ml of pyridine in a 15-ml glass test tube (Pyrex, Corning, NJ). Then, an aliquot (20-100 µl) of the obtained solution and 100 µl of 1,2,4-butanetriol standard solution (0.89 mg/ml, internal standard) were mixed and derivatized by MSTFA (100 µl) at 38 °C for 15 min. The sample was then filtered and injected at an injection volume of 1 µl into a MXT-Biodiesel TG column (14 m, 0.53 mm, 0.16 µm, Restek, Bellefonte, PA). Helium was used as the carrier gas at a flow rate of 3 ml/min. The injector and column temperatures were ramped from 50 to 110 °C at 5 °C/min with the detector temperature maintained constant at 380 °C. A calibration curve was constructed by analyzing pure

glycerol at different concentration levels.

For FAME analysis, the organic fraction sample (without saponification) was weighed (20-50 mg) and dissolved in 5 ml of anhydrous hexane in a 15-ml glass test tube (Pyrex, Corning, NJ). An aliquot of the obtained solution and 100  $\mu$ l of methyl heptadecanoate standard solution (internal standard) were mixed and filtered through a PTFE filter (porosity: 0.22 $\mu$ m; diameter: 13mm, Fisher Scientific, Pittsburgh, PA) into a 1.5-ml GC vial. Each sample (1  $\mu$ l) was injected into a Stabliwax-DA column (30 m, 0.32 mm id, 0.5  $\mu$ m df, Restek, Bellefonte, PA) at an injection temperature of 200 °C. The column temperature was ramped from 100 to 250 °C at 5 °C/min with detector temperature maintained constant at 250 °C. Helium was used as the carrier gas at a flow rate of 1 ml/min. The calibration curve was constructed by analyzing standard FAME solution at different concentration levels.

The fatty acid profiles of the FFAs in organic fractions (with saponification) were analyzed as follows: sample (60-150 mg) was weighed into a Teflon-capped test tube, followed by the addition of 2 ml of 10% w/w BF<sub>3</sub>-Methanol. The tube was heated in a water bath maintained at 60 °C for 15 min, after which 1 ml of hexane and 1 ml of water were added. The top hexane phase containing methyl esters derivatives of FFAs was analyzed by GC according to the FAME analysis procedure described above.

#### *4.2.10 Titrimetric determination of FFA content*

The FFA contents of crude glycerol and of organic fractions (without and with saponification) were determined with reference to AOCS Official Method Ca 5a-40.

#### *4.2.11 Statistical analysis*

Statistical analysis of the obtained data was conducted by IBM SPSS Statistics 19 (Armonk, NY). The significance of the difference between samples was tested by ANOVA procedure at  $\alpha=0.05$ .

### **4.3 Results and Discussion**

#### *4.3.1 Physical properties of crude glycerol*

The density of five crude glycerol samples varied from 1.01 and 1.20 g/cm<sup>3</sup>, lower than that of pure glycerol (1.31 g/cm<sup>3</sup>) (Table 4.1), due to the presence of some lighter impurities such as fatty acids methyl esters (FAMES), fatty acids, methanol, and water in crude glycerol. All samples, except CG-Soy1, had pH values close to 10 because of residual alkalis such as NaOH or KOH left from the biodiesel production process. CG-Soy1 had a lower pH value (6.9) close to that of pure glycerol (6.4) due to the removal of residual alkalis by post-processing treatment in the biodiesel plant. The pH values of the eleven crude glycerol samples from different biodiesel plants in Australia varied from 2.0 to 10.8 (Hansen et al., 2009). The viscosities of our five crude glycerol samples ranged from 15 to 1213 mPa·s, due to their different compositions. Waste vegetable oil-based crude glycerol (CG-WV) had the highest viscosity of 1213 mPa·s.

#### *4.3.2 Comparative glycerol determination in crude glycerol*

The quantification of glycerol can be achieved by a variety of analytic techniques such as titrimetric method, HPLC, and GC (Pyle et al., 2008; AOCS Ca 14-56, 1997;

ASTM D6584-10a, 2010). The free glycerol content of CG-WV determined by the iodometric-periodic acid method, HPLC, and GC was 27.6, 27.9, and 27.4 %, respectively (Table 4.2), which were comparable to each other. The relative standard deviations (% *RSD*) of all three methods were below 2%. Therefore, all following glycerol contents reported were determined by HPLC since it allows the simultaneous determination of glycerol and methanol in crude glycerol.

#### 4.3.3 *Glycerol and methanol in crude glycerol*

A representative HPLC chromatogram for the determination of glycerol and methanol in crude glycerol indicates that the separation and elution of glycerol and methanol were achieved within 10 min (Figure 4.2). During the saponification process, glycerides in crude glycerol, if any, were converted to glycerol and soap (Figure 4.3 (b)). Therefore, the glycerol in aqueous fractions with saponification included not only the free glycerol that originally existed in crude glycerol but also the combined glycerol released from glycerides by saponification. The free glycerol contents of the five crude glycerol samples varied widely from 22.9 to 63.0% (Table 4.3). The glycerol contents of the eleven crude glycerol samples obtained from different biodiesel plants in Australia varied from 38.4 to 96.5% (Hansen et al., 2009). In contrast, the glycerol contents of the crude glycerol prepared in the lab using seven different seed oils were much more consistent, ranging from 62.5 to 76.6 % (Thompson and He, 2006). For all crude glycerol samples, except CG-WV, the total glycerol contents were close to their respective free glycerol contents (Table 4.3). A statistical analysis showed that there were no significant differences ( $p > 0.05$ ) between these two types of glycerol contents, indicating the low

contents of combined glycerol, i.e., glycerides, in crude glycerol. CG-WV had a total glycerol content (28.9 %) slightly higher than its free glycerol content (27.9 %), indicating its higher content of glycerides, compared to the other samples.

The methanol contents of five crude glycerol samples varied widely from 6.2 to 12.6 % (Table 4.3). During the biodiesel production process, an excess of methanol is usually used to increase biodiesel yield (Ma and Hanna, 1999). After the production process, excess methanol is generally recovered by a distillation process (Hajek and Skopal, 2010). The residual methanol in crude glycerol varies with the methanol inputs and the recovery efficiencies in different biodiesel plants.

#### *4.3.4 FFAs, FAMES, and glycerides in organic fractions*

The organic fractions of crude glycerol obtained without saponification varied from BDL (below detection limit) to 55.8 % (Table 4.3). CG-Soy1 had no detectable levels of organic fraction because it had been refined to remove most of its organic impurities. Figure 4.4 and 4.5 show representative GC chromatograms for the determination of FAMES and glycerides in the obtained organic fractions, respectively. The FFA contents of the organic fractions of four crude glycerol samples ranged between 35.7 and 96.4 % (Table 4.4). The FFAs determined in organic fractions included not only FFAs originally existed in crude glycerol but also those converted from soap by acidification (Figure 4.3(c)) (Pyle et al., 2008; Xiu et al., 2010). The existence of soap in crude glycerol can be attributed to the occurrence of saponification, an unfavorable side reaction, during the biodiesel production process (Ma and Hanna, 1999). The total FAME contents (sum of all individual methyl esters) of the organic fractions of four crude

glycerol samples ranged between 5.2 and 51.6 %. The presence of FAMES in crude glycerol was most likely caused by the incomplete separation between ester and glycerol layers during the biodiesel production process (Ma and Hanna, 1999). Compared to FFAs and FAMES, glycerides were at low levels (<5 %) in organic fractions, except for CG-WV (12.6%). The low glyceride contents of CG-Soy2, CG-Soy3, and CG-SW corresponded well with the above results that the free glycerol contents were similar to the total glycerol contents (Table 4.3).

For crude glycerol fractionation with saponification, the obtained organic fractions of five crude glycerol samples varied between BDL to 52.3 % (Table 4.3). The organic fractions consisted almost entirely of FFAs (data not shown). Therefore, the saponification treatment significantly changed the composition of the obtained organic fractions. This is probably because the saponification process converted FAMES and/or glycerides in crude glycerol to soap and other compounds and the soap was further converted to FFAs by acidification (Figure 4.3). The saponification process also lowered the organic fraction in CG-Soy2, CG-Soy3, and CG-WV compared to non-saponified samples (Table 4.3), due to the weight losses of organic fractions associated with the conversion of FAMES and/or glycerides to FFAs. CG-SW showed no significant difference between the contents of these two types of organic fractions (Table 4.3) due to its low contents of FAMES and glycerides (Table 4.4). The fatty acid profile analyses of the FFAs in organic fractions showed that all samples had high contents of oleic (23.3 to 35.2 %), linoleic (25.6 to 46.8 %), and palmitic acids (10.0 to 12.9 %) (Table 4.5), which were similar to the fatty acid profiles of soybean and some other vegetable oils (Petrovic,

2008).

#### *4.3.5 Elemental analysis*

The C and N content of five crude glycerol samples ranged from 24.3 to 54.2% and from 0.3 to 1.2 %, respectively (Table 4.6). The C and N content of seven crude glycerol samples prepared in lab ranged from 24.0 to 37.7 % and 0.04 to 0.12 %, respectively (Thompson and He, 2006). The higher C content of crude glycerol obtained in this study can be explained by the higher contents of certain impurities in crude glycerol such as soaps, FAMES, and glycerides, which have higher C contents than glycerol. The high content of K in CG-SW and Na in CG-Soy1, CG-Soy2, CG-Soy3, and CG-WV can be attributed to the use of K- and Na-based alkalis, respectively, during the biodiesel production process (Ma and Hanna, 1999).

#### *4.3.6 Soap, water, and ash in crude glycerol*

The soap contents of all crude glycerol samples, except CG-Soy1, were relatively high (20.5 to 31.4 %), while all crude glycerol samples had low FFA contents ( $\leq 3.0\%$ ) (Table 4.7). This indicates that the FFAs in organic fractions (without saponification, Table 4.4) were mainly derived from the acidification of the soap that existed in crude glycerol. The water and ash contents of the five crude glycerol samples ranged from 1.0 to 28.7 % and from 2.7 to 5.7 %, respectively. In addition, for all crude glycerol samples, the sums of soap, FAMES, and glyceride content of crude glycerol (Table 4.7) were higher than their respective organic fractions (Table 4.3) that consisted of FFAs, FAMES, and glycerides. This is because the soap was converted to FFAs during the acidification

process (Figure 4.3(c)): soap has a higher molecular weight than its corresponding FFA, and thus the weight of obtained organic fractions were lower than the sum of soap, FAMEs, and glycerides in crude glycerol.

#### *4.3.7 Composition of crude glycerol*

The chemical compositions of all crude glycerol samples, except the CG-Soy1 (partially refined), were aptly described by eight components, i.e., glycerol, methanol, water, soap, FAMEs, glycerides, FFAs, and ash (Table 4.7). The glycerol, methanol, FAMEs, soap, and water in total accounted over 85% of the mass of crude glycerol, while the total of glycerides, FFAs, and ash was generally less than 15% (Table 4.7). The compositions of the five crude glycerol samples varied significantly; for example, glycerol contents ranged from 22.9 to 63.0 %. Therefore, it is necessary to characterize the composition of each crude glycerol before considering it for value-added conversions.

#### **4.4 Conclusions**

The physical and chemical properties of five biodiesel-derived crude glycerol samples, from different biodiesel plants, were successfully determined by using a combination of analytical techniques. Glycerol content in the five crude glycerol samples ranged widely from 22.9 to 63.0 %. Compositional analyses showed that unpurified crude glycerol samples contain non-glycerol impurities including water, methanol, FAMEs, soap, FFAs, glycerides, and ash. The proportions of these compounds in crude glycerol varied widely with different biodiesel plants. For some crude glycerol samples, the contents of impurity compounds even exceeded that of glycerol, and the effects of

these impurities should be taken into consideration during the development of any value-added processes for crude glycerol.

Table 4.1: Physical properties of crude glycerol<sup>a</sup>

Samples	Density (g/cm <sup>3</sup> )	pH	Viscosity (mPa·s)
CG-Soy1	1.20 ± 0.01	6.9 ± 0.0	15 ± 0.1
CG-Soy2	1.02 ± 0.02	9.7 ± 0.0	162 ± 11
CG-Soy3	1.01 ± 0.00	9.5 ± 0.0	110 ± 7
CG-WV	1.01 ± 0.00	9.4 ± 0.0	1213 ± 129
CG-SW	1.11 ± 0.01	10.0 ± 0.0	838 ± 28
Pure glycerol	1.31 ± 0.00	6.4 ± 0.0	930 ± 12

a: data expressed as mean of three replicates ± standard deviation;

Table 4.2: Comparative determination of the free glycerol content of CG-WV

Replicates	Glycerol content (wt. %)		
	iodometry <sup>d</sup>	HPLC	GC
1	27.5	27.7	27.5
2	28.1	27.9	27.7
3	26.9	27.8	27.2
4	28.3	27.9	27.5
5	27.0	28.3	27.6
6	27.8	27.8	26.9
7	27.9	28.0	27.3
Mean <sup>a</sup>	27.6	27.9	27.4
Std. <sup>b</sup>	0.5	0.2	0.3
RSD <sup>c</sup> (%)	1.9	0.7	1.0

a: mean of three replicates; b: standard deviation; c: relative standard deviation; d: iodometric-periodic method

Table 4.3: Glycerol, methanol, and organic fraction contents of crude glycerol<sup>a</sup>

Samples	Without Saponification		With Saponification		Methanol (wt. %)
	Free Glycerol (wt. %)	Organic fraction <sup>b</sup> (wt. %)	Total Glycerol (wt. %)	Organic fraction (wt. %)	
CG-Soy1	63.0 ± 0.3	BDL <sup>c</sup>	63.3 ± 0.7	BDL	6.2 ± 0.0
CG- Soy2	22.9 ± 0.2	45.0 ± 0.3	22.9 ± 0.1	43.1 ± 0.5	10.9 ± 0.2
CG- Soy3	33.3 ± 0.1	43.4 ± 0.7	33.3 ± 0.3	40.5 ± 0.5	12.6 ± 0.1
CG-WV	27.9 ± 0.2	55.8 ± 0.7	28.9 ± 0.6	52.3 ± 0.3	8.6 ± 0.0
CG-SW	57.1 ± 0.0	26.1 ± 0.5	57.3 ± 0.6	26.0 ± 0.1	11.3 ± 0.0

a: data expressed as mean of three replicates ± standard deviation; b: mainly consist of FAMES, FFAs, and glycerides; c: below detection limit.

Table 4.4: Composition of organic fractions obtained without saponification<sup>a</sup>

Samples <sup>b</sup>	CG-Soy2	CG-Soy3	CG-WV	CG-SW	
FFAs (wt. %)	50.0 ± 0.2	51.6 ± 0.1	35.7 ± 0.6	96.4 ± 0.4	
Glycerides <sup>c</sup> (wt. %)	Mono-	1.6 ± 0.1	2.2 ± 0.4	5.2 ± 0.3	0.7 ± 0.0
	Di-	1.1 ± 0.2	1.6 ± 0.1	7.4 ± 3.3	0.9 ± 0.0
FAMES (wt. %)	Palmitate	4.9 ± 0.2	4.5 ± 0.1	6.9 ± 0.2	0.3 ± 0.1
	Stearate	1.8 ± 0.1	1.5 ± 0.1	2.8 ± 0.2	BDL <sup>e</sup>
	Oleate	14.0 ± 0.5	11.0 ± 0.2	14.7 ± 0.6	0.8 ± 0.2
	Linoleate	14.8 ± 0.6	14.2 ± 0.4	12.7 ± 0.7	2.7 ± 0.0
	Linolenate	1.9 ± 0.2	2.0 ± 0.1	1.3 ± 0.1	1.4 ± 0.7
	Others <sup>d</sup>	9.9 ± 1.3	11.3 ± 0.7	13.2 ± 2.5	BDL

a: data expressed as mean of three replicates ± standard deviation and all percentages were expressed on the weight basis of organic fractions; b: CG-Soy1 not listed because of no detectable organic fractions; c: triglycerides below detection limit for all CG samples; d: balance after quantification of FFAs, glycerides, and five common FAMES; e: below detection limit.

Table 4.5: Composition of organic fractions obtained with saponification<sup>a</sup>

Samples	CG-Soy2	CG-Soy3	CG-WV	CG-SW
Palmitic acid (wt.%)	12.9 ± 1.0	10.4 ± 1.4	14.1 ± 0.5	10.0 ± 1.7
Stearic acid (wt.%)	4.6 ± 0.6	3.5 ± 0.8	6.3 ± 0.1	1.2 ± 0.3
Oleic acid (wt.%)	35.2 ± 2.7	25.9 ± 3.9	29.3 ± 0.3	23.3 ± 4.1
Linoleic acid (wt.%)	37.6 ± 2.9	36.0 ± 3.4	25.6 ± 1.5	46.8 ± 8.6
Linolenic acid (wt.%)	4.0 ± 1.1	4.5 ± 1.1	2.1 ± 1.0	1.2 ± 0.2
Others <sup>b</sup> (wt.%)	5.7 ± 3.3	19.7 ± 4.1	22.7 ± 1.0	17.5 ± 7.5

a: data expressed as mean of three replicates ± standard deviation; b: balance after quantification of five common FAMES;

Table 4.6: Elemental analysis of crude glycerol <sup>a</sup>

Samples	CG-Soy1	CG-Soy2	CG-Soy3	CG-WV	CG-SW
C (wt. %)	24.3 ± 0.2	44.3 ± 0.4	46.8 ± 0.4	54.2 ± 0.1	42.5 ± 0.3
N (wt. %)	0.3 ± 0.1	0.6 ± 0.1	0.7 ± 0.1	0.9 ± 0.3	1.2 ± 0.1
Na (wt. %)	1.2 ± 0.2	1.9 ± 0.3	1.9 ± 0.2	1.6 ± 0.2	<0.01
K (wt. %)	0.01 ± 0.003	0.01 ± 0.002	0.1 ± 0.01	0.05 ± 0.01	3.9 ± 0.3
P (ppm)	38.7 ± 4.8	101.3 ± 15.5	24.7 ± 8.8	233.8 ± 33.6	BDL
Ca (ppm)	BDL <sup>b</sup>	8.4 ± 3.7	4.0 ± 4.8	20.5 ± 9.5	17.4 ± 2.4
Mg (ppm)	BDL	3.7 ± 0.6	BDL	14.2 ± 3.0	BDL
Fe (ppm)	31.6 ± 19.0	34.2 ± 12.0	52.8 ± 24.9	92.1 ± 33.0	37.4 ± 15.6

a: data expressed as mean of three replicates ± standard deviation; Al, Mn, Co, Cu, and Zn were determined to be below detection limit and not listed; b: below detection limit.

Table 4.7: Composition of crude glycerol<sup>a</sup>

Samples	CG-Soy1	CG-Soy2	CG-Soy3	CG-WV	CG-SW
Glycerol (wt. %)	63.0 ± 0.3	22.9 ± 0.2	33.3 ± 0.1	27.8 ± 0.2	57.1 ± 0.0
Methanol (wt. %)	6.2 ± 0.0	10.9 ± 0.2	12.6 ± 0.1	8.6 ± 0.0	11.3 ± 0.0
Water (wt. %)	28.7 ± 0.3	18.2 ± 0.1	6.5 ± 0.1	4.1 ± 0.1	1.0 ± 0.1
Soap (wt. %)	BDL	26.2 ± 0.2	26.1 ± 0.1	20.5 ± 0.1	31.4 ± 0.1
FAMES <sup>b</sup> (wt. %)	BDL	21.3 ± 0.2	19.3 ± 0.3	28.8 ± 1.1	0.5 ± 0.1
Glycerides <sup>b</sup> (wt. %)	BDL	1.2 ± 0.2	1.6 ± 0.3	7.0 ± 0.5	0.4 ± 0.1
FFAs <sup>c</sup> (wt. %)	BDL	1.0 ± 0.1	1.4 ± 0.1	3.0 ± 0.1	BDL
Ash (wt. %)	2.7 ± 0.1	3.0 ± 0.0	2.8 ± 0.1	2.7 ± 0.0	5.7 ± 0.2
Total (wt. %)	100.6	104.8	103.7	102.7	107.5

a: data expressed as mean of three replicates ± standard deviation; b: glycerides and FAMES contents determined from their known contents in organic fraction (Table 4.4) and the contents of organic fraction in crude glycerol (Table 4.3); c: FFAs originally existed in crude glycerol, not including those converted from soap acidification.

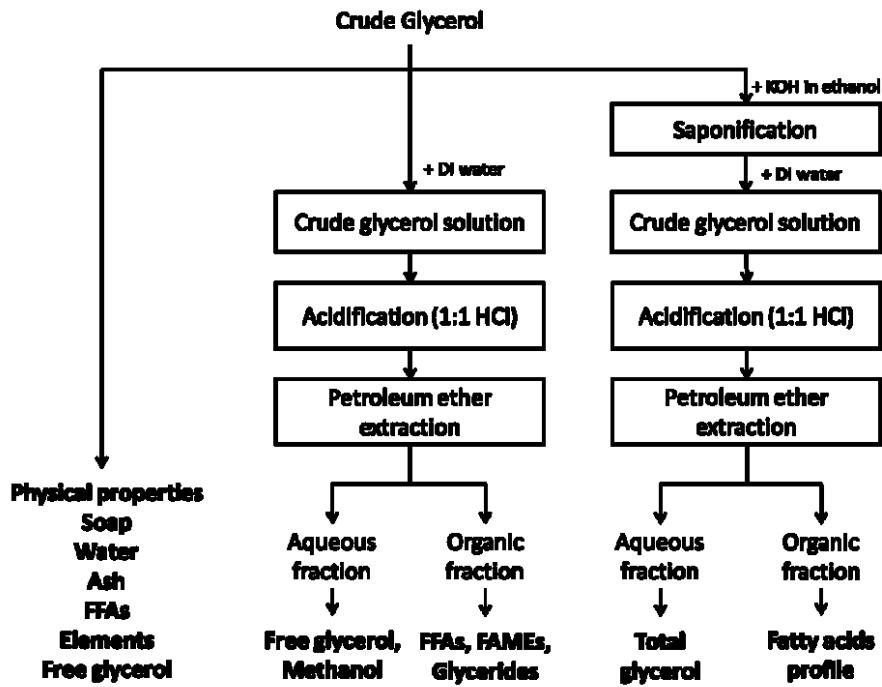


Figure 4.1: Scheme of crude glycerol fractionation and characterization

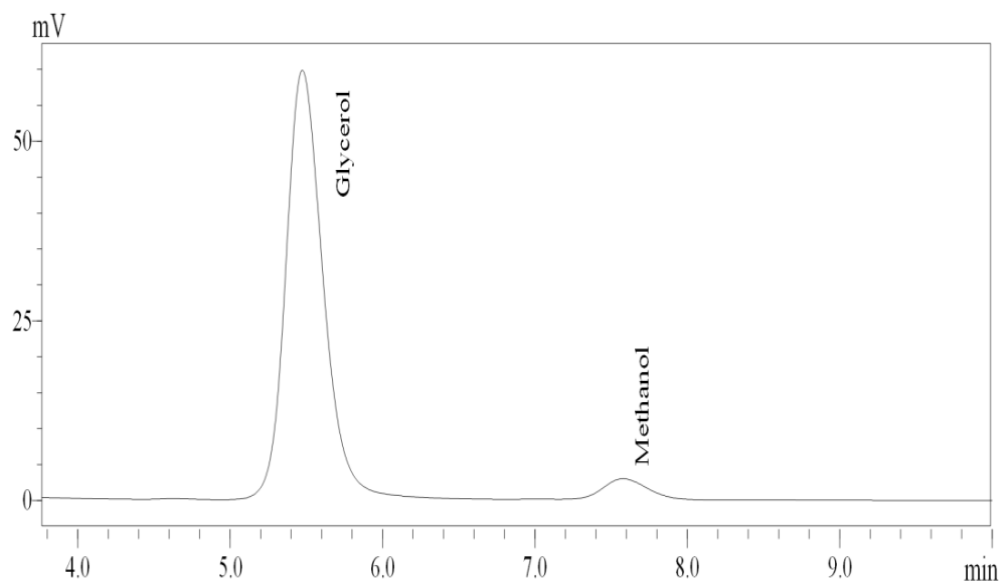


Figure 4.2: Representative HPLC chromatogram for the determination of glycerol and methanol in crude glycerol

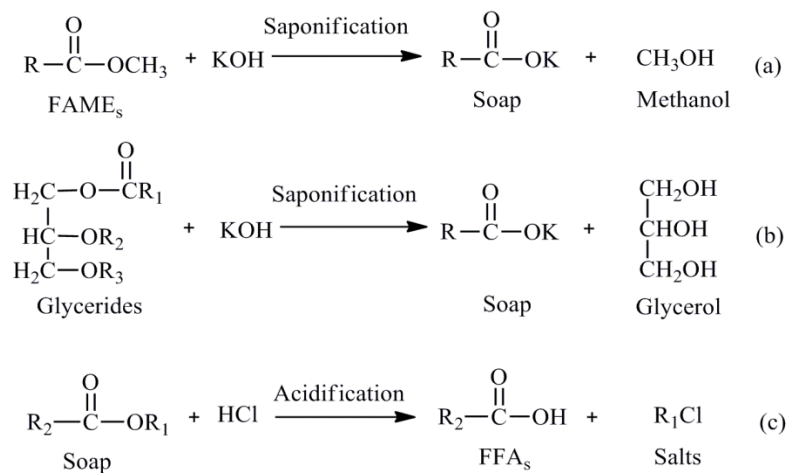


Figure 4.3: Chemical reactions occurring in crude glycerol fractionation processes: (a):  $R$ : aliphatic tails; (b):  $R_1$ : aliphatic tails;  $R_2$  and  $R_3$ : -H or -COR ( $R$ : aliphatic tails); (c):  $R_1$ : Na or K;  $R_2$ : aliphatic tails

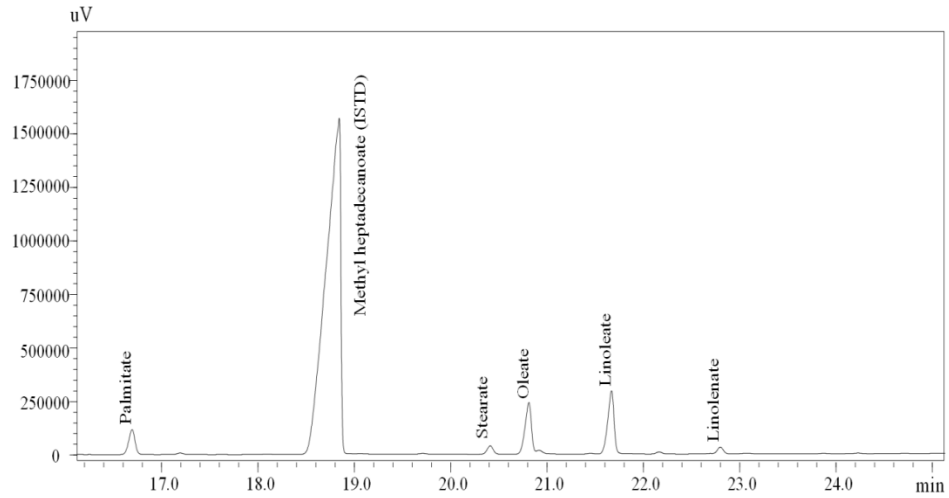


Figure 4.4: Representative GC chromatogram for the determination of FAMES in organic fractions obtained without saponification

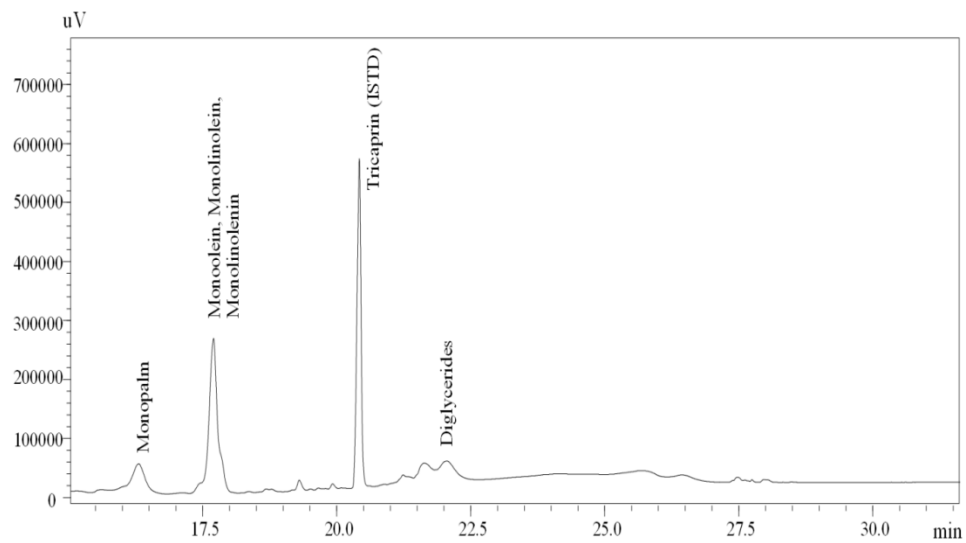


Figure 4.5: Representative GC chromatogram for the determination of glycerides in organic fractions obtained without saponification

## **Chapter 5 Effects of Crude Glycerol Impurities on the Properties of Base-catalyzed Liquefaction-derived Polyols and PU Foams**

The effects of various crude glycerol impurities on the properties of polyols and PU foams derived from base-catalyzed biomass liquefaction were investigated. Inorganic salts, including NaCl and Na<sub>2</sub>SO<sub>4</sub>, had no significant effects on biomass conversion and the hydroxyl numbers of polyols. Organic impurities, including FFA, FAMEs, and glycerides, significantly affected the properties of polyols and PU foams produced. A first-order linear model was developed and validated for the prediction of the hydroxyl numbers of polyols from the contents of organic impurities in crude glycerol. As the contents of organic impurities increased from 5 to 85 % in crude glycerol, biomass conversion decreased from 64.5 to 37.7 % and the hydroxyl numbers of polyols decreased from 1285 to 130 mg KOH/g; concomitantly, the  $M_w$  of polyols increased from 249 to 1013 g/mol. In general, crude glycerol containing 45-70 % of organic impurities was optimal for the production of polyols and PU foams with acceptable properties.

### **5.1 Introduction**

Crude glycerol produced by biodiesel plants generally contains not only glycerol but also other impurities such as soap, FFA, FAMEs, glycerides, methanol, water, and ash (Hu et al., 2012a). The proportions of these impurities in crude glycerol vary widely with sample origins, and sometimes the content of impurities even exceeds that of

glycerol in crude glycerol (Hu et al., 2012a). The significant presence of these impurities underscores the necessity of taking into account their roles in any value-added conversion processes developed for crude glycerol.

The effects of crude glycerol impurities, including inorganic salts and organic impurities (i.e. FFA, FAMEs, glycerides), on the properties of base-catalyzed liquefaction-derived polyols and PU foams were investigated. It is worth mentioning that the effects of FFA investigated in this study actually represent the combined effects of FFA and soap in crude glycerol since FFA and soap are inter-convertible via simple acid-base reactions.

## **5.2 Materials and Methods**

### *5.2.1 Materials*

Corn stover was harvested from the OARDC farm (Wooster, OH), air-dried, ground (1mm mesh screen), and oven-dried at 105 °C for 24 h before being used for liquefaction. Chemicals purchased from Fisher Scientific (Pittsburgh, PA) included glycerol, oleic acid, imidazole, NaOH pellets, concentrated HCl (35-38 % wt.), standard HCl solution (0.1 N), and standard NaOH solution (0.1 N and 10 N). Chemicals purchased from Sigma Aldrich (St. Louis, MO) included anhydrous hexane, anhydrous Na<sub>2</sub>SO<sub>4</sub>, NaCl, phthalic anhydride, methyl heptadecanoate, standard FAME mix (GLC-10), HPLC-grade H<sub>2</sub>SO<sub>4</sub> (50 % wt.). Chemicals purchased from Pharmco-AAPER (Shelbyville, KY) included pyridine, 1,4-dioxane, HPLC-grade THF (tetrahydrofuran) chloroform, 98 % concentrated sulfuric acid, ethanol, methanol, and petroleum ether.

Standard stock solutions of monoolein, diolein, triolein, 1,2,4-butanetriol, tricaprins, and derivatization reagent N-methyl-N-trimethylsilyltrifluoroacetamide (MSTFA) were purchased from Restek (Bellefonte, PA). All chemicals used were of reagent grade or higher purity.

Technical grade mono-glycerides, containing approximately 40 % of 1-oleoyl-rac-glycerol, 15-40 % diglyceride, and 15-40 % triglyceride, was purchased from Sigma Aldrich (St. Louis, MO) and used as the model compound of glycerides. Crude glycerol and biodiesel samples were obtained from Bio100 Technologies, LLC. (Mansfield, OH). The obtained biodiesel sample, used as the model compound of FAMES, was determined to contain five major types of FAMES: methyl palmitate (11.7 %), methyl stearate (5.1 %), methyl oleate (22.6 %), methyl linoleate (52.9 %), and methyl linolenate (6.4 %). Additives used in PU foaming were obtained from Air Products & Chemicals, Inc. (Allentown, PA). Polymeric MDI (methylene-4,4'-diphenyl diisocyanate) was obtained from Bayer Material Science (Pittsburgh, PA).

### *5.2.2 Experimental design and statistical analysis*

The effects of inorganic salts, including NaCl and Na<sub>2</sub>SO<sub>4</sub>, on the properties of polyols were investigated independently at 0 and 4 % (wt. of pure glycerol) levels. Salt (either NaCl or Na<sub>2</sub>SO<sub>4</sub>) was mixed with pure glycerol at desired treatment level and the obtained mixture was used as a liquefaction solvent for polyol production. The effects of organic impurities, including FFA, FAMES, and glycerides, on the properties of polyols and PU foams were investigated using a Box-Behnken design (Table 5.1). FFA, FAMES, and glycerides were independent variables (predictors), while the properties of polyols

(biomass conversion, acid and hydroxyl numbers, and  $M_w$ ) and PU foams (density and compressive strength) were dependent variables (responses). The independent variables were coded according to the following equation:

$$x_i = \frac{X_i - X_0}{\Delta X}, i = 1, 2, 3, \text{ where,}$$

$x_i$  represents coded independent variable,  $X_i$  represents real-value independent variable,  $X_0$  represents the value of  $X_i$  at center point, and  $\Delta X$  represents step-change value. A detailed illustration of the coded and real-value experimental levels used in this study is shown in Table 5.2. The experimental design and data analysis were performed using JMP 9.0.0 (SAS Institute Inc., Cary, NC)

### 5.2.3 Preparation of liquefaction solvents

Oleic acid, biodiesel, and tech-grade mono-glycerides were used as the model compounds of FFA, FAMEs, and glycerides, respectively. For each treatment, model crude glycerol was prepared by mixing pure glycerol, oleic acid, biodiesel, and tech-grade mono-glycerides according to the levels specified in the Table 5.1; the amount of pure glycerol used in each treatment was the balance of 100 % after considering the content of organic impurities (i.e. FFA, FAMEs, and glycerides) in crude glycerol.

To verify the mathematical model relating organic impurities to the hydroxyl numbers of polyols, crude glycerol produced by industrial biodiesel plants was used as liquefaction solvent. Before being used in liquefaction process, crude glycerol was pretreated to remove salts, water, and methanol as follows: crude glycerol was acidified

by adding sufficient concentrated HCl (35-38% wt., 11.55 N) to completely convert soap to FFA. Then, crude glycerol was dried by rotary evaporation at 70 °C under vacuum to constant weight to remove water and methanol. After that, the crude glycerol was centrifuged at 10,000 rpm (ca. 11,600 g) for 10 min to separate crude glycerol into three phases: top (mainly FFA, FAME, and glycerides), middle (mainly glycerol), and bottom (mainly salts) phases. The top and middle phases were collected and used as liquefaction solvent.

#### *5.2.4 Liquefaction process for polyol production*

The biomass liquefaction for polyol production was conducted according to the procedure described in Section 3.2.2 using the following liquefaction conditions: 240 °C, 180 min, 3 % wt. of NaOH and 10 % wt. of corn stover. Weight percentages were based on the weight of liquefaction solvent.

#### *5.2.5 Determination of biomass conversion*

The determination of biomass conversion was conducted according to the procedure described in Section 3.2.3.

#### *5.2.6 Characterization of liquefaction-derived polyols*

The determination of acid and hydroxyl numbers of polyols followed the procedures described in Section 3.2.4. The  $M_w$  of polyols were determined using a LC-20 AB HPLC system (Shimadzu, Columbia, MD) equipped with a RID-10A refractive index detector and a GPC column (Styragel HR1 THF, 7.8 × 300 mm, Waters, Milford, MA).

The mobile phase used was HPLC-grade THF at a flow rate of 1 ml/min. The column and RID temperatures were maintained at 35 °C and 40 °C, respectively. The injection volume was 10 µl. An external calibration curve was constructed by analyzing standard polystyrene with  $M_w$  ranging from 200 to 2000 g/mol. The data was analyzed by using Shimadzu LCsolution Version 1.25.

### *5.2.7 Preparation and characterization of PU Foams*

The preparation and characterization (density and compressive strength) of PU Foams followed the procedures described in Section 3.2.6 and 3.2.7, respectively. For morphological study, PU foam samples were cut into  $4 \times 4 \times 3 \text{ mm}^3$  and attached to the substrate. Each sample was coated with a thin layer of platinum (0.2 kÅ) by a Hummer 6.2 Sputtering System (Anatech Ltd, Battle Creek, MI) before analysis. The scanning electron microscopy (SEM) of the sample was conducted on a Hitachi S-3500 N scanning electron microscope (Chiyoda, Tokyo, Japan).

## **5.3 Results and Discussion**

### *5.3.1 Effects of inorganic salts on biomass conversion and hydroxyl numbers of polyols*

Biomass conversion decreased slightly from 71.4 to 70.6 % and 71.4 to 67.8 % when NaCl and Na<sub>2</sub>SO<sub>4</sub> content in crude glycerol increased from 0 to 4 %, respectively (Figure 5.1). The hydroxyl numbers of polyols produced at 0 and 4 % salt levels showed no significant differences ( $p > 0.05$ ) (ca. 1335 mg KOH/g), indicating the insignificant effects of inorganic salts on liquefaction efficiency.

### 5.3.2 *Effects of organic impurities on acid and hydroxyl numbers of polyols*

Methanol and water were found to be completely eliminated by evaporation during the heating of the solvent to liquefaction temperature (240 °C) and so were not considered further. The effects of organic impurities, including FFA, FAMEs, and glycerides, on the properties of polyols and PU foams were investigated. The polyols produced showed low acid numbers less than 5 mg KOH/g (data not shown) at all treatment levels, which agrees with the results from our previous reports (Hu et al., 2012b; Luo et al., 2013). Generally, polyol need to have low acid number (< 5 mg KOH/g) for PU foam applications because acids in polyol can react with and deactivate the amine catalysts used in foaming formulations, leading to decreased catalytic efficiency. Polyols produced from acid-catalyzed liquefaction process usually possess high acid numbers ranging from 15 to 40 mg KOH/g and need to be treated before PU applications (Kurimoto et al., 1999; Kurimoto et al., 2000; Lee et al., 2000; Lee and Lin, 2008).

The hydroxyl number of polyol is vital for PU applications because it directly relates to the quantity of isocyanates used in PU formulations. In this study, through the use of a response surface design, regression models were built between the hydroxyl numbers of polyols and crude glycerol organic impurities. The fitted second-order equation is shown below:

$$Y = 1447.75 - 11.48X_1 - 15.14X_2 - 32.18X_3 - 0.04X_1^2 + 0.01X_2^2 + 1.19X_3^2 - 0.10X_1X_2 - 0.01X_1X_3 + 0.30X_2X_3$$

where  $Y$  is the hydroxyl number of polyols,  $X_1$ ,  $X_2$ , and  $X_3$  are real-value content of FFA, FAMEs, and glycerides in crude glycerol, respectively.

A summary of the ANOVA (analysis of variance) of the model is shown in Table 5.3. The model had a  $p$ -value less than 0.0001, suggesting the model could explain the variations among different treatments. The coefficient of determination,  $R^2$ , is a common term used to evaluate the goodness of fit of regression models. Normally, a model with  $R^2 \geq 0.9$  is considered to be of high correlation (Li et al., 2005; Chen et al., 2009). The fitted model had a high  $R^2$  of 0.99, indicating that 99 % of total variance can be explained by the model and that a high correlation exists between predictors and responses. A  $F$ -test showed that only linear terms, i.e. FFA ( $X_1$ ), FAMEs ( $X_2$ ), and glycerides ( $X_3$ ), were significant in the model ( $p < 0.05$ ). This indicates that the relationship between the hydroxyl numbers of polyols and organic impurities may be adequately described by a simple first-order linear model. Therefore, the experimental data was further fitted into a first-order linear model as follows:

$$Y = 1449.75 - 15.18X_1 - 15.28X_2 - 14.43X_3$$

Table 5.4 shows a summary of the ANOVA of the fitted first-order model. Similar to the second-order model discussed above, the linear model also was highly significant ( $p < 0.0001$ ) and had a high  $R^2$  value (0.99). In addition, all predictors ( $X_1$ ,  $X_2$ , and  $X_3$ ) in the model were shown to be significant by  $F$ -test ( $p < 0.05$ ). The hydroxyl numbers of polyols predicted by the linear model were listed along with the measured values in Table 5.1. The differences between the predicted and measured values were

mostly less than 5 %, suggesting the sufficiency of the model. The linear model was further verified by using two industrially-derived crude glycerol samples as liquefaction solvents for polyol production. The results showed that the differences between the predicted and measured hydroxyl numbers were less than 5 % (Table 5.5), indicating the high prediction accuracy of the model.

Based on the built linear model, the response surfaces of polyol hydroxyl numbers with organic impurities were obtained (Figure 5.2a, 5.2b, and 5.2c). The hydroxyl numbers of polyols decreased with increasing levels of organic impurities in crude glycerol. For example, increasing contents of FFA and FAMES from 0 to 40 % dramatically decreased polyol hydroxyl numbers from 1285 to 778 mg KOH/g and from 1285 to 794 mg KOH/g, respectively. This can be explained by the physical replacement of glycerol and the consumption of glycerol via chemical reactions such as esterification and transesterification by FFA and FAMES. Compared to that of FFA and FAMES, increasing glycerides content in crude glycerol decreased the hydroxyl numbers of polyols less dramatically (Figure 5.2b and 5.2c). Commercial polyols for rigid or semi-rigid PU foam applications generally have hydroxyl numbers ranging from 34 to 800 mg KOH/g (Dow Product literature, 2013). In this study, polyols produced from crude glycerol with organic impurities over 45 % exhibited hydroxyl numbers less than 800 mg KOH/g (Table 5.1) and thus have the potential to produce rigid or semi-rigid PU foams.

### *5.3.3 Effects of organic impurities on biomass conversion, molecular weights and functionalities of polyols*

Biomass conversion decreased from 64.5 to 37.3 % with increasing contents of organic impurities in crude glycerol (Table 5.1). This is due to that increasing levels of organic impurities in crude glycerol decreased liquefaction agent (i.e. glycerol)/biomass ratio, which led to lower liquefaction efficiency. In addition, liquefaction agent/biomass ratio may be further decreased by the esterification and transesterification reactions that occurred between glycerol and organic impurities during liquefaction process (Hu et al., 2012b; Luo et al., 2013).

The  $M_w$  of polyols increased with increasing levels of FFA and FAMES in crude glycerol (Table 5.6). For example, compared to the polyol ( $M_w$ : 249 g/mol) produced at 0 % of FFA and FAMES, polyols produced at 40 % of FFA, FAMES, or their mixture had higher  $M_w$  around 454-472 g/mol. Polyol produced at 80 % of FFA and FAMES had even higher  $M_w$  of 1013 g/mol. The higher  $M_w$  at higher levels of FFA and FAMES could be explained by the intensified polymerization reactions, such as esterification or transesterification among glycerol, FFA, and FAMES, during the liquefaction process (Hu et al., 2012b; Luo et al., 2013). The functionalities of polyols increased from 5.7 to 6.2-6.7 when FFA and/or FAMES contents increased from 0 to 40 % (Table 5.6). These values are comparable to the functionalities of some commercially-produced glycerol-initiated polyether polyols ( $f_n$ : 3.0 to 6.9) (Dow Product literature, 2013). Polyol produced at 80 % of FFA and FAMES had a much lower functionality of 2.3 (Table 5.6), due to the low glycerol content (15 %) of the crude glycerol used and the occurrence of

condensation reactions that consumed hydroxyl groups. Polyols with appropriate  $M_w$  are essential in providing PU with desired soft segment properties. Depending on the specific application needs, the  $M_w$  of polyols can range from approximately 3000 to 6000 g/mol for flexible PU foams and from approximately 200 to 1000 g/mol for rigid or semi-rigid PU foams (Randall and Lee, 2002c). Polyols produced from petrochemical solvent-based liquefaction processes generally have  $M_w$  ranging from 500 to 900 g/mol (Lee et al., 2000; Kurimoto et al., 2001a), which are suitable for rigid or semi-rigid PU foam applications. In this study, polyols produced from crude glycerol containing 45 % or more of organic impurities showed  $M_w$  comparable to those derived from petrochemical solvent-based biomass liquefaction process. This suggests that organic impurities are beneficial in producing polyols with appropriate  $M_w$  for common PU applications.

#### *5.3.4 Effects of organic impurities on PU foam properties*

Generally, the presence of organic impurities in crude glycerol decreased the density of PU foams (Figure 5.3). PU foams produced at 5 % of organic impurities had the highest density of 0.071 g/cm<sup>3</sup>, which was significant higher than the density (0.037-0.048 g/cm<sup>3</sup>) of those produced at 45-70 % of organic impurities. The decreasing density of PU foams indicate that PU with less dense structures were produced at higher FFA and FAMES levels, which can be attributed to the lower hydroxyl numbers of their corresponding polyols. In contrast, the compressive strength of PU foams increased from 127 to 188 kPa when the contents of organic impurities increased from 5 to 60 % (Figure 5.3). After that, the compressive strength PU foams decreased to approximately 140 kPa at 70 % of organic impurities. Since polyol hydroxyl numbers decreased with increasing

levels of organic impurities (Section 5.2.2), PU foams produced at higher organic impurities levels consumed less isocyanates for foam production than those at lower levels, which is preferred for the cost-reduction of PU production. These results indicate that organic impurities, particularly FFA and FAMEs, helped improve not only the properties (density and compressive strength) but also the economics of crude glycerol-based PU foams. However, it should be noted that PU foam produced at 85 % of organic impurities collapsed during the foaming process, probably due to the low functionality (2.3, Table 5.6) and low biomass conversion (37.7 %, Table 5.1) of its corresponding polyol. This indicates that organic impurity content in crude glycerol should be controlled at appropriate levels for optimal PU properties. In this study, PU foams produced at organic impurity contents from 45 to 70 % did not collapse and had better mechanical properties (i.e. higher compressive strength but lower densities) than those produced at low impurities level (i.e. 5 % glycerides) (Figure 5.3).

It has been previously reported that the mechanical strength of PU increased with increasing hydroxyl numbers and functionalities of vegetable oil-based polyols. Zlatanovic et al. (2004) prepared epoxidized polyols with different hydroxyl numbers and functionalities from different types of vegetable oils. PU produced from polyols with higher hydroxyl numbers and functionalities showed higher mechanical strength due to their higher crosslinking densities. In this study, the higher compressive strength of PU foams produced at higher organic impurities levels could be partially attributed to the higher functionalities of their corresponding polyols (Table 5.6). In addition, polyol reactivity also could be used to explain this observation. The polyol produced at 5 % of

organic impurities had an extremely high hydroxyl number (1285 mg KOH/g, Table 5.1) but a low  $M_w$  (249 g/mol, Table 5.6). It may contain a large number of secondary hydroxyl groups and/or hydroxyl groups located structurally close to each other. Both types of hydroxyl groups could decrease polyol reactivity due to the low reactivity of secondary hydroxyl groups and/or the steric hindrance encountered during the polymerizations between polyols and isocyanates. This eventually could result in slow curing rates and/or even incompletely cured PU structures with disrupted cell structures and non-uniform cell sizes (Figure 5.4). In contrast, polyols produced at 45-70 % of organic impurities had lower hydroxyl numbers (405-794 mg KOH/g, Table 5.1) and higher  $M_w$  (400-1000 g/mol, Table 5.6). During the PU foaming process, these polyols showed higher reactivity and faster curing rates with isocyanates than that produced at 5 % of organic impurities (data not shown), suggesting their lower content of secondary and/or structurally closely located hydroxyl groups. The higher reactivity of these polyols could eventually lead to PU foams with more cured structures and higher compressive strength. Compared to the PU foam produced at a lower impurity level (5 % glycerides, Figure 5.4), the PU foam produced at a higher impurity level (20 % FFA, 20 % FAMEs and 5 % glycerides, Figure 5.4) had a less disrupted structure and a smaller average cell size, which could contribute to its higher mechanical strength.

#### **5.4. Conclusions**

Inorganic salts had negligible effects on polyol properties, while organic impurities, including FFA, FAMEs, and glycerides, significantly affected the properties of base-catalyzed liquefaction-derived polyols and PU foams. Despite their negative

effects on biomass conversion, organic impurities, particularly FFA and FAMEs, were essential in producing polyols with appropriate hydroxyl numbers and  $M_w$  for rigid or semi-rigid PU foam applications. The presence of appropriate content of organic impurities in crude glycerol (45-70 %) also helped improve the properties (density and compressive strength) of PU foams produced.

Table 5.1: Box-Behnken design with three variables and general properties of polyols

Run	FFA ( $x_1$ )	FAME ( $x_2$ )	Glycerides ( $x_3$ )	Biomass conversion (%)	Hydroxyl number (mg KOH/g)	
					Measured	Predicted
1	0	1	1	45.8	406	391
2	0	1	-1	49.5	528	535
3	-1	1	0	47.8	794	766
4	-1	0	1	49.6	1035	1000
5	0	0	0	54.8	755	769
6	1	-1	0	49.9	778	771
7	0	0	0	52.8	786	769
8	-1	0	-1	52.9	1140	1144
9	0	-1	-1	51.1	1241	1146
10	1	1	0	37.7	130	159
11	-1	-1	0	64.5	1285	1378
12	0	0	0	54.0	752	769
13	1	0	-1	47.3	513	537
14	0	-1	1	51.9	999	1002
15	1	0	1	45.5	405	393
16	0	0	0	55.2	749	769

Table 5.2: Coding of the independent variables

Independent variables	Levels		
	-1	0	1
FFA (wt. %) <sup>a</sup>	0	20	40
FAMES (wt. %)	0	20	40
Glycerides (wt. %)	0	5	10

Note: a: wt. % represents the weight percentages of crude glycerol impurities in model crude glycerol.

Table 5.3: ANOVA of the fitted second-order model for polyol hydroxyl numbers

Source	Degree of freedom	Mean square	F-value	Probe>F
Model	9	171141	126.06	<0.0001*
$X_1$	1	32412	23.87	0.0027*
$X_2$	1	56451	41.58	0.0007*
$X_3$	1	15927	11.73	0.0141*
$X_1X_2$	1	6162	4.54	0.0772
$X_1X_3$	1	2	0.00	0.9688
$X_2X_3$	1	3600	2.65	0.1546
$X_1^2$	1	1156	0.85	0.3917
$X_2^2$	1	42	0.03	0.8658
$X_3^2$	1	3540	2.61	0.1575
Residual	6	1358		
Lack of fit	3	2420	8.20	0.0588
Pure error	3	295		

Note:  $R^2=0.99$ ; adjusted  $R^2=0.99$

Table 5.4: ANOVA of the fitted first-order model for polyol hydroxyl numbers

Source	Degree of freedom	Mean square	F-value	Probe>F
Model	3	508589	269.47	<0.0001*
$X_1$	1	736898	390.43	<0.0001*
$X_2$	1	747253	395.92	<0.0001*
$X_3$	1	41616	22.05	0.0005*
Residual	12	1887		
Lack of fit	9	2418	8.20	0.0588
Pure error	3	295		

Note:  $R^2=0.99$ ; adjusted  $R^2=0.98$

Table 5.5: Verification of the developed linear model for predicting polyol hydroxyl numbers

Samples	Crude glycerol composition (wt. %)				Polyol hydroxyl number (mg KOH/g)	
	Glycerol	FFA	FAME	Glycerides	Predicted	Measured
CG-A	51.5	23.3	23.9	1.3	712	687
CG-B	73.3	7.6	12.9	6.2	1048	1076

Table 5.6: Effects of FFA and FAMEs on molecular weights and functionalities of polyols

Treatments	Contents in liquefaction solvents (%) <sup>a</sup>		Molecular weight (g/mol) <sup>b</sup>			$f_n^d$
	FFA	FAMEs	$M_n$	$M_w$	PDI	
1	0	0	224 ± 7 <sup>c</sup>	249 ± 9	1.11 ± 0.01	5.7 ± 0.2
2	20	20	305 ± 2	455 ± 1	1.49 ± 0.00	6.2 ± 0.0
3	40	0	304 ± 3	454 ± 6	1.49 ± 0.00	6.3 ± 0.1
4	0	40	307 ± 9	472 ± 21	1.54 ± 0.02	6.7 ± 0.3
5	40	40	816 ± 73	1013 ± 85	1.24 ± 0.01	2.3 ± 0.2

Note: a: all liquefaction solvents contained 5 % glycerides, in addition to FFA, FAMEs, and glycerol; b:  $M_n$ : number-average molecular weight;  $M_w$ : weight-average molecular weight; PDI: polydispersity; c: mean ± standard deviation of two replicates; d: functionality

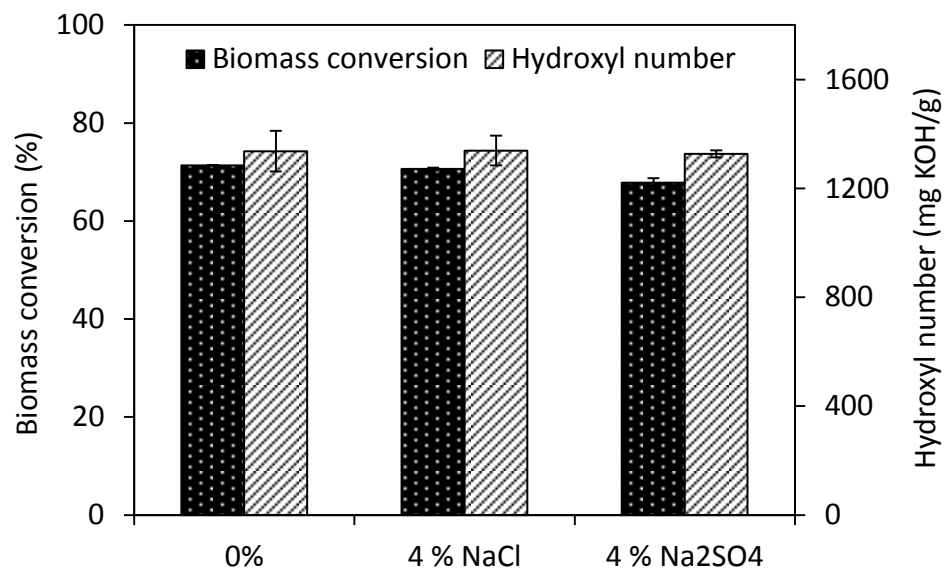
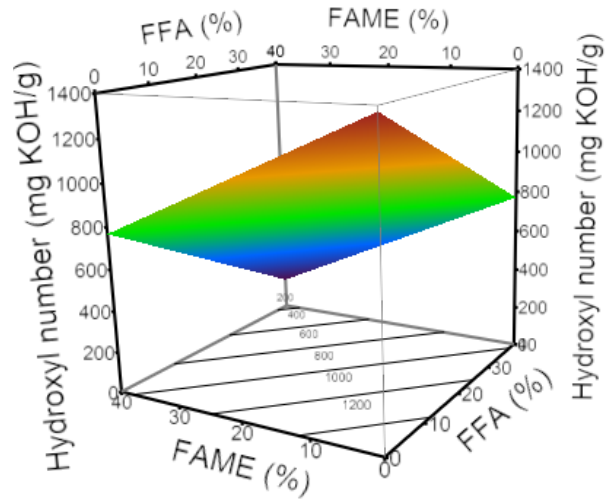
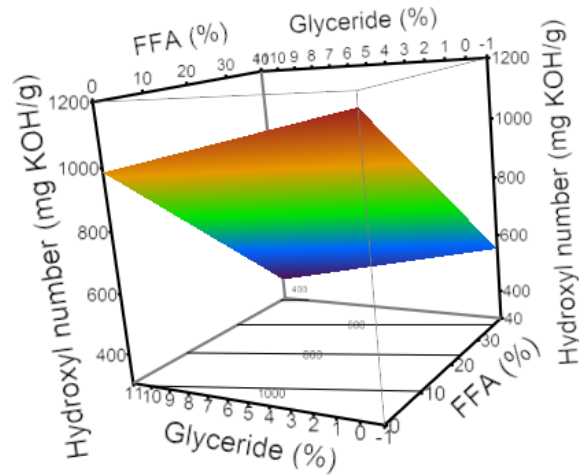


Figure 5.1: Effects of inorganic salts (NaCl and Na<sub>2</sub>SO<sub>4</sub>) on biomass conversion and the hydroxyl numbers of polyols



(a)

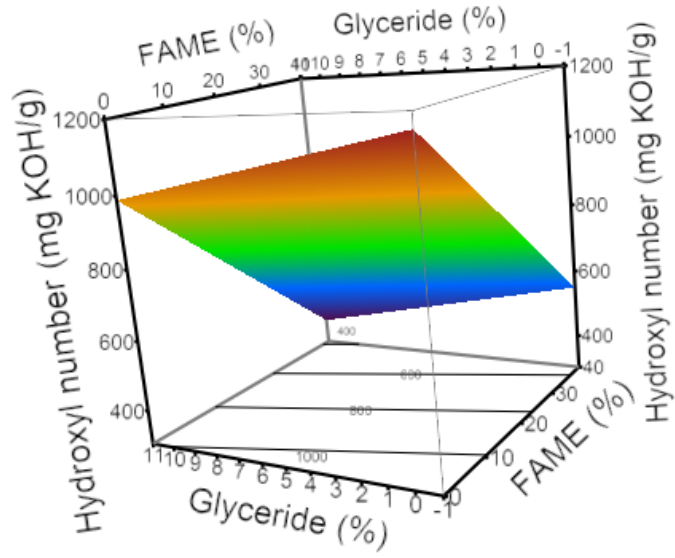


(b)

Continued

Figure 5.2: Response surface plots and its corresponding contour plots of the dependence of the hydroxyl number of polyols on: (a) FFA and FAME (at glyceride: 5 %); (b) FFA and glyceride (at FAME: 20 %); (c) FAME and glyceride (at FFA: 20 %)

Figure 5.2 continued



(c)

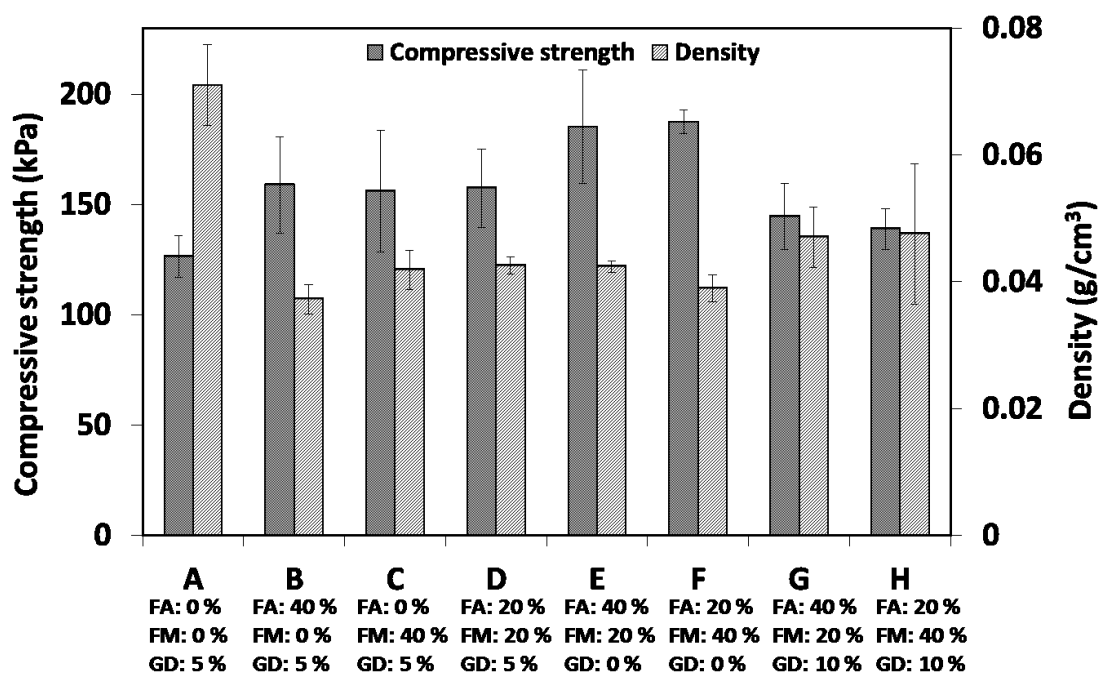


Figure 5.3: Effects of organic impurities on compressive strength and density of PU foams (Note: FA: FFA; FM: FAMES; GD: glycerides)

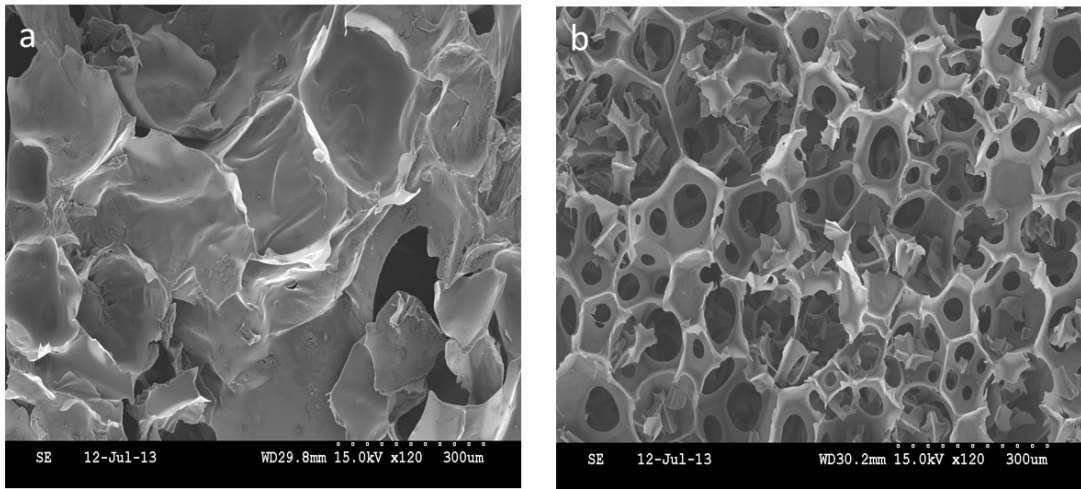


Figure 5.4: SEM images of PU foams produced from crude glycerol containing: (a) 5 % glycerides; (b) 20 % FFA, 20 % FAMEs and 5 % glycerides

## **Chapter 6 Effects of Crude Glycerol Impurities on the Properties of Acid-catalyzed Liquefaction-derived Polyols and PU Foams**

The effects of crude glycerol impurities on the properties of polyols and PU foams derived from acid-catalyzed biomass liquefaction process were investigated. Both inorganic salts (NaCl and Na<sub>2</sub>SO<sub>4</sub>) and organic impurities (FFA, FAMES, and glycerides) decreased biomass conversion and significantly affected the properties of polyols produced. Via a response surface methodology, regression models were developed and validated to describe the relationships between organic impurities and biomass conversion and between organic impurities and the hydroxyl numbers of polyols. In general, polyols produced from crude glycerol containing 0-45 % of organic impurities showed hydroxyl numbers varying from 700 to 1301 mg KOH/g, acid number from 19 to 28 mg KOH/g, viscosities from 2.4 to 29.2 Pa.s, and  $M_w$  from 244 to 550 g/mol. Polyols produced from crude glycerol with 40 % or more of organic impurities showed appropriate hydroxyl numbers and  $M_w$  for rigid or semi-rigid PU foam applications. PU foams produced in this study showed comparable properties (density and compressive strength) to their analogs derived from petrochemical solvent-based liquefaction process.

### **6.1 Introduction**

Compared to base-catalyzed liquefaction processes, acid-catalyzed biomass liquefaction processes are usually conducted at lower temperatures (150-180 °C versus

240-250 °C for base-catalyzed processes) and is more commonly used for biomass liquefaction. Its dramatically different liquefaction conditions could lead to different fates for the crude glycerol impurities and biomass components during the biomass liquefaction process, producing polyols and PU foams with different properties.

## 6.2 Materials and Methods

### 6.2.1 Materials

Corn stover and other chemicals used were the same as those described in Section 5.2.1.

### 6.2.2 Experimental design and statistical analysis

The individual effects of salts, NaCl and Na<sub>2</sub>SO<sub>4</sub>, on polyol properties were investigated at 0 %, 2 % and 4 % (wt. of pure glycerol) levels. The effects of organic impurities, including FFA, FAMES, and glycerides, on polyol and PU foam properties were investigated using a three-factor central-composite design (Table 6.1). FFA, FAMES, and glycerides were independent variables (predictors), and polyol and PU foam properties were dependent variables (responses) in this study. The independent variables were coded according to the following equation:

$$x_i = \frac{X_i - X_0}{\Delta X}, i = 1,2,3$$

Where  $x_i$  represent coded independent variables,  $X_i$  represent real-value independent variables,  $X_0$  represents the value of  $X_i$  at center point, and  $\Delta X$  represents step change value (FFA and FAMES: 10; glycerides: 2.5). A detailed illustration of the coding and the

actual values of experimental levels used in this study is shown in Table 6.2. The experimental design and statistical analysis in this study were conducted using JMP 9.0.0 and SAS 9.3 (SAS Institute Inc., Cary, NC)

#### *6.2.3 Preparation of liquefaction solvents*

The preparation of liquefaction solvents used in this study followed the procedures described in Section 5.2.3.

#### *6.2.4. Liquefaction process for polyol production*

The biomass liquefaction for polyol production was conducted according to the procedure described in Section 3.2.2 using the following liquefaction conditions: 150 °C, 90 min, 3 % wt. of H<sub>2</sub>SO<sub>4</sub> (concentrated, 98 %) and 10 % wt. of corn stover. Weight percentages were based on the weight of liquefaction solvent.

#### *6.2.5. Determination of biomass conversion*

The determination of biomass conversion was conducted according to the procedure described in Section 3.2.3.

#### *6.2.6. Characterization of liquefaction-derived polyols*

The determination of acid and hydroxyl numbers of polyols followed the procedures described in Section 3.2.4. The  $M_w$  of polyols were determined according to the procedure described in Section 5.2.6.

### *6.2.7. Preparation and characterization of PU Foams*

The preparation and characterization (density and compressive strength) of PU foams were conducted by following the procedures described in Section 3.2.6 and 3.2.7, respectively. The morphological study of PU foams by SEM followed the procedure described in Section 5.2.7.

## **6.3 Results and Discussion**

### *6.3.1 Effects of inorganic salts on polyol properties*

Biomass conversion decreased significantly ( $p < 0.05$ ) from 92.6 to 53.4 % and 92.6 to 55.5 % when NaCl and Na<sub>2</sub>SO<sub>4</sub> content in crude glycerol increased from 0 to 4 %, respectively (Figure 6.1). In addition, biomass conversion at 2 % NaCl level (57.4 %) was much less than that at 2 % of Na<sub>2</sub>SO<sub>4</sub> (80.2 %), indicating the stronger negative effect of NaCl (Figure 6.1). This was probably due to the higher molarity of NaCl in crude glycerol resulted from its lower molar mass (NaCl: 58 g/mol; Na<sub>2</sub>SO<sub>4</sub>: 144 g/mol). Increasing salts content also led to significant increases in polyol viscosities, probably due to decreased biomass conversions (Chen and Lu, 2009; Lee et al., 2000). The hydroxyl numbers of polyols increased significantly ( $p < 0.05$ ) from 1301 to 1500 mg KOH/g and from 1301 to 1489 mg KOH/g when NaCl and Na<sub>2</sub>SO<sub>4</sub> content increased from 0 to 4 %, respectively (Figure 6.2). The higher hydroxyl numbers could be explained by the lower biomass conversions since less glycerol was consumed for biomass liquefaction. The significant effects of salts on acid-catalyzed liquefaction differ

from our previous finding that inorganic salts had no significant effects on the properties of polyols produced from the base-catalyzed liquefaction process.

Decrease in biomass conversion was well accompanied by the decrease in the acid numbers of polyols (Figure 6.1 and 6.2), which agrees well with the results from previous reports (Lee et al., 2000; Hassan and Shukry, 2008). Higher biomass conversion is usually obtained at higher acid potential due to the stronger catalytic effects of acids. In this study, the decreased acid potential was most likely caused by the consumption of acid ( $\text{H}_2\text{SO}_4$ ) by salts ( $\text{NaCl}$  and  $\text{Na}_2\text{SO}_4$ ) via two major chemical reactions (Figure 6.3) (Patnaik, 2007; Christ, 1999). Since the liquefaction process was conducted under atmospheric pressure and high temperature, the  $\text{HCl}$  produced from the reaction between  $\text{NaCl}$  and  $\text{Na}_2\text{SO}_4$  could largely escape from the reactor and led to decreased acid potential in liquefaction system. The reaction between  $\text{Na}_2\text{SO}_4$  and  $\text{H}_2\text{SO}_4$  also led to decreased biomass conversion because the produced  $\text{NaHSO}_4$  is a weak acid that has a lower catalytic efficiency than  $\text{H}_2\text{SO}_4$ .

### *6.3.2 Effects of organic impurities on biomass conversion*

It was not possible to apply the organic impurity levels effective in base-catalyzed liquefaction to the acid-catalyzed liquefaction. Significant recondensations occurred at early stages of the liquefaction process when crude glycerol contained high contents of organic impurities (> 50 %, data not shown). Increasing contents of organic impurities decreased glycerol contents in crude glycerol through physical replacement and chemical reactions such as esterification and transesterification (Hu et al., 2012b; Luo et al., 2013). When organic impurity contents become substantially high (>50 %), low glycerol

contents in liquefaction solvent led to low glycerol/biomass ratios and thus early occurrence of detrimental recondensations. Therefore, the designed organic impurity levels in this study were adjusted to lower levels (FFA and FAMES: 0-20 %; glycerides: 0-5 %) to accommodate the acid-catalyzed biomass liquefaction process.

The relationship between biomass conversion and organic impurities was fitted into both first- and second-order models. It was found that the fitted second-order model (data not shown) had a higher  $R^2$  (0.90) but lower adjusted  $R^2$  (0.79) than the fitted first-order model ( $R^2$ : 0.86; adjusted  $R^2$ : 0.83). This suggests that the second-order terms added little to the explanatory power of the second-order model. Therefore, the fitted first-order model was considered the preferred model and was shown below:

$$Y = 94.08 - 0.518X_1 - 0.464X_2 - 0.636X_3$$

where  $Y$  is biomass conversion,  $X_1$ ,  $X_2$ , and  $X_3$  are real-value contents of FFA, FAMES, and glycerides in crude glycerol, respectively.

A summary of the ANOVA of the fitted first-order model indicates that the model could explain the variations among treatments (Table 6.3). FFA ( $X_1$ ) and FAMES ( $X_2$ ), due to their small  $p$ -values ( $p < 0.0001$ ), were identified as significant terms in the model, indicating their significant effects on biomass conversion. The fitted model was further verified by using two industrially-derived crude glycerol samples (CG-A and CG-B) for polyol production (Table 6.5). Polyol produced from CG-A showed a measured biomass conversion (77.9 %) higher than the predicted one (70.0 %). The relatively large difference (around 10 %) between these two values may be explained by the model's low

extrapolation power since the combined content of FFA and FAMEs (47.2 %) in CG-A exceeded the designed experimental levels (0 to 40 %). CG-B had FFA and FAMEs contents within the designed experimental levels and showed a predicted biomass conversion (80.2 %) close to the measured one (82.3 %), indicating the model's good predictability.

As shown in the model, all coefficients were negative, suggesting that increasing contents of organic impurities in crude glycerol led to decreased biomass conversion. This agrees well with the data shown in Table 6.1 that biomass conversion decreased from 92.6 to 69.3 % with increasing contents of organic impurities from 0 to 40 %. The decreased biomass conversion at higher organic impurity levels were due to decreased glycerol/biomass ratios. Compared to the base-catalyzed liquefaction process, the acid-catalyzed liquefaction process had higher biomass conversion at the same level of organic impurities. For example, crude glycerol with 45 % of organic impurities led to a biomass conversion of 71.2 % in the acid-catalyzed process, but a much lower biomass conversion of 54.2 % in the base-catalyzed process (Table 5.1 and 6.1).

### *6.3.3 Effects of organic impurities on hydroxyl numbers of polyols*

To describe the relationship between polyol hydroxyl numbers and organic impurities, the obtained results were fitted into both first- and second-order models. It was found that the fitted second-order model showed both a higher  $R^2$  (0.99) and adjusted  $R^2$  (0.98) than the fitted first-order model ( $R^2$ : 0.95; adjusted  $R^2$ : 0.94, data not shown), indicating the explanatory power of the second-order terms in the second-order model. Therefore, the second-order model was considered as the optimal model:

$$Y = 1303.78 - 8.54X_1 - 5.93X_2 + 3.48X_3 - 0.20X_1^2 - 0.32X_2^2 - 2.36X_3^2 - 0.11X_1X_2 - 0.28X_1X_3 + 0.07X_2X_3$$

where  $Y$  is polyol hydroxyl number,  $X_1$ ,  $X_2$ , and  $X_3$  are real-value contents of FFA, FAMEs, and glycerides in crude glycerol, respectively.

Table 6.4 shows a summary of the ANOVA of the fitted model. The model was highly significant ( $p < 0.0001$ ) and of high correlation ( $R^2 = 0.99$ ). FFA ( $X_1$ ,  $p < 0.05$ ) was identified as the significant factor affecting polyol hydroxyl numbers. FAMEs ( $X_2$ ) and squared FAMEs ( $X_2^2$ ) showed low  $p$  values less than or around 0.1, indicating their potential effects on polyol hydroxyl numbers as well. As shown in Table 6.5, the model was verified to be of high predictability (difference between the measured and predicted value less than 5 %). Figure 6.4 (a, b and c) show the response surfaces of polyol hydroxyl numbers with FFA, FAMEs, and glycerides based on the fitted second-order model. As expected, the hydroxyl numbers of polyols decreased with increasing contents of FFA and FAMEs in crude glycerol due to their gradual replacements and consumption of glycerol by esterification and transesterification reactions. Polyol hydroxyl numbers decreased slightly with increasing glyceride contents (Figure 6.4, a and b). The hydroxyl numbers of polyols decreased from 1301 to 700 mg KOH/g with increasing organic impurity contents from 0 to 45 %. Compared to polyols derived from the base-catalyzed process, polyols derived from the acid-catalyzed process showed higher hydroxyl numbers due to the use of crude glycerol with higher glycerol contents. Similar to the base-catalyzed process, polyols with suitable hydroxyl numbers (<800 mg KOH/g) and  $M_w$  for rigid or semi-rigid PU foam applications were produced from crude glycerol

containing 40 % or more of organic impurities. However, since the acid-catalyzed process needs crude glycerol with impurity contents less than 50 % to avoid detrimental recondensations (Section 6.3.2), crude glycerol containing 40-50 % of organic impurities was considered to be suitable for the acid-catalyzed liquefaction process.

#### *6.3.4 Effects of organic impurities on acid numbers and viscosities of polyols*

The acid numbers of polyols increased slightly from 20 to 23 mg KOH/g with increasing contents of FFA from 0 to 20 % (Figure 6.5), probably due to the presence of residual FFA (tested to be  $2.1 \pm 0.2$  %) in polyol produced at 20 % FFA level. For FAMES content increasing from 0 to 20 %, the acid number of polyols also slightly increased from 20 to 23 mg KOH/g (Figure 6.5), probably due to the hydrolysis of FAMES to FFA (FFA content tested to be  $1.8 \pm 0.2$  % in produced polyol) during liquefaction process. Increasing glyceride content from 0 to 5 % caused no significant change in polyol acid numbers (20 mg KOH/g for both 0 and 5 % glycerides levels). The acid numbers of polyols produced in this study were higher than those produced from the base-catalyzed liquefaction process ( $< 5$  mg KOH/g), but were similar to those derived from conventional acid-catalyzed biomass liquefaction processes (Lee et al., 2000; Yan et al., 2008). The viscosities of polyols increased significantly ( $p < 0.05$ ) from 2.4 to 10.9, 6.5 and 3.9 Pa.s for the respective increase of FFA, FAMES and glycerides contents from 0 to 20 %, 20 % and 5 % (Figure 6.5). The increased polyol viscosities could be explained by decreased biomass conversion (Chen and Lu, 2009; Lee et al., 2000) as well as intensified condensation reactions during liquefaction process at higher organic impurity levels (Hu et al., 2012b; Luo et al., 2013).

### 6.3.5 Effects of organic impurities on molecular weights of polyols

Similar to the observations made in base-catalyzed process, the  $M_w$  of polyols increased with increasing levels of organic impurities in crude glycerol (Table 6.6) (Hu et al., 2012b; Luo et al., 2013). The functionalities of polyols ( $f_n$ : 5.6 to 7.6) also increased with increasing contents of organic impurities in crude glycerol, and generally their values were comparable to those of polyols produced from the base-catalyzed process. Polyols derived from petrochemical solvent-based liquefaction processes have shown  $M_w$  varying from 500-900 g/mol (Kurimoto et al., 2001a; Lee et al., 2000). In this study, polyol produced from crude glycerol containing 40 % or more of organic impurities showed  $M_w$  close to or over 500 g/mol, further supporting the important roles of organic impurities in improving polyol properties.

### 6.3.6 Effects of organic impurities on PU foam properties

The presence of organic impurities in crude glycerol significantly ( $p < 0.05$ ) decreased the density of PU foams (Figure 6.6), which agrees with the result obtained in the base-catalyzed liquefaction process. The decreased density at higher organic impurity levels were mainly caused by the lower hydroxyl numbers of polyols produced. The compressive strength of PU foams decreased significantly ( $p < 0.05$ ) from 174 to 149 kPa, 76 kPa and 166 kPa when FFA, FAMEs, and glyceride contents increased from 0 to 20%, 20% and 5%, respectively (Figure 6.6). This was contrary to our previous observations made in the base-catalyzed liquefaction process, during which the compressive strength of PU foams increased with increasing contents of organic impurities. The disagreement between the acid- and base-catalyzed processes could be explained by the different

experimental levels and/or different reactions involved. In this study, the decreased strength of PU foams was mostly due to the lower hydroxyl numbers of polyols produced at higher impurity levels, which led to lower hard segment content and lower intermolecular hydrogen bonding in PU (Lu and Larock, 2008). Among all organic impurities, FAMES (at 20 %) caused the most dramatic decrease in PU foam strength (Figure 6.6), probably due to the high content of residual FAMES ( $5.7 \pm 0.1$  %) present in the polyol produced. Since FAMES have little reactivity with isocyanate, their presence in polyols might cause disrupted foam structures that decrease PU strength (Figure 6.7). However, despite the negative effects of organic impurities, PU foams produced in this study still exhibited comparable compressive strength to their analogs derived from petrochemical solvent-based liquefaction processes (Lee et al., 2000; Chen and Lu, 2009).

### *6.3.7 Comparison between the acid- and base-catalyzed biomass liquefaction processes*

Table 6.7 shows a comparison between the properties of polyols and PU foams derived from the acid- and base-catalyzed biomass liquefaction processes. Compared to the base-catalyzed process, the acid-catalyzed process resulted in a much higher biomass conversion, indicating its higher liquefaction efficiency. The higher biomass conversion obtained in the acid-catalyzed process also means that more hydroxyl groups were consumed for the solvolytic liquefaction of biomass, producing polyol with lower hydroxyl number (Table 6.7). In addition, because of its higher liquefaction efficiency, the acid-catalyzed process also produced polyol with lower viscosity and higher  $M_w$  than those from the base-catalyzed process (Table 6.7). However, compared to the acid-

catalyzed process, the base-catalyzed process had the advantages of producing polyol with lower acid number and PU foam with higher compressive strength. Polyols with high acid numbers are unfavorable and need to be treated before being used for PU applications. Moreover, the base-catalyzed process was also more robust for accommodating crude glycerol with a wider range of compositions (crude glycerol with 45-70 % of organic impurities). In comparison, as previously discussed, the acid-catalyzed liquefaction process needs crude glycerol with 40-50 % of organic impurities to achieve the balance between inhibition of early occurrence of detrimental recondensations and production of polyols with suitable properties for PU foam applications.

#### **6.4 Conclusions**

Biomass conversion decreased with increasing levels of inorganic salts (NaCl and Na<sub>2</sub>SO<sub>4</sub>) and organic impurities, including FFA, FAMES, and glycerides, in crude glycerol. Despite their negative effects on biomass conversion, organic impurities were beneficial in producing polyols with appropriate hydroxyl numbers (<800 mg KOH/g) and  $M_w$  (>500 g/mol) for rigid or semi-rigid PU foam applications. All PU foams produced in this study showed compressive strength comparable to those derived from petrochemical solvent-based liquefaction process. Compared to the base-catalyzed liquefaction processes, the acid-catalyzed process had higher liquefaction efficiency and produced polyols with lower viscosities, but higher acid numbers.

Table 6.1: Central composite design and general properties of polyols

Run	FFA ( $x_1$ )	FAME ( $x_2$ )	Glycerides ( $x_3$ )	Biomass conversion (%)		Hydroxyl number (mg KOH/g)	
				Measured	Predicted	Measured	Predicted
1	-1	-1	1	90.5	90.9	1249	1262
2	-1	1	-1	88.2	84.8	1042	1058
3	1	-1	-1	86.7	83.7	1058	1054
4	1	1	1	71.2	71.3	700	703
5	-1	-1	-1	92.6	94.1	1301	1304
6	-1	1	1	80.5	81.6	1014	1023
7	1	-1	1	79.1	80.5	996	985
8	1	1	-1	69.3	74.4	773	765
9	1	0	0	78.8	77.5	903	923
10	-1	0	0	85.1	87.8	1250	1208
11	0	1	0	79.3	78.0	942	922
12	0	-1	0	86.0	87.3	1187	1186
13	0	0	1	82.5	81.1	1059	1045
14	0	0	-1	82.9	84.3	1104	1097
15	0	0	0	82.2	82.7	1062	1085
16	0	0	0	84.4	82.7	1074	1085
17	0	0	0	83.1	82.7	1068	1085
18	0	0	0	85.6	82.7	1095	1085

Table 6.2: Coding of the independent variables

Independent variables	Levels		
	-1	0	1
FFA (wt. %) <sup>a</sup>	0	10	20
FAMES (wt. %)	0	10	20
Glycerides (wt. %)	0	2.5	5

Note: a: wt. % represents the weight percentages of experimental variables (i.e. crude glycerol impurities) in model crude glycerol.

Table 6.3: ANOVA of the first-order model for biomass conversion

Source	Degree of freedom	Mean square	F-value	Probe>F
Model	3	169.63	29.32	<0.0001*
$X_1$	1	268.32	46.38	<0.0001*
$X_2$	1	215.30	37.21	<0.0001*
$X_3$	1	25.28	4.37	0.0553
Residual	14	5.79		
Lack of fit	11	6.76	3.05	0.1946
Pure error	3	2.22		

Note:  $R^2=0.86$ ; adjusted  $R^2=0.83$

Table 6.4: ANOVA of the second-order model for polyol hydroxyl numbers

Source	Degree of freedom	Mean square	F-value	Probe>F
Model	9	44402	76.79	<0.0001 *
$X_1$	1	3993	6.91	0.0303*
$X_2$	1	1925	3.33	0.1055
$X_3$	1	41	0.07	0.7956
$X_1X_2$	1	946	1.64	0.2367
$X_1X_3$	1	378	0.65	0.4421
$X_2X_3$	1	21	0.04	0.8532
$X_1^2$	1	1054	1.82	0.2139
$X_2^2$	1	2727	4.72	0.0616
$X_3^2$	1	588	1.02	0.3429
Residual	8	578		
Lack of fit	5	801	3.89	0.1466
Pure error	3	206		

Note:  $R^2=0.99$ ; adjusted  $R^2=0.98$

Table 6.5: Verification of the developed models for predicting biomass conversion and polyol hydroxyl numbers

Samples	Organic impurities (wt. %)			Biomass conversion (%)		Polyol hydroxyl number (mg KOH/g)	
	FFA	FAME	Glycerides	Predicted	Measured	Predicted	Measured
CG-A	23.3	23.9	1.3	70.0	77.9	608	629
CG-B	7.6	12.9	6.2	80.2	82.3	1011	966

Table 6.6: Effects of organic impurities on polyol molecular weights and functionalities

Sample	Organic impurities (wt. %) <sup>a</sup>			Molecular weight (g/mol) <sup>b</sup>			$f_n^d$
	FFA	FAMEs	Glycerides	$M_n$	$M_w$	PDI	
1	0	0	0	$214 \pm 4^c$	$244 \pm 8$	$1.14 \pm 0.02$	$5.6 \pm 0.2$
2	0	0	5	$217 \pm 3$	$262 \pm 13$	$1.21 \pm 0.04$	$5.8 \pm 0.3$
3	0	20	0	$230 \pm 4$	$309 \pm 22$	$1.34 \pm 0.07$	$5.7 \pm 0.4$
4	20	0	0	$248 \pm 1$	$401 \pm 8$	$1.62 \pm 0.03$	$7.6 \pm 0.1$
5	20	20	5	$306 \pm 4$	$550 \pm 5$	$1.80 \pm 0.01$	$6.8 \pm 0.2$

Note: a: balance of 100 % being glycerol; b:  $M_n$ : number-average molecular weight;  $M_w$ : weight-average molecular weight; PDI: polydispersity; c: mean  $\pm$  standard deviation of two replicates; d: functionality

Table 6.7: Comparison between the properties of polyols and PU foams derived from acid- and base-catalyzed liquefaction processes

	B.C. <sup>c</sup> (%)	Polyol properties			PU foam properties		
		OH <sup>d</sup> (mg KOH/g)	Acid number (mg KOH/g)	Viscosity (Pa.s)	$M_w^e$ (g/mol)	Density (g/cm <sup>3</sup> )	C.S. <sup>f</sup> (kPa)
Acid <sup>a</sup>	71.2	700	28	29.2	550	0.033	121
Base <sup>b</sup>	54.2	761	<5	>100	455	0.043	157

Note; a and b: acid- and base-catalyzed liquefaction, using crude glycerol containing 55 % of glycerol, 20 % of FFA, 20 % of FAMES, and 5 % of glycerides; c: biomass conversion; d: hydroxyl number; e: weight-averaged molecular weight; f: compressive strength

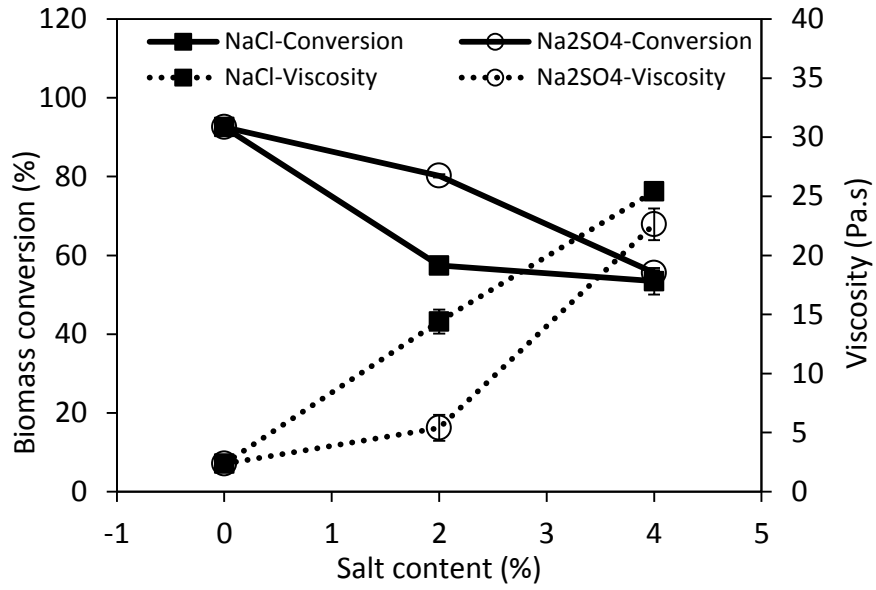


Figure 6.1: Effects of NaCl and Na<sub>2</sub>SO<sub>4</sub> on biomass conversion and viscosities of polyols

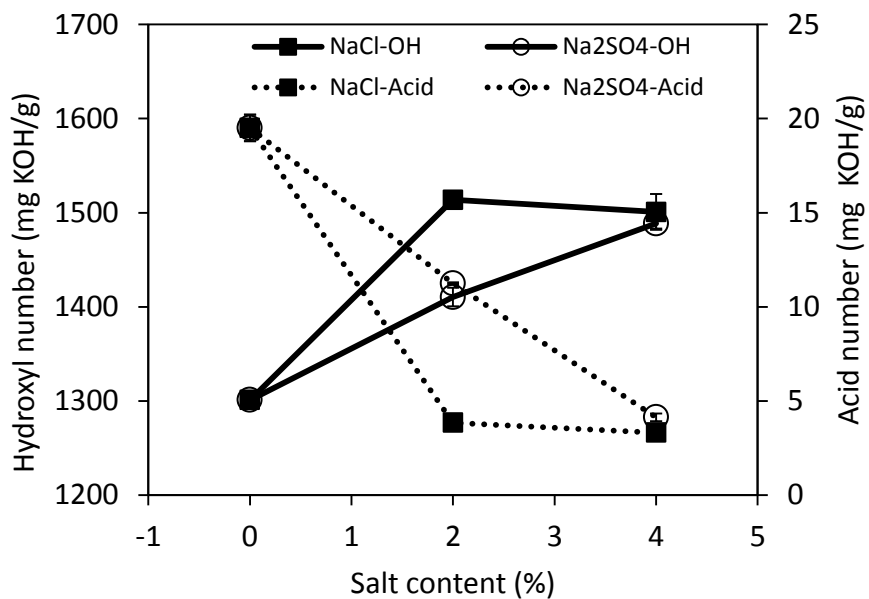


Figure 6.2: Effects of NaCl and Na<sub>2</sub>SO<sub>4</sub> on hydroxyl and acid numbers of polyols

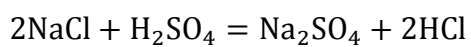
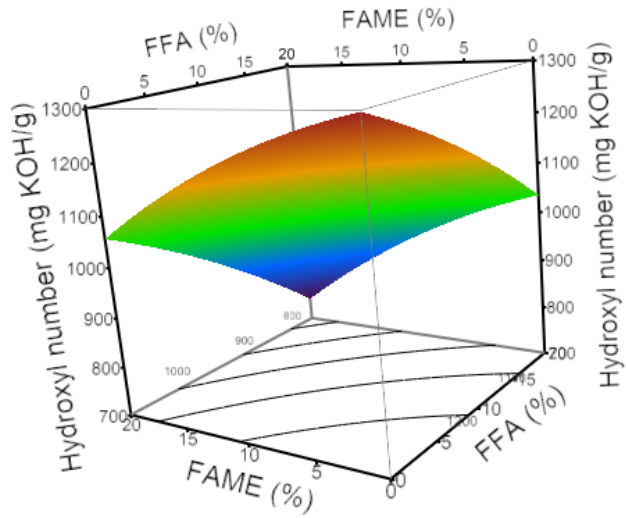
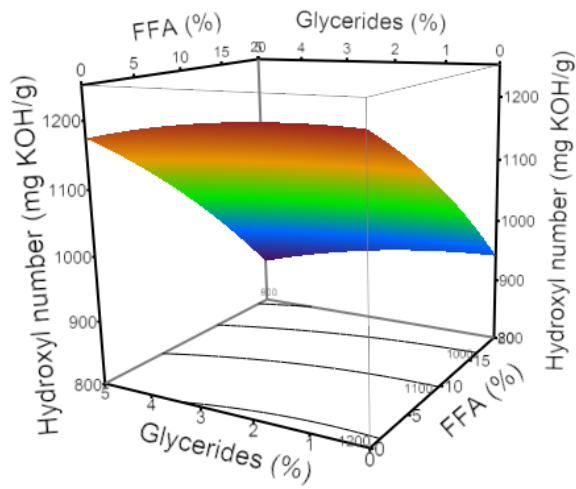


Figure 6.3: Chemical reactions occurring between salts and sulfuric acid during acid-catalyzed biomass liquefaction process



(a)

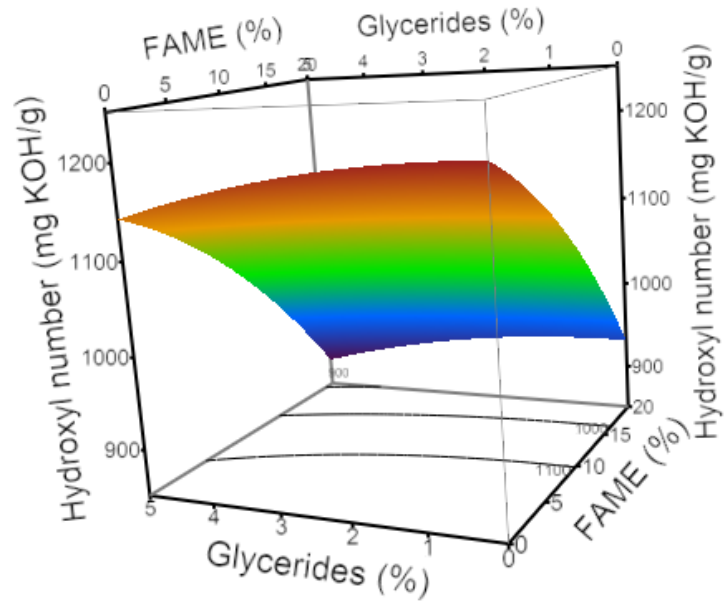


(b)

Continued

Figure 6.4: Response surface plots and its corresponding contour plots of the dependence of polyol hydroxyl numbers on: (a) FFA and FAME (at glyceride: 2.5 %); (b) FFA and glycerides (at FAMES: 10 %); (c) FAMES and glycerides (at FFA: 10 %)

Figure 6.4 continued



(c)

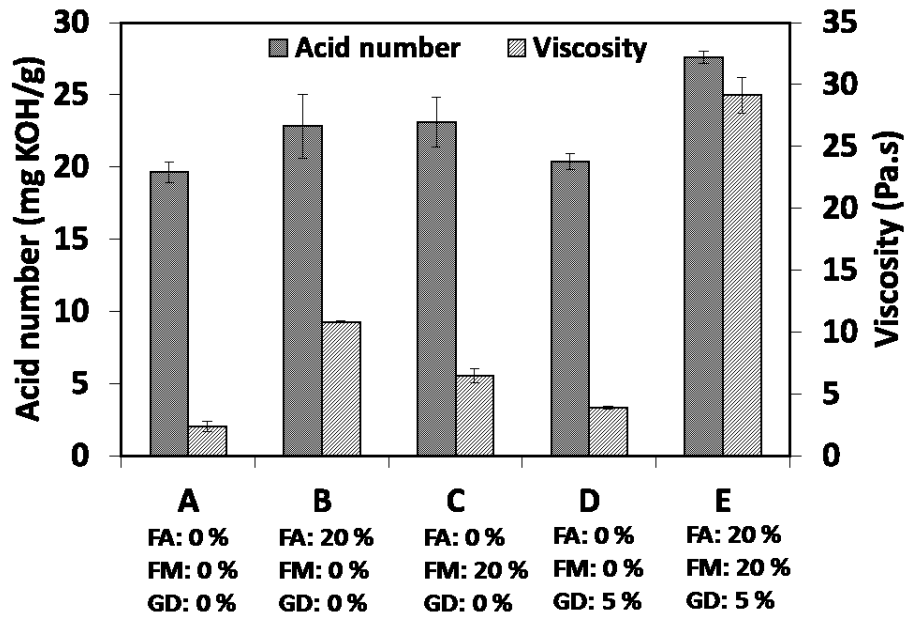


Figure 6.5: Effects of organic impurities on acid numbers and viscosities of polyols  
 (Note: FA: FFA; FM: FAMES; GD: glycerides)

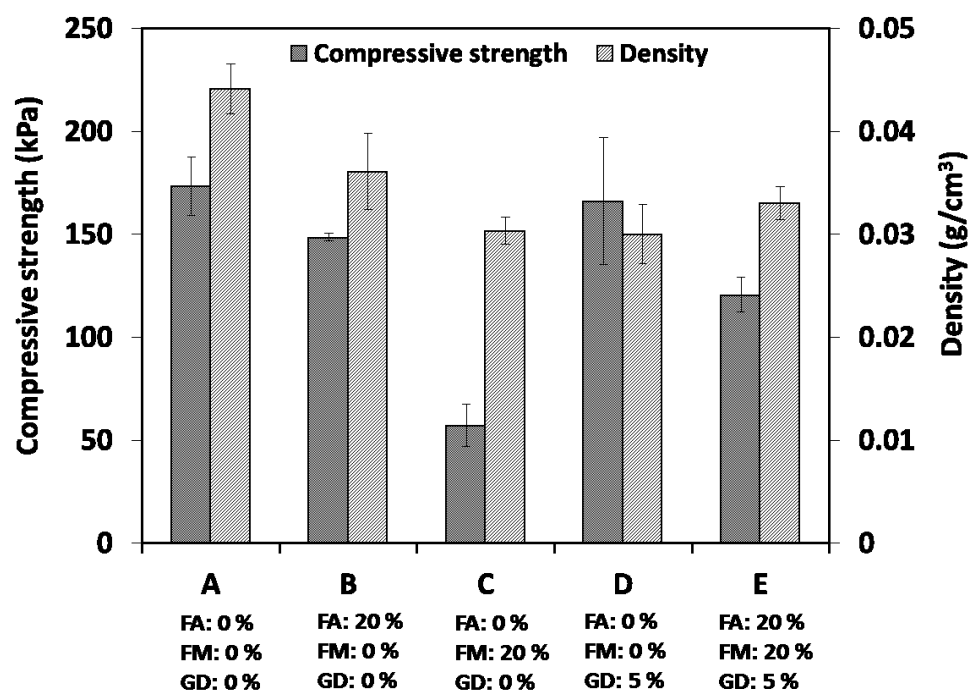


Figure 6.6: Effects of organic impurities on compressive strength and density of PU foams (Note: FA: FFA; FM: FAMES; GD: glycerides)

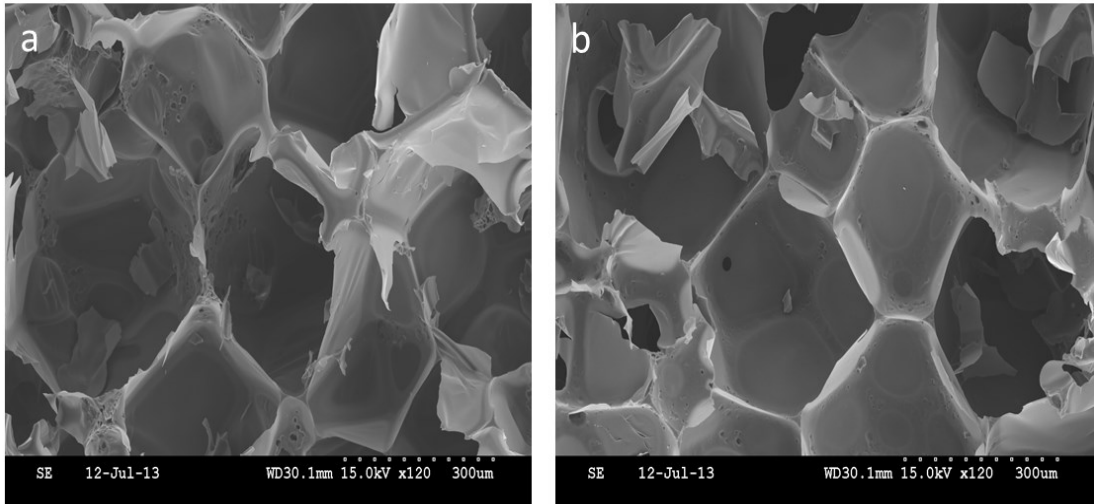


Figure 6.7: SEM images of PU foams produced from crude glycerol containing: (a) 0 % impurities; (b) 20 % FFA, 20 % FAMES and 5 % glycerides

## **Chapter 7 Polyols and PU Foams from a Two-step Sequential Liquefaction of Lignocellulosic Biomass by Crude Glycerol**

A two-step sequential process was developed for crude glycerol-based liquefaction of lignocellulosic biomass. The first acid-catalyzed process exhibited high efficiency in liquefying biomass and promoting esterification between free fatty acids (FFA) and glycerol/other hydroxylated compounds. The second base-catalyzed step mainly featured the occurrence of various condensation reactions, such as transesterification and etherification. Crude glycerol with organic impurity contents varying from 26 to 40 % were tested in the two-step process. The polyols produced showed hydroxyl numbers ranging from 536 to 936 mg KOH/g, viscosities from 20.6 to 28.0 Pa.s, and  $M_w$  from 444 to 769 g/mol. PU foams produced had density ranging from 0.04 to 0.05 g/cm<sup>3</sup>, compressive strength from 223 to 420 kPa, and thermal conductivity from 32.2 to 38.9 mW/m.k. Polyols and PU foams produced from the two-step liquefaction process had improved properties over those derived from one-step acid- or base-catalyzed liquefaction process.

### **7.1 Introduction**

To combine the advantages of both base- and acid-catalyzed liquefaction, this study aimed to develop a two-step sequential biomass liquefaction process for the production of polyols from crude glycerol and lignocellulosic biomass. The first-step

biomass liquefaction process was conducted under acid-catalysis to achieve high biomass conversion, while the second-step biomass liquefaction process was conducted under base-catalysis to produce polyols with lower residual FFA and FAMEs contents and with higher  $M_w$  and lower acid numbers. It was expected that the two-step sequential liquefaction process could help produce polyols with improved properties over those produced from one-step base- or acid-catalyzed liquefaction process.

## **7.2 Materials and Methods**

### *7.2.1 Materials*

Corn stover and other chemicals used were the same as those described in Section 5.2.1. The liquefaction solvents used in this study included one model crude glycerol (60 % glycerol, 20 % oleic acid and 20 % FAMEs) and two crude glycerol samples (CGA and B) obtained from Bio100 Technologies, LLC. (Mansfield, OH). Before being used for liquefaction, crude glycerol samples were pretreated to remove salts, water, and methanol according to the procedure described in Section 5.2.3. The composition of pretreated CG A and CG B was determined according to the procedures described in Chapter 4. Table 7.1 shows the composition of crude glycerol used in this study.

### *7.2.2 Two-step sequential liquefaction process for polyol production*

The first-step acid-catalyzed liquefaction was conducted according to the procedure described in Section 3.2.2 using the following liquefaction conditions: 150 °C, 30-165 min, 3 % wt. of H<sub>2</sub>SO<sub>4</sub> (concentrated, 98 %) and 10 % wt. of corn stover. Weight percentages were based on the weight of liquefaction solvent. After the first-step

liquefaction, the flask was immediately removed from the heating mantle, and the acid number of the obtained polyol was determined in accordance with the procedure described previously (Section 3.2.4). According to the determined acid number, a pre-determined amount of NaOH was added into the flask to reach a final NaOH content (wt. % of polyol) of 0.5 % in polyol (after neutralization of acids in polyol). Then, the flask was heated again by the heating mantle to 240 °C, and the base-catalyzed liquefaction was conducted at 240 °C for 45-180 min under a constant flow of nitrogen gas. Upon completion, polyol was obtained upon recovery from the flask. All liquefaction treatments were conducted in duplicates.

#### *7.2.3 Determination of biomass conversion*

The determination of biomass conversion was conducted according to the procedure described in Section 3.2.3.

#### *7.2.4 Characterization of liquefaction-derived polyols*

The determination of acid and hydroxyl numbers of polyols followed the procedures described in Section 3.2.4. The  $M_w$  of polyols were determined according to the procedure described in Section 5.2.6.

#### *7.2.5 Preparation and characterization of PU Foams*

PU foams were prepared according to the procedure described in Section 3.2.6. The only difference is that the mixture was poured into a plastic container (approximately 20 cm in diameter) for foaming after vigorously stirring for 15 s. The determination of

the density and compressive strength of PU foams followed the procedures described in Section 3.2.7. The thermal conductivity of PU foam was determined using a Fox 304 heat flow meter (LaserComp Inc. Saugus, MA). The temperatures of top and bottom plates were maintained 40 and 65 °C, respectively.

## **7.3 Results and Discussion**

### *7.3.1. First step: acid-catalyzed biomass liquefaction process*

In this study, unless otherwise specified, model crude glycerol (Table 7.1) was used as a liquefaction solvent to study the progression of the two-step liquefaction process. A very rapid biomass liquefaction stage was observed (79 %, 30 min) at the beginning of liquefaction process, after which biomass liquefaction proceeded at a much slower rate until reaching its maximum degree at 90 min (88.1 %) (Figure 7.1). The rapid liquefaction achieved at the first stage is largely due to the degradation of easily accessible biomass components such as lignin, hemicellulose, and amorphous cellulose, while the slower second stage mainly features the degradation of well-packed and less accessible crystalline cellulose (Lee et al., 2002; Chen and Lu, 2009; Zhang et al., 2012a). When acid-catalyzed biomass liquefaction is conducted for a prolonged reaction time, significant increases in solid residue contents are usually observed due to the occurrence of detrimental recondensations (Wang and Chen, 2007; Chen and Lu, 2009). In this study, significant decrease in biomass conversion was observed at a reaction time of 165 min (43.5 %, Figure 7.1), signifying the occurrence of detrimental recondensations. The FFA and FAMES contents in polyols decreased from 17.7 to 2.5 %

and from 17.7 to 3.3 % when liquefaction time increased from 0 to 165 min (Figure 7.1), respectively, mainly due to their reactions with glycerol/other hydroxylated compounds via esterification and transesterification (Hu et al., 2012b; Luo et al., 2013). Compared to FAMEs, FFA was consumed and converted at a faster rate during liquefaction, suggesting the faster rate of esterification than transesterification under acid-catalysis.

The acid numbers of polyols decreased significantly ( $p < 0.05$ ) from 32 to 25 mg KOH/g with increasing liquefaction time from 30 to 60 min and then stayed almost unchanged after that (Figure 7.2). The hydroxyl numbers of polyols decreased from 835 to 441 mg KOH/g for increasing liquefaction time from 30 to 165 min (Figure 7.2). The decreasing hydroxyl numbers of polyols were attributable to various complex reactions such as dehydration, condensation, and thermal oxidation that occurred among liquefaction components during the liquefaction process (Yao et al., 1996; Lee et al., 2000). Particularly, in this study, esterification and transesterification occurred between glycerol and organic impurities (i.e. FFA and FAMEs) contributed greatly to the decrease of polyol hydroxyl numbers. In summary, acid-catalyzed liquefaction process was highly effective in liquefying biomass, achieving high biomass conversion (88.1 %) under optimal liquefaction conditions (150 °C, 90 min). However, the polyol produced under the optimal conditions still contained residual FFA (3.1 %) and FAMEs (9.9 %), which are not preferred for PU applications.

### 7.3.2 Second step: base-catalyzed biomass liquefaction process

The unreacted residual FFA and FAMES present in the polyol derived from the first-step acid-catalyzed process were expected to be completely converted during the second-step base-catalyzed process. Particularly, the basic liquefaction medium could potentially accelerate the transesterification between FAMES and glycerol (Borugadda and Goud, 2012). In this study, FFA and FAMES contents in polyols produced from the second-step base-catalyzed process at different reaction times (45-180 min) were determined. All produced polyols showed low acid numbers ( $< 2$  mg KOH/g) and low FAMES content ( $< 1$  %), indicating the near-complete conversion of FFA and FAMES. Biomass conversion increased slightly from 88.1 to 92.1 % as liquefaction time increased from 0 to 45 min, and after that biomass conversion stayed almost steady (Figure 7.3). The slow liquefaction rate could be explained by the recalcitrant nature of crystalline cellulose and/or by the low liquefaction efficiency of the base-catalyzed process. The hydroxyl numbers of polyols decreased from 644 to 536 mg KOH/g when liquefaction time increased from 0 to 180 min (Figure 7.3), due to the condensation reactions occurred among liquefaction components such as transesterification, dehydration (Hu et al., 2012b; Luo et al., 2013), and etherification (Ionescu and Petrovic, 2010). As shown in Figure 7.4, glycerol contents in polyols decreased gradually with increasing liquefaction time, which further confirms the occurrence of condensation reactions. The monoglyceride contents in polyols increased significantly ( $p < 0.05$ ) from 4.0 to 14.0 % when liquefaction time increased from 0 to 45 min, after which they stayed almost unchanged until a slight decrease was observed at 180 min. The increase of monoglyceride content in polyol was

most likely due to the transesterification occurring between glycerol and FAMES and/or between glycerol and di- or tri-glycerides (Noureddini et al., 2004; Echeverri et al., 2011).

### *7.3.3 Properties of polyols produced from two-step liquefaction process*

In addition to the model crude glycerol, two industrially-derived crude glycerol samples also (CG-A and CG-B) were tested for polyol production using the developed two-step liquefaction process. The properties of the polyols produced are shown in Table 7.2. High biomass conversions (>80 %) were obtained for all polyols produced by the two-step liquefaction process. Polyol-A (produced from CG-A) had the highest biomass conversion due to the highest glycerol content of CG-A (74.0 %, Table 7.1) among all crude glycerol samples. Generally, biomass conversions obtained in this study are comparable to those obtained from petrochemical solvent-based liquefaction process. Depending on different feedstocks and liquefaction conditions, biomass conversions varying from approximately 60 to 95 % have been obtained for petrochemical solvent-based biomass liquefaction processes (Liang et al., 2006; Wang and Chen, 2007; Hassan and Shukry, 2008; Wang et al., 2008; Yan et al., 2008; Chen and Lu, 2009; Zhang et al., 2012a). Table 7.2 also shows that the hydroxyl numbers and  $M_w$  of polyols varied respectively from 536 to 936 mg KOH/g and from 444 to 769 mg KOH/g with different crude glycerol compositions. Polyol-A had the highest hydroxyl number but the lowest  $M_w$  due to the highest glycerol content of CG-A. Compared to polyol-A, polyol-M and polyol-B had lower hydroxyl numbers and higher  $M_w$  due to the higher contents of organic impurities in CG-M and CG-B.

As previously shown in Chapter 6, when crude glycerol containing 45 % of organic impurities was used as liquefaction solvent, polyols produced from the acid- and base-catalyzed biomass liquefaction processes had hydroxyl numbers of 700 and 761 mg KOH/g, and  $M_w$  of 550 and 455 g/mol, respectively (Table 6.7). In this study, CG-M and CG-B contained similar levels of organic impurity levels (approximately 40 %), but the produced polyols (polyol-M and polyol-B) had lower hydroxyl numbers and higher  $M_w$  (hydroxyl numbers of 536 and 572 mg KOH/g, and  $M_w$  of 752 and 769 g/mol, Table 7.2). This could be attributed to the intensified condensation/polymerization reactions induced by the two-step liquefaction process. The lower hydroxyl numbers and higher  $M_w$  of polyols obtained in this study are considered as beneficial for PU applications, as discussed previously. Furthermore, as shown in Table 7.2, the polyols produced from the two-step process also had low acid numbers ( $< 2$  mg KOH/g) and low viscosities (20.6 to 28.0 Pa.s) suitable for PU applications.

#### *7.3.4 Properties of PU foams derived from the two-step liquefaction process*

All polyols showed high reactivity during PU foaming process, as indicated by their short cream, tack-free, and free rise time (Table 7.3). Compared to PU-M and PU-B, PU-A had longer cream, tack-free and free rise time, suggesting the lower reactivity of polyol-A. The produced PU foams showed compressive strength ranging from 223 to 420 kPa, which were higher than those derived from base- or acid-catalyzed liquefaction process (Chapter 5 and 6). The higher compressive strength of PU foams produced in this study could be attributed to the higher functionalities ( $f_n$ : 7.2-7.8) and/or higher reactivity

of the polyols produced. These results further support that the two-step liquefaction process improved the properties of polyols and PU foams.

PU foams are excellent thermal insulation materials due to their low thermal conductivity, good dimensional stability, and good adhesion to a variety of substrates (Randall and Lee, 2002a). Hakim et al. (2011) tested the thermal conductivity of PU foams prepared from mixtures of biomass liquefaction-derived and petroleum-derived polyols. The thermal conductivity of the prepared foams decreased approximately from 35 to 28 mW/m.k with increasing density from 0.025 to 0.05 g/cm<sup>3</sup>. This was explained by the decreased radiant heat transfer due to higher density (Hakim et al., 2011). In this study, PU foams derived from crude glycerol with different compositions showed thermal conductivity ranging from 32.2 to 38.9 mW/m.k.. In general, these values were comparable to the results from the work of Hakim et al. (2011) and met the standard specifications for PU foams used for structural sandwich panel core applications (ASTM E1730-09, 2009). Among all foams, PU-A had the highest density and the lowest thermal conductivity, which agrees with the findings of Hakim et al. (2011).

Generally, PU foams are considered as thermally unstable materials due to the presence of labile urethane bonds, which usually start to degrade somewhere between 150 and 220 °C, depending on the types of isocyanates and polyols used (Lee et al., 2002). As shown in Figure 7.5, all PU foams showed TGA curves with similar shapes, suggesting their similar thermal degradation behavior. The onset of PU foam degradation (5 % weight loss) occurred at around 250 °C, which can be ascribed to the relatively unstable urethane bonds and/or pyranose rings and isocyanates (Chen and Lu, 2009;

Hakim et al., 2011; Zhao et al., 2012). The second stage degradation occurring approximately between 380 and 510 °C can be assigned to the degradation of polyol components such as derivatives of cellulose or lignin (Chen and Lu, 2009; Liu et al., 2009; Hakim et al., 2011; Zhao et al., 2012). The thermal stability and degradation behavior of PU foams produced in this study were similar to those of PU foams derived from petrochemical solvent-based liquefaction process (Lee et al., 2002; Chen and Lu, 2009; Zhao et al., 2012). For example, in the study of Zhao et al. (2012), PU foams prepared from liquefied mountain pine showed two-stages degradation that occurred at around 250 and 400 °C, respectively.

#### **7.4 Conclusions**

Polyols and PU foams with promising properties were produced from a novel two-step sequential biomass liquefaction process using crude glycerol as the liquefaction solvent. The first-step acid-catalyzed liquefaction process was highly effective in liquefying biomass and promoting the esterification reactions between FFA and glycerol/other hydroxylated compounds. The second-step base-catalyzed liquefaction process mainly featured condensation reactions, such as transesterification, dehydration, and etherification. The polyols and PU foams produced from the developed two-step liquefaction process had improved properties over their analogs derived from one-step acid- or base-catalyzed biomass liquefaction processes. In addition, the mechanical and thermal properties of the polyols and PU foams produced were comparable to those derived from petrochemical solvent-based biomass liquefaction processes.

Table 7.1: Composition of crude glycerol used in the two-step liquefaction process

Liquefaction solvents	Composition (wt. %)			
	Glycerol	FFA	FAMEs	glycerides
Model crude glycerol <sup>a</sup>	60	20	20	0
CG-A	74.0	12.4	11.5	2.1
CG-B	60.8	30.1	7.6	1.5

Note: a: oleic acid used as the model compound of FFA in model crude glycerol

Table 7.2: The properties of polyols produced the two-step liquefaction process

Polyol <sup>a</sup>	Biomass conversion (%)	Polyol properties <sup>b</sup>				
		Hydroxyl number (mg KOH/g)	Acid number (mg KOH/g)	Viscosity (Pa.s)	$M_w$ (g/mol)	$f_n$
Polyol-M	91.5 ± 2.8	536 ± 17	< 2	21.2 ± 1.1	752 ± 4	7.2
Polyol-A	97.9 ± 0.3	936 ± 11	< 2	20.6 ± 2.7	444 ± 2	7.4
Polyol-B	83.6 ± 5.9	572 ± 5	< 2	28.0 ± 5.4	769 ± 19	7.8

Note: a: Polyol-M, -A, and -B refer to polyol produced from model crude glycerol, CG-A, and CG-B (Table 7.1), respectively; b:  $M_w$ : molecular weight,  $f_n$ : functionality

Table 7.3: The properties of PU foams produced the two-step liquefaction process

PU foam <sup>a</sup>	Foaming process			PU foam properties		
	Cream time (s)	Tack-free time (s)	Free rise time (s)	Density (g/cm <sup>3</sup> )	Compressive strength (kPa)	Thermal conductivity (mW/m.k.)
PU-M	10	38	50	0.042 ± 0.000	281 ± 25	38.9 ± 5.3
PU-A	20	60	90	0.050 ± 0.000	420 ± 35	32.2 ± 1.7
PU-B	12	50	77	0.040 ± 0.001	223 ± 28	34.3 ± 3.3

Note: a: PU-M, -A, and -B refer to PU foam derived from model crude glycerol, CG-A, and CG-B (Table 7.1), respectively;

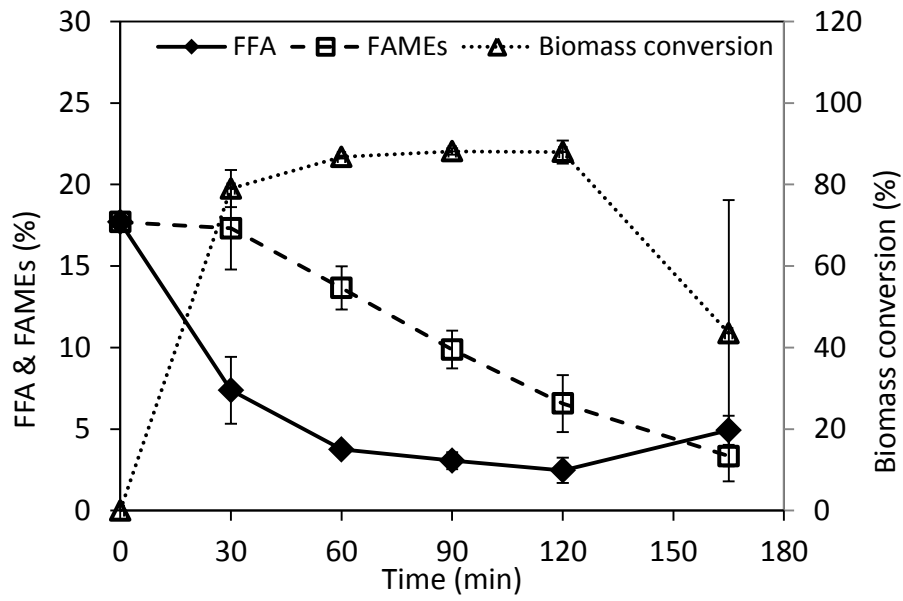


Figure 7.1: The change (s) of FFA and FAMES contents in polyols and of biomass conversion during acid-catalyzed liquefaction process

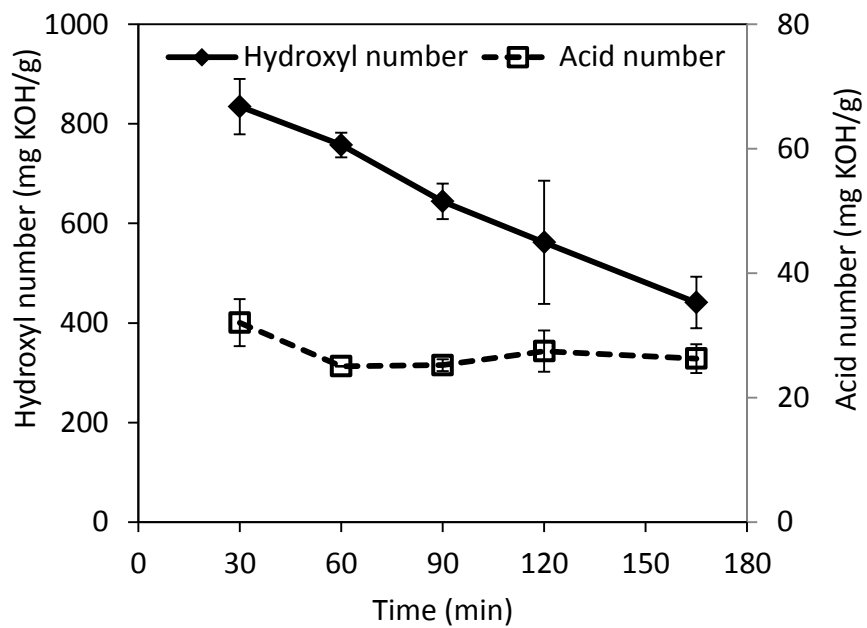


Figure 7.2: The changes of hydroxyl and acid numbers of polyols during acid-catalyzed liquefaction process

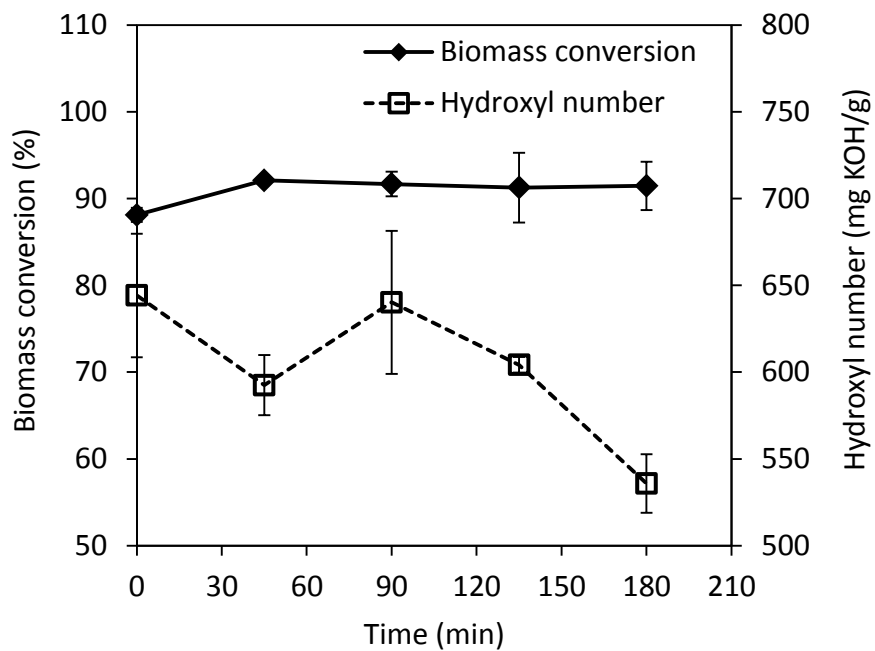


Figure 7.3: The changes of biomass conversions and polyol hydroxyl numbers during base-catalyzed liquefaction (data points at 0 min represent the properties of polyol obtained from acid-catalyzed liquefaction (150 °C, 90 min))

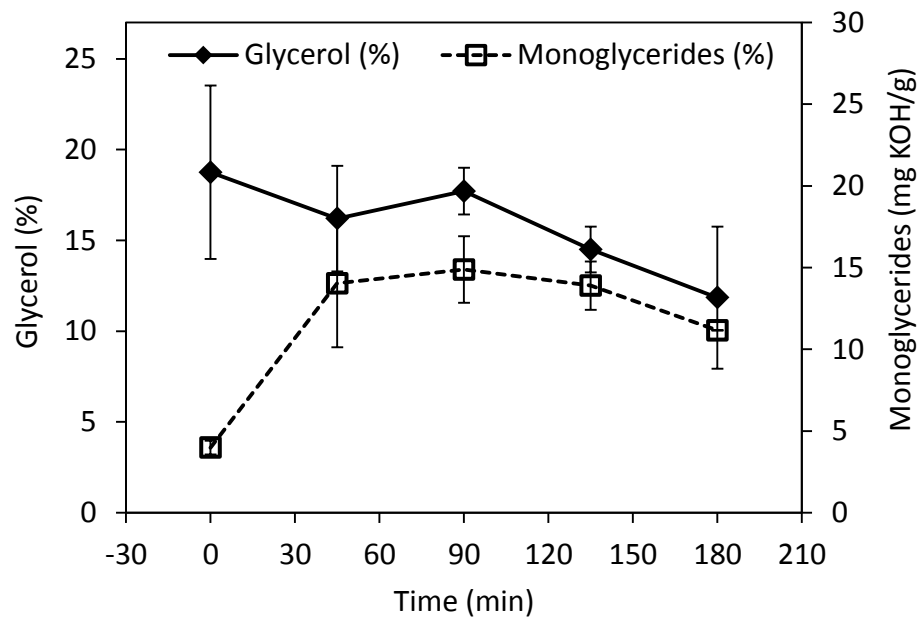


Figure 7.4: The changes of glycerol and monoglyceride contents in polyols during base-catalyzed liquefaction (data points at 0 min represent the values of polyol obtained from acid-catalyzed liquefaction (150 °C, 90 min))

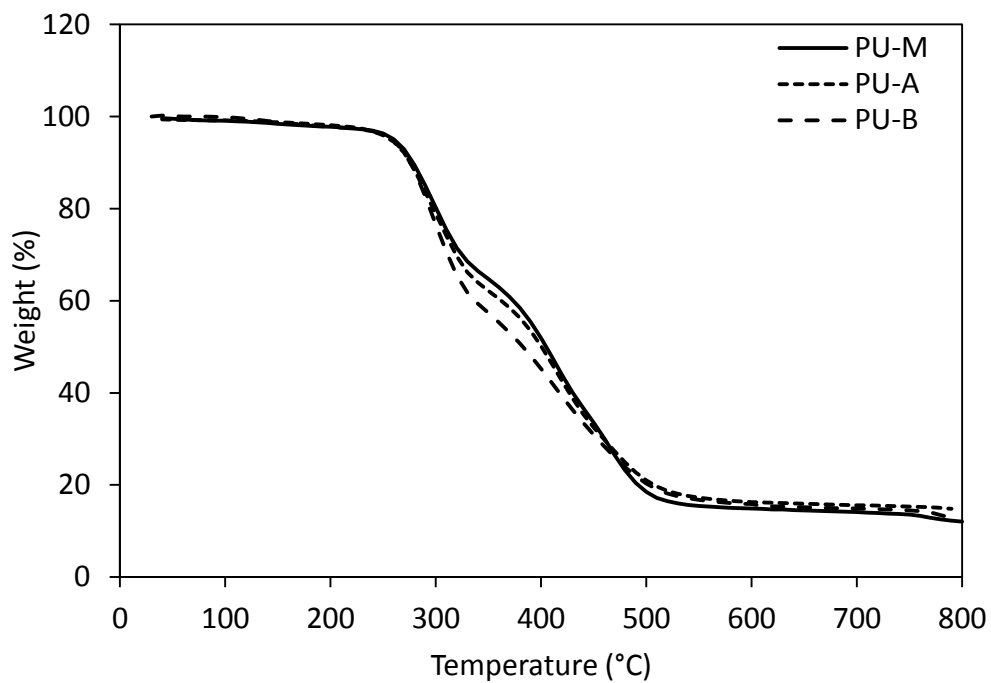


Figure 7.5: TGA curves of PU foams derived from two-step biomass liquefaction process

## Chapter 8 Polyols and Waterborne PU Dispersions from Crude Glycerol

Crude glycerol-based polyol (CG-POL) and waterborne polyurethane dispersions (CG-WPUDs) were prepared. CG-POL was produced through a thermochemical conversion process using crude glycerol as a sole feedstock. The thermochemical conversion process was optimized to achieve maximum conversion of crude glycerol impurities, mainly FFA and FAMEs, into polyol. Under optimized reaction conditions (190 °C, 120 min, and 6.6 % soap), CG-POL contained low levels of residual FFA (<1 %) and FAMEs (<2.5 %), indicating their high conversion into polyol. The CG-POL produced had a hydroxyl number of 378 mg KOH/g, functionality of 4.7, acid number of < 5 mg KOH/g, and  $M_w$  of 702 g/mol. The CG-POL was successfully used to prepare CG-WPUDs. The glass transition temperatures ( $T_g$ ) of PU films cast from CG-WPUDs increased from 63 to 81 °C with increasing hard segment contents from 41.0 to 63.2 %. The PU films produced had good thermal stability up to 240 °C. CG-WPUDs-based coatings showed excellent adhesion to steel panel surface, pencil hardness as high as F, but relatively low flexibility. This study demonstrates that crude glycerol can be used as a sole feedstock for the production of bio-based polyols and WPUDs.

### 8.1. Introduction

Although PU foams still account for the largest market share among all PU products, the market share of other PU products, such as elastomers and coatings, has

been steadily increasing (Randall and Lee, 2002d). PU coatings have been widely used in various commercial applications due to their excellent chemical, solvent, and abrasion resistance, as well as toughness combined with good low-temperature flexibility (Coutinho et al., 2001). Traditionally, PU coatings are solvent-based and present significant emissions of volatile organic compounds (VOCs). In recent years, the use of solvent-based coating systems has been largely reduced because of the increasingly stringent VOC emission regulations. As a result, environmentally-friendly PU coating technologies, such as waterborne PU dispersions (WPUDs), have been gaining increasing attention and rapid development in recent years (Bai et al., 2006; Lu and Larock, 2008; Madbouly and Otaigbe, 2009).

WPUDs are binary colloidal systems in which PU particles of very small sizes (i.e. 20-200 nm) are dispersed in a continuous phase of water (Asif et al., 2004). The high surface energy resulting from the small particle size distribution largely facilitates film formation on substrate surfaces after water evaporation with little or no VOC emissions (Lu and Larock, 2008; Wang et al., 1999). Compared to their solvent-based analogs, WPUDs have several advantages, such as low toxicity, low viscosity at high  $M_w$ , and low environmental hazards (Kim, 1996; Lu and Larock, 2008). However, WPUDs also suffer from several drawbacks, such as low hydrolytic stability, low water and solvent resistance, and low thermal stability (Kim, 1996; Bai et al., 2007; Wang et al., 2011), which can be alleviated by the increase of crosslinking density and incorporation of nanoparticles in PU (Bai et al., 2007; Bai et al., 2008; Pathak et al., 2009; Lee et al., 2011; Sow et al., 2011; Wang et al., 2011).

In recent years, concerns over the depletion and increasing prices of fossil fuels have sparked research interests in developing bio-based WPUDs from polyols derived from renewable sources. Particularly, the research group of Larock has published extensive reports in this field (Lu and Larock, 2007; Lu and Larock, 2008; Lu and Larock, 2010a; Lu and Larock, 2010b; Lu and Larock, 2011; Xia and Larock, 2011a ; Xia and Larock, 2011b; Xia and Larock, 2011c). Through the use of different vegetable oils and additives (e.g. crosslinkers, nanocomposites), the properties of vegetable oil-derived WPUDs may be customized to suit a wide range of applications. In one example, the effects of polyol functionality and hard segment content on the properties of soybean oil-derived WPUDs were evaluated (Lu and Larock, 2008). It was found that PU films derived from polyols with higher functionality and hydroxyl numbers had higher rigidity and mechanical strength due to their higher crosslinking density and stronger intermolecular hydrogen bonding (Lu and Larock, 2008). Similarly, Larock's research group also showed that incorporation of crosslinker and nanocomposites into vegetable oil-derived WPUDs also can increase mechanical strength of PU (Xia and Larock, 2011a ; Xia and Larock, 2011b). In addition, the properties of vegetable oil-derived WPUDs also can be improved or tailored through the preparation of PU/acrylic hybrid dispersions (Lu and Larock, 2007; Lu and Larock, 2011; Lu et al., 2011).

Studies presented previously (Chapter 4, 5, 6, and 7) have shown that crude glycerol, a low-value biodiesel byproduct, has great potential in liquefying lignocellulosic biomass for the production of bio-based polyols and PU foams. In this study, the feasibility of using crude glycerol as a sole feedstock for polyol production was

investigated. The crude glycerol-based polyol (CG-POL) produced was further investigated for its potential in WPUDs applications. Crude glycerol-based WPUDs (CG-WPUDs) were prepared in anionic form using dimethylol propionic acid (DMPA) as an internal emulsifier, and the effects of hard segment content on the properties of WPUDs were investigated.

## **8.2. Materials and Methods**

### *8.2.1. Materials*

Chemicals purchased from Fisher Scientific (Pittsburgh, PA) included imidazole and standard NaOH solution (0.1 N and 10 N). Chemicals purchased from Sigma Aldrich (St. Louis, MO) included phthalic anhydride, dibutyltin dilaurate (DBTDL), DMPA, isophorone isocyanate (IPDI). Chemicals purchased from Pharmco-AAPER (Shelbyville, KY) included pyridine, 1,4-dioxane, acetone, triethylamine (TEA), HPLC-grade THF (tetrahydrofuran), 98 % concentrated H<sub>2</sub>SO<sub>4</sub>. All chemicals purchased above were of reagent grade or higher purity. Crude glycerol was obtained from Bio100 Technologies, LLC. (Mansfield, OH) and determined to contain glycerol (23.1 %), soap (26.1 %), FAMEs (24.8 %), methanol (7.9 %), water (17 %), FFA (2 %), and ash (3 %).

### *8.2.2. Thermochemical conversion of crude glycerol to polyol*

Thermochemical conversion of crude glycerol to polyol was carried out in a 500-ml three-neck flask, equipped with a vacuum pump, a condenser and a thermometer under constant stirring at 500 rpm. Crude glycerol and a predetermined amount of 98 % concentrated sulfuric acid were added into the flask and then heated to desired reaction

temperature (160–190 °C) using a temperature-controlled heating mantle (Thermo Electron Corp., Madison, WI). Then, the reaction temperature was hold constantly to conduct the reaction for a predetermined reaction time (15–120 min), after which the flask was immediately removed from the heating mantle and cooled to room temperature in a fume food. Polyol was obtained upon the recovery from the flask.

### *8.2.3 Characterization of crude glycerol-based polyols*

The determination of acid and hydroxyl numbers of polyols followed the procedures described in Section 3.2.4. The  $M_w$  of polyols were determined according to the procedure described in Section 5.2.6.

### *8.2.4 Preparation of crude glycerol-based waterborne PU dispersions (CG-WPUDs)*

The preparation of CG-WPUDs was carried out at 80 °C in a 250 ml three-neck round bottom flask. Polyol (5.0 g), a pre-determined amount of DMPA and IPDI were weighed into the flask, followed by the addition of a few drops of DBTDL as catalyst and approximately 30 ml of acetone as solvent. The flask was then immersed into an oil bath kept constantly at 80 °C. A nitrogen inlet was connected to the flask to conduct the reaction under a nitrogen atmosphere and a reflux condenser was connected to reflux acetone back to the flask. The reaction was conducted until the reaction between polyol and isocyanate was completed, as indicated by the disappearance of NCO absorption peak under Fourier transform infrared spectroscopy (FT-IR). During the reaction, acetone was added as necessary to decrease the viscosity of polymer solution. After the completion of polymerization, an appropriate amount of TEA (molar ratio of

TEA/DMPA: 1.2/1) was added to the polymer solution and the reaction was conducted for 1 h at 50 °C. Then, the polymer solution was dispersed into deionized water under high-speed stirring. Acetone in the dispersion was then removed at 40 °C by a vacuum-assisted rotary evaporator. The produced CG-WPUDs had solid contents of approximately 20 %.

#### *8.2.5 Preparation and characterization of CG-WPUDs-derived PU films*

For the preparation of PU films, CG-WPUDs were poured into a Teflon-coated metal molds, air-dried in fume hood for 24 h, and then vacuum-dried at 60 °C for 24 h. FT-IR analyses of PU films were conducted on a Spectrum Two spectrometer (PerkinElmer Inc., Waltham, MA) using an attenuated total reflectance (ATR) diamond cell. All spectra obtained were ATR and baseline corrected using Spectrum 10 software. Differential scanning calorimetry (DSC) was carried out on a Q20 DSC analyzer (TA Instruments, New Castle, DE) equipped with refrigerated cooling. Each PU film sample (5.0-10.0 mg) was first heated to 100 °C to erase its thermal history, cooled to -70 °C, and then heated again to 200 °C. An equilibration time of 3 min was applied after each heating and cooling cycle at ramping rates of +/-10 °C min<sup>-1</sup>. The glass transition temperature ( $T_g$ ) was determined as the inflection point in DSC thermogram obtained in the second heating scan. The thermal stability of PU was analyzed using a Q50 Thermogravimetric Analyzer (TGA, TA Instruments, New Castle, DE). Each PU sample (8.0-15.0 mg) was heated from 30 to 800 °C at a rate of 20 °C/min under a nitrogen atmosphere. Analyses of both DSC and TGA data were conducted using Universal Analysis 2000 (TA instruments, New Castle, DE).

### *8.2.6 Characterization of the coating performance of CG-WPUDs*

CG-WPUDs were applied to phosphated cold-rolled steel panels (R-46-I, 4 × 6 × 0.032'', matte finish, Q-lab Corp., Westlake, OH) by a foam brush. The coated panels were dried in a fume hood overnight and then at 60 °C in a vacuum oven for 48 h. The tape adhesion, pencil hardness, and mandrel bending tests on coated steel panels were conducted according to ASTM D3359, ASTM D3363 and ASTM D522, respectively.

## **8.3 Results and Discussion**

### *8.3.1 Thermochemical conversion of crude glycerol to polyol*

The esterification of glycerol with fatty acids can be catalyzed by metal carboxylates, i.e. inorganic salts (e.g. sodium, potassium, zinc, etc) of fatty acids, which can act as emulsifying agents to increase the contact between reactants (i.e. glycerol and fatty acids) (Macierzanka and Szelag, 2004). In this study, soap present in crude glycerol can act as an emulsifier to improve the contact between FFA and glycerol and thus accelerate esterification reactions. In addition, soap also may act as a base catalyst to accelerate the transesterification between FAMES and glycerol. To investigate the effect of soap content on polyol production, crude glycerol (initial soap content: 26.1 %) was partially neutralized by H<sub>2</sub>SO<sub>4</sub> to different soap contents (2.5, 5, 10, and 15 %). When crude glycerol was heated to desired reaction temperature (160-190 °C), water (17 %) and methanol (7.9 %) originally existing in crude glycerol were completely removed from the liquefaction system under vacuum. As a result, the actual soap contents in liquefaction system were determined to be 3.3, 6.6, 13.3, and 20 %.

At different soap contents, the liquefaction system had different initial FFA contents (Figure 8.1) because different amounts of FFA were produced from soap acidification at different soap levels (Luo et al., 2013). FFA content in polyol decreased with increasing reaction time at all soap levels, due to the esterification occurring between glycerol and FFA (Figure 8.1). After 120 min, polyols produced at 6.6, 13.3 and 20 % soap levels exhibited low FFA contents (<2 %), while a relatively high residual FFA content (6.7 %) was observed at 3.3 % soap level. The higher residual FFA content at 3.3 % soap level may have resulted from the liquefaction system's higher initial FFA content (31.8 %) and/or by its lower soap content causing a lower catalytic effect on esterification reactions. Similarly, FAMES contents in polyols also decreased gradually with increasing reaction time at all soap levels, due to the occurrence of transesterification reactions between FAMES and glycerol (Figure 8.2), and FAMES content decreased faster at higher soap levels. After a reaction time of 120 min, the polyols produced at 13.3 and 20 % soap levels had very low FAMES contents (<1 %), whereas those at 3.3 and 6.6 % soap levels had high residual FAMES contents (>15 %). This higher residual FAMES contents at 3.3 and 6.6 % soap levels could be explained by the lower catalytic effects and/or by the stronger competition from the esterification between FFA and glycerol at lower soap levels.

The time-dependent changes of FFA and FAMES contents in polyols at different reaction temperatures (160-190 °C) are shown in Figure 8.3 and 8.4, respectively. The decrease of FFA content with increasing reaction time was relatively slow at 160 and 170 °C, and the residual FFA content was 8.8 and 6.3 %, respectively, after a reaction time of

120 min (Figure 8.3). Significant improvements in FFA conversion rates were observed when temperature increased to 180 and 190 °C, and the polyols produced at 120 min showed low FFA contents (< 2 %, Figure 8.3). The decrease of FAMEs content with increasing time was relatively slow at 160, 170 and 180 °C, and the produced polyols had high contents of residual FAMEs (>15 %) after a reaction time of 120 min (Figure 8.4). Dramatic increase in FAMEs conversion rate was observed when the reaction temperature was increased to 190 °C, and the produced polyol had a low FAMEs content of approximately 2.5 %.

Based on the results discussed above, both FFA and FAMEs were converted more rapidly at higher soap levels, due to the intensified emulsifying and/or catalytic effects of soap; however, crude glycerol with higher soap contents also led to the production of polyols with higher soap contents, which are unfavorable for PU applications. Thus, soap content in crude glycerol needs to be optimized to balance these two contradictory effects. In this study, the optimal soap content was determined to be 6.6 %, at which the produced polyols (190 °C and 120 min) showed low FFA (<1 %) and FAMEs (ca. 2.5 %) contents. Table 8.1 shows the compositions of original crude glycerol, crude glycerol after the removal of water and methanol, and crude glycerol-based polyol produced under optimized reaction conditions. The large existence of glycerides (mono- and di-) in the produced polyol supported the extensive occurrence of esterification and transesterification reactions during the thermochemical conversion process, which agrees with our previous findings (Luo et al., 2013). Characterization of the polyol produced

showed that it had a hydroxyl number of 378 mg KOH/g, functionality of 4.7, acid number of < 5 mg KOH/g, and  $M_w$  of 702 g/mol.

### *8.3.2 Production of crude glycerol-based waterborne PU dispersions (CG-WPUDs)*

Crude glycerol-based polyol (CG-POL) produced from the optimized thermochemical process had a relatively high hydroxyl number (378 mg KOH/g) and functionality (4.7), which may lead to gelation and high crosslinking of PU networks that are difficult to disperse in water (Lu and Larock, 2008). Previous studies on the synthesis of petroleum-derived WPUDs mostly used polyols with low functionalities (ca. 2.0) and a prepolymer process that uses excess isocyanate (Kim and Lee, 1996; Wang et al., 1999; Delpech and Coutinho, 2000; Coutinho et al., 2001; Nanda and Wicks, 2006; Garcia-Pacios et al., 2011; Lee et al., 2011). The use of low-functionality polyols and the prepolymer process ensures low viscosity of the polymer solution/melt, which reduces the use of organic solvents, such as acetone and methyl ethyl ketone (MEK), during polymerization process. Similarly, the synthesis of WPUDs from bio-based (i.e. mostly vegetable oil-based) polyols have been previously reported and the polyols used also had low functionalities around 2.0 (Lu and Larock, 2007; Lu and Larock, 2011); however, most of these bio-based WPUDs were synthesized using NCO/OH ratios equal or close to 1, unlike the excess isocyanates used in the prepolymer process (Lu and Larock, 2008; Lu and Larock, 2010b; Ni et al., 2010). By using this method, Lu and Larock (2008) prepared WPUDs from soybean oil-based polyols with high crosslinking density and functionality as high as 4.

In this study, the synthesis of crude glycerol-based WPUDs (CG-WPUDs) was first conducted using a literature-described prepolymer process that applies excess isocyanate (Kim and Lee, 1996). However, it was observed that a large amount of acetone-insoluble compounds were produced within 30 min of reaction at 80 °C (data not shown), probably due to the formation of highly-crosslinked PU thermosets from CG-POL ( $f_n$ : 4.7). When the polymerization was conducted at 1:1 NCO/OH molar ratio, this problem was largely resolved as long as acetone was added as necessary to keep polymer solution at low viscosity. Through this approach, no significant formation of acetone-insoluble compounds was observed during the polymerization process, and the produced CG-WPUDs showed good stability under ambient conditions.

The progression of polymerization was monitored by FT-IR at the wavenumber of 2270  $\text{cm}^{-1}$ , which is assigned to the absorption peak of the isocyanate group (-NCO) (Lu and Larock, 2010b). It can be seen that the intensity of -NCO adsorption peak at 2270  $\text{cm}^{-1}$  decreased gradually with increasing reaction time from 5 to 45 h until its complete disappearance at 45 h, suggesting completion of the polymerization (Figure 8.5). The reaction time required for completion of the polymerization (45 h) in this study was much longer than the reaction time (ca. 3 h) reported in previous studies, where WPUDs were synthesized from vegetable oil-based polyols and aromatic isocyanates (Lu and Larock, 2010b; Ni et al., 2010). This could be explained by: (a) the low reactivity of CG-POL due to the presence of secondary hydroxyl groups, which are much less reactive than primary hydroxyl groups (Ionescu et al., 2007); (b) the low reactivity of the isocyanate (i.e. IPDI) used in this study, which has the lowest reactivity among all isocyanates and is much less

reactive than aromatic isocyanates (Randall and Lee, 2002a); (c) the addition of organic solvent (i.e. acetone) into reaction system before polymerization may have led to diluted monomer concentrations in this study, while organic solvent was added after set polymerization times (0.5 to 3 h) in previous studies (Lu and Larock, 2008; Lu and Larock, 2010b; Ni et al., 2010).

### *8.3.3 Properties of PU films cast from CG-WPUDs*

Hydrogen bonding, formed between the N-H of the amide group and the urethane carbonyl, the ether oxygen, or the carbonyl group in PU, has significant impacts on PU properties (Lu and Larock, 2008). A higher degree of hydrogen bonding, due to increased polyol functionality or hard segment content in PU, has been found to lead to stronger crosslinking, higher  $T_g$  and higher mechanical strength of PU films (Lu and Larock, 2008). FT-IR is a powerful tool for examining the presence and relative intensity of hydrogen bonding in PU. The characteristic absorption peaks of the stretching of -NH ( $3300\text{-}3500\text{ cm}^{-1}$ ) and -NCO ( $1700\text{-}1740\text{ cm}^{-1}$ ) groups in PU are particularly useful for this purpose (Lu and Larock, 2008; Lu and Larock, 2010b). The strong absorption peaks at  $3353\text{ cm}^{-1}$  and at  $1709$  and  $1727\text{ cm}^{-1}$  in the spectra of four PU films with different hard segment contents can be attributed to the stretching of hydrogen bonded -NH and -C=O, respectively (Figure 8.6) (Sung and Schneider, 1977; Srichatrapimuk and Cooper, 1978; Pollack et al., 1989; Pattanayak and Jana, 2005; Lu and Larock, 2008). In contrast, the relatively weak absorption peaks at  $3464$  and  $1739\text{ cm}^{-1}$  were assigned to the stretching of free -NH and -C=O groups in PU, respectively. These results suggest that most -NH and -C=O groups in PU are hydrogen bonded, which is in good agreement

with previous reports on soybean oil-derived PU (Lu and Larock, 2008; Lu and Larock, 2010b). The spectra of all four PU films showed similar absorption peaks of  $\text{-C=O}$  stretching, indicating their similar degrees of hydrogen bonding (Figure 8.6).

No melting or crystallization peaks were observed in any PU films cast from CG-WPUDs for temperatures up to 200 °C, indicating the amorphous structures of PU films (Figure 8.7). The  $T_g$  of CGPU-63.5 and CGPU-58.2 were determined to be 81 and 76 °C, respectively. The addition of a commercial polyether polyol (hydroxyl number: 34 mg KOH/g;  $f_n$ : 2.6) into WPUD formulations helped produce PU films with lower  $T_g$  (PCGPU-51.5: 69 °C; PCGPU-41: 66 °C), due to the increased chain flexibility imparted by polyether chains. In general, the  $T_g$  of PU produced in this study increased with increasing hard segment content in PU (Table 8.1 and 8.3), which agrees well with previous findings on vegetable oil-based PU (Lu and Larock, 2008). The increased  $T_g$  at higher hard segment content was attributed to the increased crosslinking density in PU causing a restriction on the mobility of polymer chains (Zlatanic et al., 2004; Lu and Larock, 2008). The  $T_g$  of prepared PU films cast from soybean oil-based WPUDs increased from 8.9 to 33.5 °C with increasing polyol functionalities ( $f_n$ : 2.4-4.0) and hydroxyl numbers (135-200 mg KOH/g) (Lu and Larock, 2008). The relatively higher  $T_g$  (66-81 °C) observed in this study can be attributed to the higher functionality ( $f_n$ : 4.7) and higher hydroxyl number (378 mg KOH/g) of CG-POL. PU networks prepared from high-functionality linseed oil-based polyol (hydroxyl number: 248 mg KOH/g;  $f_n$ : 6.4) showed a similarly high  $T_g$  of 77 °C (Zlatanic et al., 2004).

Figure 8.8 and 8.9 show the TGA and derivative TGA curves of PU films cast from CG-WPUDs, respectively. Generally, PU are considered to have low thermal stability due to the presence of labile urethane bonds, which usually start to degrade at temperatures between 150 and 220 °C, depending on the types of isocyanates and polyols used in PU production (Lee et al., 2002). The dissociation of urethane bonds have been previously proposed to follow three mechanisms: dissociation to isocyanate and alcohol, formation of primary amine and olefin, and formation of secondary amine (Javni et al., 2000). In this study, PU films exhibited two major degradation stages (Figure 8.9), similar to the degradation behavior of vegetable oil-derived PU (Lu and Larock, 2008; Ni et al., 2010; Javni et al., 2000). This similarity could be attributed to the fact that CG-POL and vegetable oil-based polyols contain similar structural components such as glycerol backbone and fatty acid side chains. The first stage occurred between 240 and 310 °C can be attributed to the degradation of urethane linkages in PU, whereas the second stage occurred between 310 and 470 °C were mostly like caused by the chain scission of polymer chains in polyols (CG-POL, DMPA, and commercial polyether polyol) (Lu and Larock, 2008). As shown in Table 8.3, both  $T_5$  (5 % weight loss temperature) and  $T_{50}$  (50 % weight loss temperature) of the PU decreased with increasing hard segment contents, due to the higher content of urethane linkages in PU with higher hard segment contents (Lu and Larock, 2008). In general, PU films cast from CG-WPUDs showed thermal stability comparable to their analogs derived from vegetable oils (Javni et al., 2000; Lu and Larock, 2008; Ni et al., 2010).

#### 8.3.4 Coating performance of CG-WPUDs

All crude glycerol-based PU coatings showed excellent adhesion to steel surface and no coatings were removed from the surface by tape (5B) (Table 8.3). All PU coatings, except PCGPU-41, showed F grade pencil hardness. The lower hardness of PCGPU-41 (2B) can be explained by its higher content (Table 8.1) of polyether polyol which is much more flexible than CG-POL. PU coatings prepared from soybean oil glyceride and hybrid glyceride amide polyols exhibited pencil hardness (F) and tape adhesion properties (5B) similar to the results obtained in this study (Benecke et al., 2008). The Mandrel bending test results showed that incorporation of flexible polyether polyol improved the flexibility of CG-WPUDs-based coatings. The low flexibility of CG-WPUDs-based coatings was largely resulted from the high functionality, high hydroxyl number, low  $M_w$ , and the relatively rigid molecular chains of CG-POL.

### 8.4 Conclusions

Thermochemical conversion of crude glycerol to polyol was optimized to produce CG-POL with low contents of residual FFA (<1 %) and FAMES (<2.5 %). CG-WPUDs with different hard segment contents were synthesized from CG-POL alone or CG-POL partially substituted by a commercial polyether polyol. PU films cast from CG-WPUDs showed increasing  $T_g$  but decreasing thermal stability with increasing hard segment contents. Generally, PU films cast from CG-WPUDs had higher  $T_g$  (63-81 °C) and similar thermal stability, when compared to vegetable oil-derived PU. CG-WPUDs-based coatings showed excellent adhesion to steel surface, good hardness, but low flexibility. The flexibility of CG-WPUDs-based coatings can be improved by incorporation of

flexible polyether polyols. This study suggests that biodiesel-derived crude glycerol can be used as a potential feedstock to produce bio-based polyols and WPUDs.

Table 8.1: Formulation of crude glycerol based waterborne polyurethane dispersions (CG-WPUDs) prepared from crude glycerol-based polyol (CG-POL)

Samples <sup>a</sup>	Relative molar ratio to hydroxyl groups in CG-POL				HS <sup>c</sup> (%)	DMPA <sup>d</sup> (%)
	NCO	OH (CG-POL)	OH (DMPA)	OH <sup>b</sup>		
CGPU-63.2	1.6	1	0.6	0	63.2	10.8
CGPU-58.2	1.4	1	0.4	0	58.2	8.1
PCGPU-51.5	1.43	1	0.4	0.03	51.5	6.6
PCGPU-41	1.5	1	0.4	0.1	41.0	5.0

Note: a: CGPU-63.2 and -58.2: WPUDs based solely on CG-POL; PCGPU-51.5 and -41: WPUDs based on CG-POL partially substituted by a commercial polyether polyol; number after dash indicates hard segment content in PU; b: hydroxyl groups from commercial polyether polyol (hydroxyl number: 34 mg KOH/g); c: hard segment; d: dimethylol propionic acid (DMPA).

Table 8.2: Composition of crude glycerol and CG-POL

Samples	Crude glycerol	Crude glycerol after the removal of water and methanol <sup>b</sup>	Polyol (CG-POL)
Free glycerol (wt %)	23.1 ± 0.2 <sup>a</sup>	30.8 ± 0.2	11.0 ± 0.2
Methanol (wt %)	7.9 ± 0.5	0	BDL <sup>c</sup>
Water (wt %)	17.0 ± 0.1	0	BDL
Soap (wt %)	26.1 ± 0.2	34.8 ± 0.2	6.1 ± 0.1
FAMES (wt %)	24.8 ± 0.3	33.0 ± 0.3	2.5 ± 0.0
FFA (wt %)	2.0 ± 0.2	2.7 ± 0.2	0.6 ± 0.1
Monoglycerides (wt %)	BDL <sup>b</sup>	BDL	33.8 ± 1.0
Diglycerides (wt %)	BDL	BDL	21.1 ± 0.4

Note: a: mean ± standard deviation of two replicates; b: the composition was calculated by subtracting the amounts of methanol and water from the total amount of crude glycerol; c: below the detection limit.

Table 8.3: Thermal properties of CG-WPUDs-derived PU films and coating performance of CG-WPUDs

Samples	DSC	TGA <sup>a</sup>		Coating performance		
	$T_g$ (°C)	$T_5$ (°C)	$T_{50}$ (°C)	Tape adhesion	Pencil hardness	Mandrel Bending at 3/8 in.
CGPU-63.2	81	235	295	5B	F	Fail
CGPU-58.2	76	238	300	5B	F	Fail
PCGPU-51.5	69	243	308	5B	F	Fail
PCGPU-41	66	253	363	5B	2B	Pass

Note: a:  $T_5$  and  $T_{50}$ : 5 and 50 % weight loss temperature

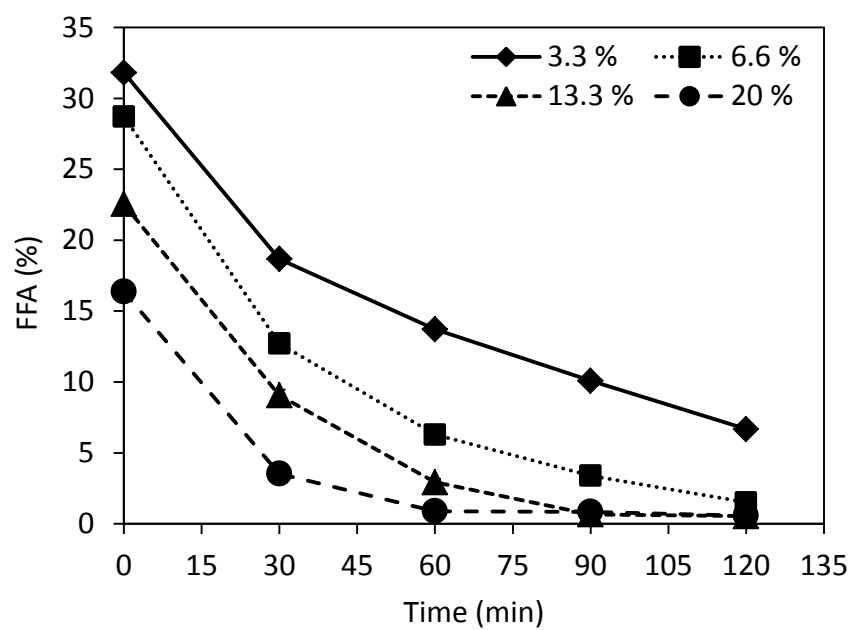


Figure 8.1: Time-dependent changes of FFA contents in polyols at different soap levels (3.3 to 20 %, reaction temperature: 180 °C)

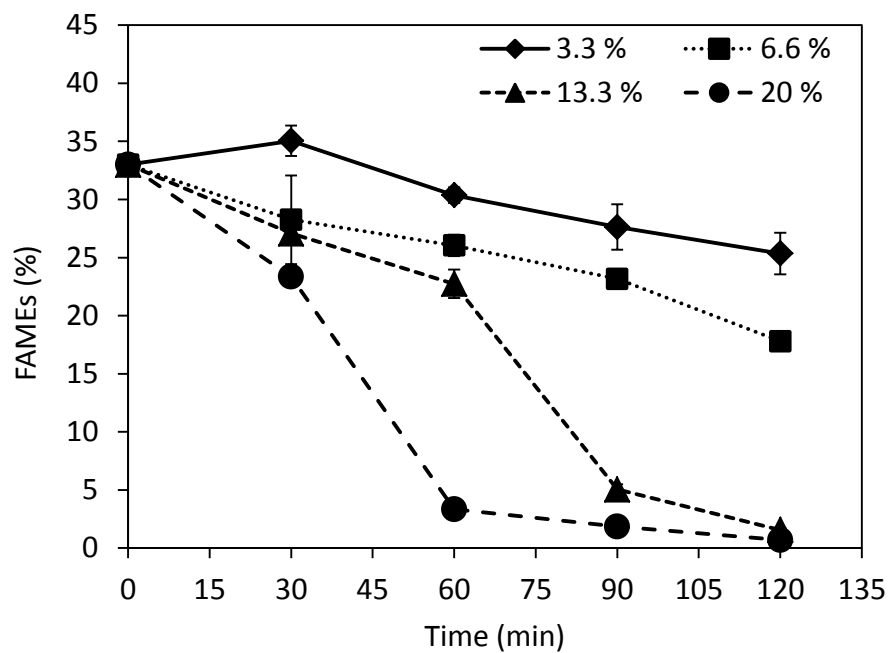


Figure 8.2: Time-dependent changes of FAMES contents in polyols at different soap levels (3.3 to 20 %, reaction temperature: 180 °C)

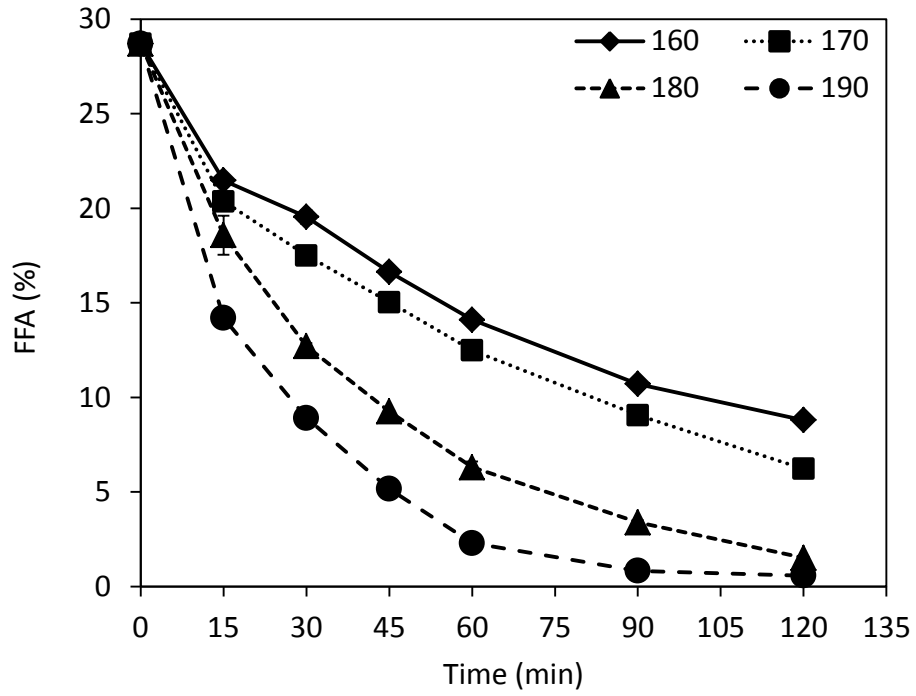


Figure 8.3: Time-dependent changes of FFA contents in polyols at different reaction temperatures (160-190 °C, soap content: 6.6 %)

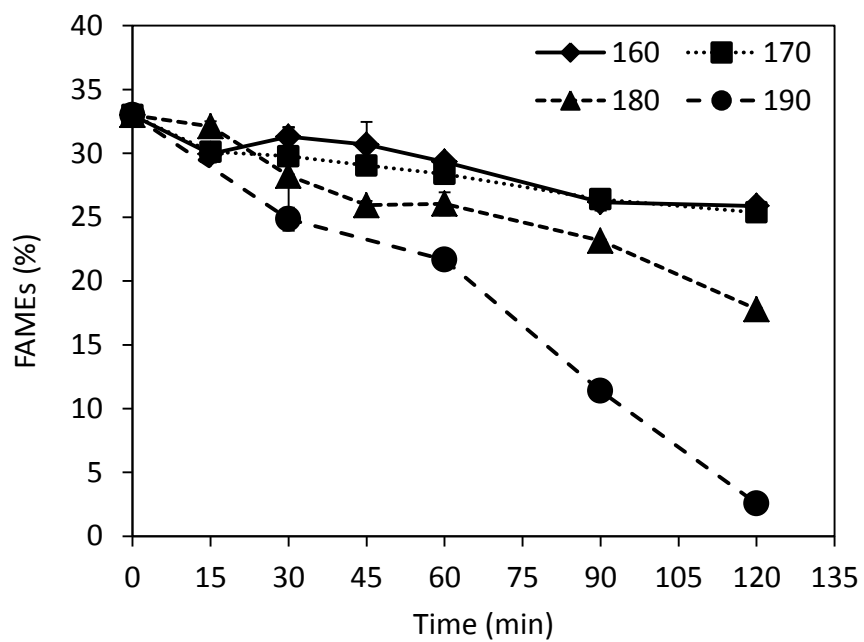


Figure 8.4: Time-dependent changes of FAMES contents in polyols at different reaction temperatures (160-190 °C, soap content: 6.6 %)

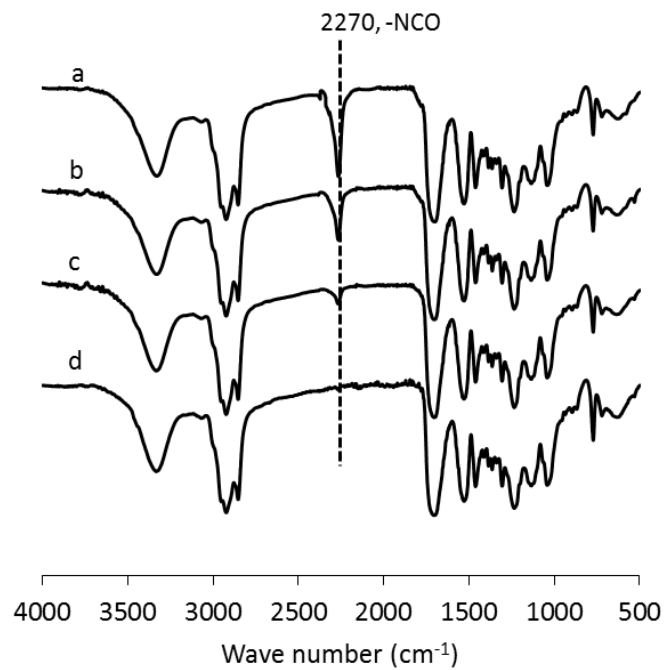


Figure 8.5: FT-IR spectra of CGPU-63.2 at different reaction time: a: 5 h; b: 10 h; c: 24 h; d: 45 h

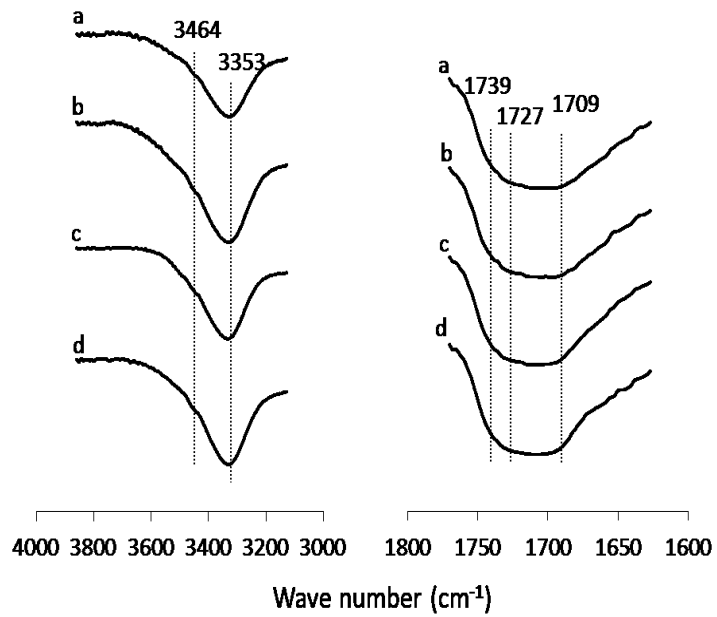


Figure 8.6: FT-IR spectra of CG-WPUDs-derived PU films: (a): CGPU-63.2, (b) CGPU-58.2, (c) PCGPU-51.5, (d) PCGPU-41

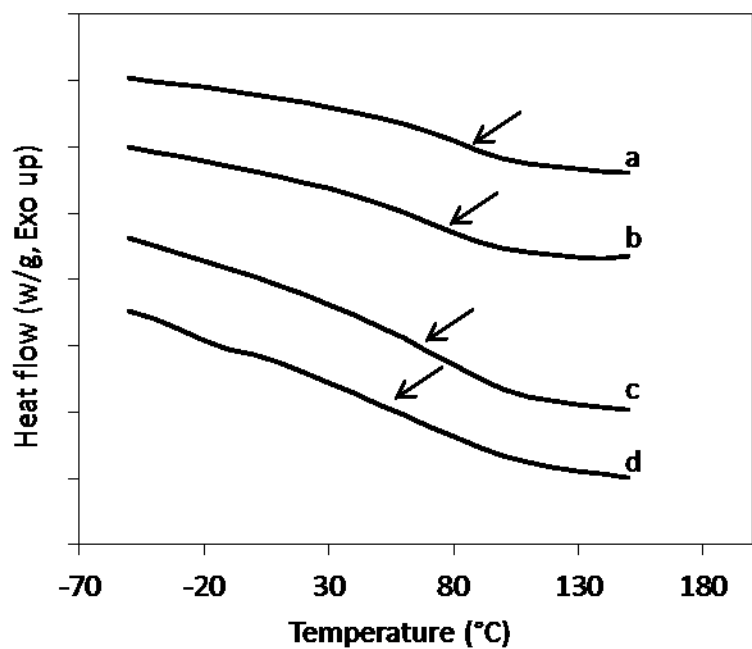


Figure 8.7: DSC thermograms of CG-WPUDs-derived PU films: (a): CGPU-63.2, (b) CGPU-58.2, (c) PCGPU-51.5, (d) PCGPU-41

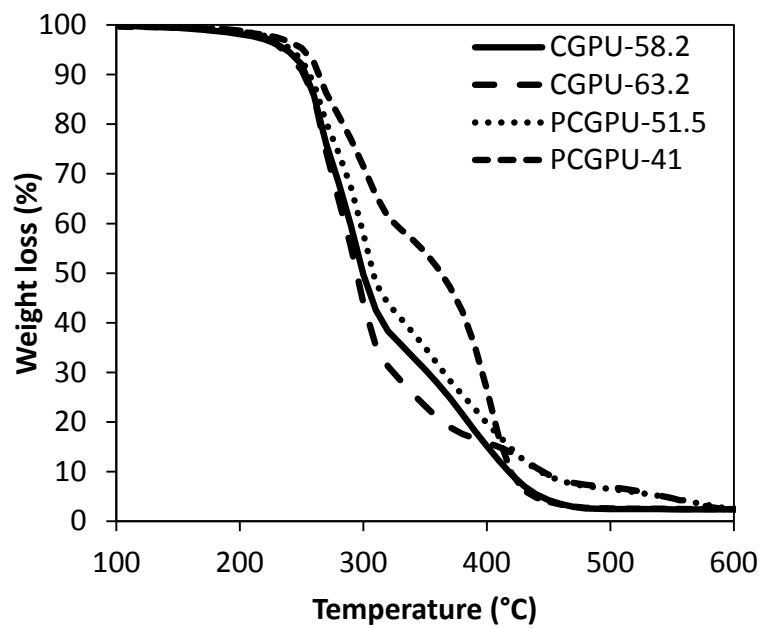


Figure 8.8: TGA curves of CG-WPUDs-derived PU films

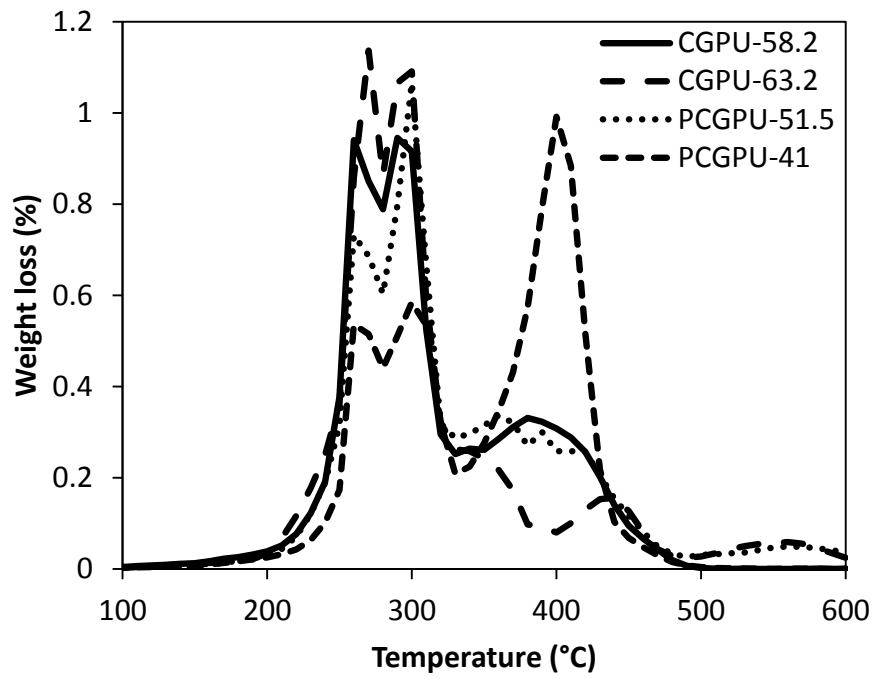


Figure 8.9: Derivative TGA curves of CG-WPUDs-derived PU films

## **Chapter 9 Conclusions and Suggestions for Future Research**

### **9.1 Conclusions**

Crude glycerol, as a low-cost byproduct from biodiesel industry, has great potential to produce bio-based polyols and PU with excellent properties. Original unpurified crude glycerol, along with lignocellulosic biomass, can be converted to high-quality polyols through base-catalyzed, acid-catalyzed, or two-step biomass liquefaction processes. To ensure the success of this conversion, the contents of organic impurities in crude glycerol, particularly FFAs/soap and FAMEs, need to be controlled at optimal levels, which differ depending on the types of liquefaction process used. Under optimal liquefaction conditions, FFA and FAMEs react synergistically with glycerol and/or biomass components to greatly improve the properties of the polyols produced. In general, polyols derived from crude glycerol and lignocellulosic biomass are particularly suited to rigid or semi-rigid PU foam applications. Crude glycerol also can be used as a sole feedstock for polyol production via a thermochemical conversion process. The polyol produced can be used to produce waterborne PU dispersions.

Industrially-derived crude glycerol has wide compositional variations due to different production practices employed by different biodiesel plants. Five industrial crude glycerol samples characterized in this study showed glycerol contents varying widely between 22.9 and 63.0 %, implying the significant presence of impurities. These

impurities mainly consisted of water, methanol, FAMEs, soap, FFAs, glycerides, and ash (inorganic salts), and their proportions in crude glycerol varied widely with crude glycerol origin. The wide compositional variations of crude glycerol present significant challenges for producing polyols and PU with consistent and tunable properties. This issue was successfully addressed through studying the effects of crude glycerol impurities on the properties of liquefaction-derived polyols and PU foams.

Both similarities and differences existed between the effects of crude glycerol impurities in base- and acid-catalyzed liquefaction processes. For base-catalyzed process, salt impurities, including  $\text{Na}_2\text{SO}_4$  and  $\text{NaCl}$ , had no significant effects on biomass conversion and polyol properties. In contrast, salt impurities negatively affected the properties of polyols in acid-catalyzed process. Organic impurities, particularly FFA and FAMEs, were strong factors determining the properties of polyols and PU foams derived from both base- and acid-catalyzed processes. The presence of FFA and FAMEs in crude glycerol was essential to produce polyols with hydroxyl numbers and  $M_w$  appropriate for rigid or semi-rigid PU foam applications. For the base-catalyzed process, crude glycerol with 45-70 % of organic impurities was suitable for producing polyols and PU foams with promising properties, whereas crude glycerol with 40-50 % of organic impurities was optimal for the acid-catalyzed process. The acid-catalyzed process had a higher biomass liquefaction efficiency than the base-catalyzed process, but produced polyols with higher acid numbers ( $> 20$  mg KOH/g). The base-catalyzed process had the advantages of producing polyols with low acid numbers ( $< 5$  mg KOH/g) suitable for PU applications and of being capable of using crude glycerol with low glycerol content ( $< 50$

%) as liquefaction solvents.

A two-step, sequential, crude glycerol-based biomass liquefaction process was developed to effectively combine the advantages of both acid- and base-catalyzed biomass liquefaction processes. The first-step acid-catalyzed process featured rapid biomass liquefaction and extensive esterification reactions between FFA and glycerol/other hydroxylated compounds. The second-step base-catalyzed process mainly featured various condensation reactions such as transesterification, dehydration, and etherification that occurred among liquefaction components. The developed two-step liquefaction process greatly improved the properties of produced polyols and PU foams over their analogs derived from acid- or base-catalyzed process alone.

Crude glycerol alone also can be converted to polyol via thermochemical conversion. The optimized thermochemical process was capable of achieving high conversion of FFA and FAMES (> 95 %) into polyols via esterification and transesterification reactions. The polyols had low contents of residual FFA (<1 %) and FAMES (<2.5 %) and were successfully used to prepare crude glycerol-based waterborne PU dispersions (CG-WPUDs). Generally, CG-WPUDs-based coatings had good thermal stability, adhesion and hardness properties, but suffered from low flexibility. The flexibility of CG-WPUDs based coatings can be improved by incorporation of flexible polyether polyols. This study further expanded the potential application of crude glycerol in polyol and PU preparation.

In summary, crude glycerol and lignocellulosic biomass have the potential to produce polyols and PU foams with properties comparable to their analogs derived from

petrochemical solvent-based liquefaction process. To produce polyols and PU foams with optimal properties, the levels of organic impurities in crude glycerol need to be controlled at optimal levels.

## 9.2 Suggestions for future research

Results obtained in this dissertation have provided strong data that support the potential of producing high-quality polyols and PU products from crude glycerol and lignocellulosic biomass. Nevertheless, challenges still exist and future work can greatly contribute to this field.

The crucial roles of FFA and FAMEs in crude glycerol-based polyol production lie on their synergistic reactions with glycerol, which help produce polyols with appropriate hydroxyl numbers and  $M_w$ . However, due to their mono-functionalities, FFA and FAMEs are unable to facilitate sufficient polymerizations to produce polyols with high  $M_w$  suitable for flexible PU applications. In addition, the long aliphatic chains of FFA and FAMEs present in polyol structures may serve as dangling components in PU, leading to decreased mechanical strength. Therefore, it is of great interest to apply further chemical modifications to increase the functionalities of FFA and FAMEs. This can be achieved by modifying double bonds present in aliphatic chains of FFA and FAMEs via methods such as epoxidation/ring opening, hydroformylation, and ozonolysis. These methods are proven processes that have been commonly used in producing vegetable oil-based polyols and have a great chance of success. Ideally, the modified FFA and FAMEs with higher functionalities could facilitate stronger polymerizations to produce polyols with higher  $M_w$  and lower contents of dangling chains.

Compared to the extensive attention paid to the effects of crude glycerol impurities on polyol and PU properties, investigations on the effects of lignocellulosic or other types of biomass on polyol and PU properties are lacking. Similar to crude glycerol, lignocellulosic biomass compositions vary with their origins (species, growth conditions, etc), which could result in significant variations in biomass liquefaction efficiency and product properties. In addition, rapid advances in the field of biofuels (ethanol, biodiesel, etc) have generated a huge amount of biorefinery-derived byproducts like dried distillers grains with solubles (DDGS), sugarcane bagasse, and lignin-rich biomass residues. Due to their very different compositions than traditional lignocellulosic biomass, these byproducts might exert dramatically different effects on crude glycerol-based liquefaction processes. Therefore, future studies investigating the effects of biomass composition on the properties of liquefaction-derived polyols and PU can greatly contribute to understanding the robustness of crude glycerol-based biomass liquefaction processes.

The CG-WPUDs based coatings produced in this study showed relatively rigid structures, high glass transition temperatures ( $T_g$ ), and low flexibility due to the high hydroxyl number and functionality ( $f_n$ ) of crude glycerol-based polyol. Future work to produce crude glycerol-based polyols with lower hydroxyl numbers and lower functionalities would be valuable for the production of CG-WPUDs with improved flexibility. One possible approach would be to carefully control the molar ratios between glycerol, FFA, and FAMES and to optimize thermochemical conversions to allow the production of polyols with high contents of monoglycerides ( $f_n: 2$ ).

Lastly, since both crude glycerol and lignocellulosic biomass are low-cost renewable materials, their uses in polyol and PU production may provide the benefits of high cost-effectiveness and reduced carbon footprint. However, life cycle analysis would be needed to justify these claims.

## References

- Ahvazi, B., Wojciechowicz, O., Ton-That, T., Hawari, J., 2011. Preparation of Lignopolyols from Wheat Straw Soda Lignin, *J. Agric. Food Chem.* 59, 10505-10516.
- Akiyama, M., Sato, S., Takahashi, R., Inui, K., Yokota, M., 2009. Dehydration-hydrogenation of glycerol into 1,2-propanediol at ambient hydrogen pressure, *Appl. Catal. A-Gen.* 371, 60-66.
- Alhanash, A., Kozhevnikova, E.F., Kozhevnikov, I.V., 2010. Gas-phase dehydration of glycerol to acrolein catalysed by caesium heteropoly salt, *Appl. Catal. A-Gen.* 378, 11-18.
- Alma, M.H., Shiraishi, N., 1998. Preparation of polyurethane-like foams from NaOH-catalyzed liquefied wood, *Holz Als Roh-Und Werkstoff.* 56, 245-246.
- Amada, Y., Koso, S., Nakagawa, Y., Tomishige, K., 2010. Hydrogenolysis of 1,2-Propanediol for the Production of Biopropanols from Glycerol, *ChemSusChem.* 3, 728-736.
- Anand, P., Saxena, R.K., 2012. A comparative study of solvent-assisted pretreatment of biodiesel derived crude glycerol on growth and 1,3-propanediol production from *Citrobacter freundii*, *New Biotechnology.* 29, 199-205.
- Aniceto, J.P.S., Portugal, I., Silva, C.M., 2012. Biomass-Based Polyols through Oxypropylation Reaction, *Chemsuschem.* 5, 1358-1368.
- AOCS Ca 14-56, 1997. AOCS Official Method Ca 14-56: Total, Free and Combined Glycerol Iodometric-Periodic Acid Method.
- Asad-ur-Rehman, Saman, W.R.G., Nomura, N., Sato, S., Matsumura, M., 2008. Pre-treatment and utilization of raw glycerol from sunflower oil biodiesel for growth and 1,3-propanediol production by *Clostridium butyricum*, *J. Chem. Technol. Biotechnol.* 83, 1072-1080.
- Asif, A., Huang, C.Y., Shi, W.F., 2004. Structure-Coproperty study of waterborne, polyurethane acrylate dispersions based on hyperbranched aliphatic polyester for UV-curable coatings, *Colloid Polym. Sci.* 283, 200-208.

ASTM D6584-10a, 2010. ASTM D6584-10a: Standard Test Method for Determination of Total Monoglyceride, Total Diglyceride, Total Triglyceride, and Free and Total Glycerin in B-100 Biodiesel Methyl Esters by Gas Chromatography.

ASTM E1730-09, 2009. ASTM E1730-09: Standard Specification for Rigid Foam for Use in Structural Sandwich Panel Cores.

Athalye, S.K., Garcia, R.A., Wen, Z., 2009. Use of Biodiesel-Derived Crude Glycerol for Producing Eicosapentaenoic Acid (EPA) by the Fungus *Pythium irregulare*, *J. Agric. Food Chem.* 57, 2739-2744.

Bai, C.Y., Zhang, X.Y., Dai, J.B., Li, W.H., 2006. A new UV curable waterborne polyurethane: Effect of C=C content on the film properties, *Progress in Organic Coatings*. 55, 291-295.

Bai, C.Y., Zhang, X.Y., Dai, J.B., Zhang, C.Y., 2007. Water resistance of the membranes for UV curable waterborne polyurethane dispersions, *Progress in Organic Coatings*. 59, 331-336.

Bai, C., Zhang, X., Dai, J., Wang, J., 2008. Synthesis of UV crosslinkable waterborne siloxane-polyurethane dispersion PDMS-PEDA-PU and the properties of the films, *Journal of Coatings Technology and Research*. 5, 251-257.

Behr, A., Eilting, J., Irawadi, K., Leschinski, J., Lindner, F., 2008. Improved utilisation of renewable resources: New important derivatives of glycerol, *Green Chem.* 10, 13-30.

Behrendt, F., Neubauer, Y., Oevermann, M., Wilmes, B., Zobel, N., 2008. Direct liquefaction of biomass, *Chem. Eng. Technol.* 31, 667-677.

Benecke, H.P., Vijayendran, B.R., Garbark, D.B., Mitchell, K.P., 2008. Low cost and highly reactive biobased polyols: A co-product of the emerging biorefinery economy, *Clean-Soil Air Water*. 36, 694-699.

Biswasw, A., Ganguly, D., 1960. Esterification of Fatty Acids with Glycerol, *Nature*. 188, 56-57.

Borugadda, V.B., Goud, V.V., 2012. Biodiesel production from renewable feedstocks: Status and opportunities, *Renewable & Sustainable Energy Reviews*. 16, 4763-4784.

Briones, R., Serrano, L., Ben Younes, R., Mondragon, I., Labidi, J., 2011. Polyol production by chemical modification of date seeds, *Industrial Crops and Products*. 34, 1035-1040.

Briones, R., Serrano, L., Labidi, J., 2012. Valorization of some lignocellulosic agro-industrial residues to obtain biopolyols, *Journal of Chemical Technology and Biotechnology*. 87, 244-249.

Briones, R., Serrano, L., Llano-Ponte, R., Labidi, J., 2011. Polyols obtained from solvolysis liquefaction of biodiesel production solid residues, *Chem. Eng. J.* 175, 169-175.

Cateto, C.A., Barreiro, M.F., Rodrigues, A.E., Belgacem, M.N., 2009. Optimization Study of Lignin Oxypropylation in View of the Preparation of Polyurethane Rigid Foams, *Ind Eng Chem Res.* 48, 2583-2589.

Chai, S., Wang, H., Liang, Y., Xu, B., 2007. Sustainable production of acrolein: investigation of solid acid-base catalysts for gas-phase dehydration of glycerol, *Green Chem.* 9, 1130-1136.

Chatzifragkou, A., Dietz, D., Komaitis, M., Zeng, A., Papanikolaou, S., 2010. Effect of Biodiesel-Derived Waste Glycerol Impurities on Biomass and 1,3-Propanediol Production of *Clostridium butyricum* VPI 1718, *Biotechnol. Bioeng.* 107, 76-84.

Chatzifragkou, A., Papanikolaou, S., 2012. Effect of impurities in biodiesel-derived waste glycerol on the performance and feasibility of biotechnological processes, *Appl. Microbiol. Biotechnol.* 95, 13-27.

Chen, F., Lu, Z., 2009. Liquefaction of Wheat Straw and Preparation of Rigid Polyurethane Foam from the Liquefaction Products, *J Appl Polym Sci.* 111, 508-516.

Chen, X., Bai, J., Cao, J., Li, Z., Xiong, J., Zhang, L., Hong, Y., Ying, H., 2009. Medium optimization for the production of cyclic adenosine 3',5'-monophosphate by *Microbacterium* sp no. 205 using response surface methodology, *Bioresour. Technol.* 100, 919-924.

Chi, Z., Pyle, D., Wen, Z., Frear, C., Chen, S., 2007. A laboratory study of producing docosahexaenoic acid from biodiesel-waste glycerol by microalgal fermentation, *Process Biochem.* 42, 1537-1545.

Chia, M., Pagan-Torres, Y.J., Hibbitts, D., Tan, Q., Pham, H.N., Datye, A.K., Neurock, M., Davis, R.J., Dumesic, J.A., 2011. Selective Hydrogenolysis of Polyols and Cyclic Ethers over Bifunctional Surface Sites on Rhodium-Rhenium Catalysts, *J. Am. Chem. Soc.* 133, 12675-12689.

Chien, Y., Lu, M., Chai, M., Boreo, F.J., 2009. Characterization of Biodiesel and Biodiesel Particulate Matter by TG, TG-MS, and FTIR, *Energy Fuels.* 23, 202-206.

Chisti, Y., 2007. Biodiesel from microalgae, *Biotechnol. Adv.* 25, 294-306.

- Chouhan, A.P.S., Sarma, A.K., 2011. Modern heterogeneous catalysts for biodiesel production: A comprehensive review, *Renewable & Sustainable Energy Reviews*. 15, 4378-4399.
- Christ, C., 1999. *Production-Integrated Environmental Protection and Waste Management in the Chemical Industry*, First edition, p.148. Wiley-VCH, 69469 Weinheim, Germany.
- Corma, A., Huber, G.W., Sauvanauda, L., O'Connor, P., 2008. Biomass to chemicals: Catalytic conversion of glycerol/water mixtures into acrolein, reaction network, *Journal of Catalysis*. 257, 163-171.
- Coutinho, F.M.B., Delpech, M.C., Alves, L.S., 2001. Anionic waterborne polyurethane dispersions based on hydroxyl-terminated polybutadiene and poly(propylene glycol): Synthesis and characterization, *J Appl Polym Sci*. 80, 566-572.
- da Silva, C.X.A., Mota, C.J.A., 2011. The influence of impurities on the acid-catalyzed reaction of glycerol with acetone, *Biomass & Bioenergy*. 35, 3547-3551.
- Delpech, M.C., Coutinho, F.M.B., 2000. Waterborne anionic polyurethanes and poly(urethane-urea)s: influence of the chain extender on mechanical and adhesive properties, *Polym. Test*. 19, 939-952.
- Diaz, I., Marquez-Alvarez, C., Mohino, F., Perez-Pariente, J., Sastre, E., 2000. Combined alkyl and sulfonic acid functionalization of MCM-41-Type silica - Part 2. Esterification of glycerol with fatty acids, *Journal of Catalysis*. 193, 295-302.
- Dobroth, Z.T., Hu, S., Coats, E.R., McDonald, A.G., 2011. Polyhydroxybutyrate synthesis on biodiesel wastewater using mixed microbial consortia, *Bioresour. Technol*. 102, 3352-3359.
- Dou, B., Rickett, G.L., Dupont, V., Williams, P.T., Chen, H., Ding, Y., Ghadiri, M., 2010. Steam reforming of crude glycerol with in situ CO(2) sorption, *Bioresour. Technol*. 101, 2436-2442.
- Dow polyols, 2011. <http://www.dow.com/polyurethane/la/en/apps/building/poly.htm>. Last accessed on 7/28/2011.
- Dow Product literature, 2013. <http://www.dow.com/scripts/litorder.asp?filepath=/polyurethane/pdfs/noreg/109-01858.pdf>, Last accessed on 05/27/13,.
- Echeverri, D.A., Cardeno, F., Rios, L.A., 2011. Glycerolysis of Soybean Oil with Crude Glycerol Containing Residual Alkaline Catalysts from Biodiesel Production, *Journal of the American Oil Chemists Society*. 88, 551-557.

- Evtiouguina, M., Barros, A., Cruz-Pinto, J., Neto, C., Belgacem, N., Pavier, C., Gandini, A., 2000. The oxypropylation of cork residues: preliminary results, *Bioresour. Technol.* 73, 187-189.
- Evtiouguina, M., Barros-Timmons, A., Cruz-Pinto, J., Neto, C., Belgacem, M., Gandini, A., 2002. Oxypropylation of cork and the use of the ensuing polyols in polyurethane formulations, *Biomacromolecules.* 3, 57-62.
- Fountoulakis, M.S., Manios, T., 2009. Enhanced methane and hydrogen production from municipal solid waste and agro-industrial by-products co-digested with crude glycerol, *Bioresour. Technol.* 100, 3043-3047.
- Gandarias, I., Requies, J., Arias, P.L., Armbruster, U., Martin, A., 2012. Liquid-phase glycerol hydrogenolysis by formic acid over Ni-Cu/Al<sub>2</sub>O<sub>3</sub> catalysts, *Journal of Catalysis.* 290, 79-89.
- Gao, L., Liu, Y., Lei, H., Peng, H., Ruan, R., 2010. Preparation of Semirigid Polyurethane Foam with Liquefied Bamboo Residues, *J Appl Polym Sci.* 116, 1694-1699.
- Garcia-Pacios, V., Costa, V., Colera, M., Miguel Martin-Martinez, J., 2011. Waterborne polyurethane dispersions obtained with polycarbonate of hexanediol intended for use as coatings, *Progress in Organic Coatings.* 71, 136-146.
- Ge, J., Zhong, W., Guo, Z., Li, W., Sakai, K., 2000. Biodegradable polyurethane materials from bark and starch. I. Highly resilient foams, *J Appl Polym Sci.* 77, 2575-2580.
- Hajek, M., Skopal, F., 2010. Treatment of glycerol phase formed by biodiesel production, *Bioresour. Technol.* 101, 3242-3245.
- Hakim, A.A.A., Nassar, M., Emam, A., Sultan, M., 2011. Preparation and characterization of rigid polyurethane foam prepared from sugar-cane bagasse polyol, *Mater. Chem. Phys.* 129, 301-307.
- Hansen, C.F., Hernandez, A., Mullan, B.P., Moore, K., Trezona-Murray, M., King, R.H., Pluske, J.R., 2009. A chemical analysis of samples of crude glycerol from the production of biodiesel in Australia, and the effects of feeding crude glycerol to growing-finishing pigs on performance, plasma metabolites and meat quality at slaughter, *Animal Production Science.* 49, 154-161.
- Hassan, E.M., Shukry, N., 2008. Polyhydric alcohol liquefaction of some lignocellulosic agricultural residues, *Industrial Crops and Products.* 27, 33-38.

Hilditch, T., Rigg, J., 1935. Experiments on the direct esterification of higher fatty acids with glycerol and with ethylene glycol. *Journal of the Chemical Society*. 1774-1778.

Hu, S., Luo, X., Wan, C., Li, Y., 2012a. Characterization of Crude Glycerol from Biodiesel Plants, *J. Agric. Food Chem.* 60, 5915-5921.

Hu, S., Wan, C., Li, Y., 2012b. Production and characterization of biopolyols and polyurethane foams from crude glycerol based liquefaction of soybean straw. *Bioresour. Technol.* 103, 227-33.

Ionescu, M., Petrovic, Z.S., 2010. High Functionality Polyether Polyols Based on Polyglycerol, *Journal of Cellular Plastics*. 46, 223-237.

Ionescu, M., Petrovic, Z.S., Wan, X., 2007. Ethoxylated soybean polyols for polyurethanes, *Journal of Polymers and the Environment*. 15, 237-243.

Jasiukaityte, E., Kunaver, M., Strlic, M., 2009. Cellulose liquefaction in acidified ethylene glycol, *Cellulose*. 16, 393-405.

Javni, I., Petrovic, Z., Guo, A., Fuller, R., 2000. Thermal stability of polyurethanes based on vegetable oils, *J Appl Polym Sci.* 77, 1723-1734.

Jin, Y., Ruan, X., Cheng, X., Lue, Q., 2011. Liquefaction of lignin by polyethyleneglycol and glycerol, *Bioresour. Technol.* 102, 3581-3583.

Johnson, D.T., Taconi, K.A., 2007. The glycerin glut: Options for the value-added conversion of crude glycerol resulting from biodiesel production, *Environ. Prog.* 26, 338-348.

Juhaida, M.F., Paridah, M.T., Hilmi, M.M., Sarani, Z., Jalaluddin, H., Zaki, A.R.M., 2010. Liquefaction of kenaf (*Hibiscus cannabinus* L.) core for wood laminating adhesive, *Bioresour. Technol.* 101, 1355-1360.

Kim, B.K., 1996. Aqueous polyurethane dispersions, *Colloid Polym. Sci.* 274, 599-611.

Kim, B.K., Lee, J.C., 1996. Waterborne polyurethanes and their properties, *Journal of Polymer Science Part A-Polymer Chemistry*. 34, 1095-1104.

Kobayashi, M., Asano, T., Kajiyama, M., Tomita, B., 2004. Analysis on residue formation during wood liquefaction with polyhydric alcohol, *Journal of Wood Science*. 50, 407-414.

Kunaver, M., Jasiukaityte, E., Cuk, N., Guthrie, J.T., 2010. Liquefaction of Wood, Synthesis and Characterization of Liquefied Wood Polyester Derivatives, *J Appl Polym Sci.* 115, 1265-1271.

- Kurimoto, Y., Doi, S., Tamura, Y., 1999. Species effects on wood-liquefaction in polyhydric alcohols, *Holzforschung*. 53, 617-622.
- Kurimoto, Y., Koizumi, A., Doi, S., Tamura, Y., Ono, H., 2001a. Wood species effects on the characteristics of liquefied wood and the properties of polyurethane films prepared from the liquefied wood, *Biomass & Bioenergy*. 21, 381-390.
- Kurimoto, Y., Takeda, M., Doi, S., Tamura, Y., Ono, H., 2001b. Network structures and thermal properties of polyurethane films prepared from liquefied wood, *Bioresour. Technol.* 77, 33-40.
- Kurimoto, Y., Takeda, M., Koizumi, A., Yamauchi, S., Doi, S., Tamura, Y., 2000. Mechanical properties of polyurethane films prepared from liquefied wood with polymeric MDI, *Bioresour. Technol.* 74, 151-157.
- Lee, S.H., Teramoto, Y., Shiraishi, N., 2002. Biodegradable polyurethane foam from liquefied waste paper and its thermal stability, biodegradability, and genotoxicity, *J Appl Polym Sci.* 83, 1482-1489.
- Lee, S.H., Yoshioka, M., Shiraishi, N., 2000. Liquefaction of corn bran (CB) in the presence of alcohols and preparation of polyurethane foam from its liquefied polyol, *J Appl Polym Sci.* 78, 319-325.
- Lee, S.K., Yoon, S.H., Chung, I., Hartwig, A., Kim, B.K., 2011. Waterborne Polyurethane Nanocomposites Having Shape Memory Effects, *Journal of Polymer Science Part A-Polymer Chemistry*. 49, 634-641.
- Lee, W., Lin, M., 2008. Preparation and application of polyurethane adhesives made from polyhydric alcohol liquefied Taiwan acacia and China fir, *J Appl Polym Sci.* 109, 23-31.
- Lehnert, K., Claus, P., 2008. Influence of Pt particle size and support type on the aqueous-phase reforming of glycerol, *Catalysis Communications*. 9, 2543-2546.
- Li, Y., Lu, J., Gu, G., Mao, Z., 2005. Characterization of the enzymatic degradation of arabinoxylans in grist containing wheat malt using response surface methodology, *Journal of the American Society of Brewing Chemists*. 63, 171-176.
- Liang, L., Mao, Z., Li, Y., Wan, C., Wang, T., Zhang, L., Zhang, L., 2006. Liquefaction of Crop Residues for Polyol Production, *Bioresources*. 1, 248-256.
- Liang, Y., Sarkany, N., Cui, Y., Blackburn, J.W., 2010. Batch stage study of lipid production from crude glycerol derived from yellow grease or animal fats through microalgal fermentation, *Bioresour. Technol.* 101, 6745-6750.

- Lin, L.Z., Nakagame, S., Yao, Y.G., Yoshioka, M., Shiraishi, N., 2001a. Liquefaction mechanism of beta-O-4 lignin model compound in the presence of phenol under acid catalysis Part 2. Reaction behavior and pathways, *Holzforschung*. 55, 625-630.
- Lin, L.Z., Yao, Y.G., Shiraishi, N., 2001b. Liquefaction mechanism of beta-O-4 lignin model compound in the presence of phenol under acid catalysis Part 1. Identification of the reaction products, *Holzforschung*. 55, 617-624.
- Lin, L.Z., Yao, Y.G., Yoshioka, M., Shiraishi, N., 1997a. Liquefaction mechanism of lignin in the presence of phenol at elevated temperature without catalysts - Studies on beta-O-4 model compound .1. Structural characterization of the reaction products, *Holzforschung*. 51, 316-324.
- Lin, L.Z., Yoshioka, M., Yao, Y.G., Shiraishi, N., 1997b. Liquefaction mechanism of lignin in the presence of phenol at elevated temperature without catalysts - Studies on beta-O-4 lignin model compound .2. Reaction pathway, *Holzforschung*. 51, 325-332.
- Lin, L.Z., Yoshioka, M., Yao, Y.G., Shiraishi, N., 1997c. Liquefaction mechanism of lignin in the presence of phenol at elevated temperature without catalysts - Studies on beta-O-4 lignin model compound .3. Multi-condensation, *Holzforschung*. 51, 333-337.
- Liu, J., Chen, F., Qiu, M., 2009. Liquefaction of Bagasse and Preparation of Rigid Polyurethane Foam from Liquefaction Products, *Journal of Biobased Materials and Bioenergy*. 3, 401-407.
- Lligadas, G., Ronda, J.C., Galia, M., Cadiz, V., 2010. Plant Oils as Platform Chemicals for Polyurethane Synthesis: Current State-of-the-Art, *Biomacromolecules*. 11, 2825-2835.
- Lu, Y., Larock, R.C., 2007. New hybrid latexes from a soybean oil-based waterborne polyurethane and acrylics via emulsion polymerization, *Biomacromolecules*. 8, 3108-3114.
- Lu, Y., Larock, R.C., 2008. Soybean-Oil-Based Waterborne Polyurethane Dispersions: Effects of Polyol Functionality and Hard Segment Content on Properties, *Biomacromolecules*. 9, 3332-3340.
- Lu, Y., Larock, R.C., 2010a. Aqueous Cationic Polyurethane Dispersions from Vegetable Oils, *Chemsuschem*. 3, 329-333.
- Lu, Y., Larock, R.C., 2010b. Soybean oil-based, aqueous cationic polyurethane dispersions: Synthesis and properties, *Progress in Organic Coatings*. 69, 31-37.
- Lu, Y., Larock, R.C., 2011. Synthesis and Properties of Grafted Latices from a Soybean Oil-Based Waterborne Polyurethane and Acrylics, *J Appl Polym Sci*. 119, 3305-3314.

- Lu, Y., Xia, Y., Larock, R.C., 2011. Surfactant-free core-shell hybrid latexes from soybean oil-based waterborne polyurethanes and poly(styrene-butyl acrylate), *Progress in Organic Coatings*. 71, 336-342.
- Luo, X., Hu, S., Zhang, X., Li, Y., 2013. Thermochemical conversion of crude glycerol to biopolyols for the production of polyurethane foams, *Bioresour. Technol.* 139, 323-329.
- Ma, F.R., Hanna, M.A., 1999. Biodiesel production: a review, *Bioresour. Technol.* 70, 1-15.
- Macierzanka, A., Szlag, H., 2004. Esterification kinetics of glycerol with fatty acids in the presence of zinc carboxylates: Preparation of modified acylglycerol emulsifiers, *Ind Eng Chem Res.* 43, 7744-7753.
- Madbouly, S.A., Otaigbe, J.U., 2009. Recent advances in synthesis, characterization and rheological properties of polyurethanes and POSS/polyurethane nanocomposites dispersions and films, *Progress in Polymer Science.* 34, 1283-1332.
- Maldas, D., Shiraishi, N., 1996. Liquefaction of wood in the presence of polyol using NaOH as a catalyst and its application to polyurethane foams, *Int. J. Polym. Mater.* 33, 61-71.
- Manosak, R., Limpattayanate, S., Hunsom, M., 2011. Sequential-refining of crude glycerol derived from waste used-oil methyl ester plant via a combined process of chemical and adsorption, *Fuel Process Technol.* 92, 92-99.
- McCoy, M., 2006. Glycerin Surplus: Plants are closing, and new uses for the chemical are being found, *Chemical & Engineering News.* 84, 7.
- Moon, C., Ahn, J., Kim, S.W., Sang, B., Um, Y., 2010. Effect of Biodiesel-derived Raw Glycerol on 1,3-Propanediol Production by Different Microorganisms, *Appl. Biochem. Biotechnol.* 161, 502-510.
- Mothes, G., Schnorpfeil, C., Ackermann, J.-., 2007. Production of PHB from crude glycerol, *Engineering in Life Sciences.* 7, 475-479.
- Mu, Y., Teng, H., Zhang, D., Wang, W., Xiu, Z., 2006. Microbial production of 1,3-propanediol by *Klebsiella pneumoniae* using crude glycerol from biodiesel preparations, *Biotechnol. Lett.* 28, 1755-1759.
- Nanda, A.K., Wicks, D.A., 2006. The influence of the ionic concentration, concentration of the polymer, degree of neutralization and chain extension on aqueous polyurethane dispersions prepared by the acetone process, *Polymer.* 47, 1805-1811.

- Ni, B., Yang, L., Wang, C., Wang, L., Finlow, D.E., 2010. Synthesis and thermal properties of soybean oil-based waterborne polyurethane coatings, *Journal of Thermal Analysis and Calorimetry*. 100, 239-246.
- Noureddini, H., Harkey, D.W., Gutsman, M.R., 2004. A continuous process for the glycerolysis of soybean oil, *Journal of the American Oil Chemists Society*. 81, 203-207.
- Ott, L., Bicker, M., Vogel, H., 2006. Catalytic dehydration of glycerol in sub- and supercritical water: a new chemical process for acrolein production, *Green Chem*. 8, 214-220.
- Pachauri, N., He, B., 2006. Value-added Utilization of Crude Glycerol from Biodiesel Production: A Survey of Current Research Activities, 2006 ASABE Annual International Meeting, Portland, Oregon.
- Pagliari, M., Ciriminna, R., Kimura, H., Rossi, M., Della Pina, C., 2007. From glycerol to value-added products, *Angewandte Chemie-International Edition*. 46, 4434-4440.
- Pathak, S.S., Sharma, A., Khanna, A.S., 2009. Value addition to waterborne polyurethane resin by silicone modification for developing high performance coating on aluminum alloy, *Progress in Organic Coatings*. 65, 206-216.
- Patnaik, P., 2007. *A Comprehensive Guide to the Hazardous Properties of Chemical Substances*, Third edition, Chapter 2: acids, mineral, p. 118. John Wiley & Sons Inc., Hoboken, NJ.
- Pattanayak, A., Jana, S.C., 2005. Thermoplastic polyurethane nanocomposites of reactive silicate clays: effects of soft segments on properties, *Polymer*. 46, 5183-5193.
- Pavier, C., Gandini, A., 2000. Oxypropylation of sugar beet pulp. 1. Optimisation of the reaction, *Industrial Crops and Products*. 12, 1-8.
- Petrovic, Z.S., 2008. Polyurethanes from vegetable oils, *Polymer Reviews*. 48, 109-155.
- Pfister, D.P., Xia, Y., Larock, R.C., 2011. Recent Advances in Vegetable Oil-Based Polyurethanes, *Chemsuschem*. 4, 703-717.
- Pollack, S., Shen, D., Hsu, S., Wang, Q., Stidham, H., 1989. Infrared and X-Ray-Diffraction Studies of a Semirigid Polyurethane, *Macromolecules*. 22, 551-557.
- Pyle, D.J., Garcia, R.A., Wen, Z., 2008. Producing docosahexaenoic acid (DHA)-rich algae from biodiesel-derived crude glycerol: Effects of impurities on DHA production and algal biomass composition, *J. Agric. Food Chem*. 56, 3933-3939.

- Ramachandran, R.P.B., van Rossum, G., van Swaaij, W.P.M., 2011. Preliminary Assessment of Synthesis Gas Production via Hybrid Steam Reforming of Methane and Glycerol, *Energy Fuels*. 25, 5755-5766.
- Randall, D., Lee, S., 2002a. Isocyanates, *The polyurethanes book*. John Wiley & Sons, LTD, UK, pp. 63-87.
- Randall, D., Lee, S., 2002b. Polyols, *The polyurethanes book*. Huntsman International LLC, The United Kingdom, pp. 89.
- Randall, D., Lee, S., 2002c. *The polyurethanes book chapter polyols, Introduction to rigid foams*, Huntsman International LLC, The United Kingdom, pp. 229-244.
- Randall, D., Lee, S., 2002d. *The polyurethanes book, Chapter 2: The global polyurethanes market*, Huntsman International LLC, The United Kingdom, pp. 9-21.
- Ruppert, A.M., Meeldijk, J.D., Kuipers, B.W.M., Erne, B.H., Weckhuysen, B.M., 2008. Glycerol etherification over highly active CaO-based materials: New mechanistic aspects and related colloidal particle formation, *Chemistry-a European Journal*. 14, 2016-2024.
- Sabourin-Provost, G., Hallenbeck, P.C., 2009. High yield conversion of a crude glycerol fraction from biodiesel production to hydrogen by photofermentation, *Bioresour. Technol.* 100, 3513-3517.
- Santibanez, C., Teresa Varnero, M., Bustamante, M., 2011. Residual Glycerol from Biodiesel Manufacturing, Waste Or Potential Source of Bioenergy: a Review, *Chilean Journal of Agricultural Research*. 71, 469-475.
- Sow, C., Riedl, B., Blanchet, P., 2011. UV-waterborne polyurethane-acrylate nanocomposite coatings containing alumina and silica nanoparticles for wood: mechanical, optical, and thermal properties assessment, *Journal of Coatings Technology and Research*. 8, 211-221.
- Srichatrapimuk, V., Cooper, S., 1978. Infrared Thermal-Analysis of Polyurethane Block Polymers, *J. Macromol. Sci. -Phys.* B15, 267-311.
- Sung, C., Schneider, N., 1977. Temperature-Dependence of Hydrogen-Bonding in Toluene Diisocyanate Based Polyurethanes, *Macromolecules*. 10, 452-458.
- ten Dam, J., Hanefeld, U., 2011. Renewable Chemicals: Dehydroxylation of Glycerol and Polyols, *Chemsuschem*. 4, 1017-1034.
- Thompson, J.C., He, B.B., 2006. Characterization of crude glycerol from biodiesel production from multiple feedstocks, *Appl. Eng. Agric.* 22, 261-265.

Venkataramanan, K.P., Boatman, J.J., Kurniawan, Y., Taconi, K.A., Bothun, G.D., Scholz, C., 2012. Impact of impurities in biodiesel-derived crude glycerol on the fermentation by *Clostridium pasteurianum* ATCC 6013, *Appl. Microbiol. Biotechnol.* 93, 1325-1335.

Wang, H., Chen, H., 2007. A novel method of utilizing the biomass resource: Rapid liquefaction of wheat straw and preparation of biodegradable polyurethane foam (PUF), *J Chin Inst Chem Eng.* 38, 95-102.

Wang, T., Li, D., Wang, L., Yin, J., Chen, X.D., Mao, Z., 2008. Effects of CS/EC ratio on structure and properties of polyurethane foams prepared from untreated liquefied corn stover with PAPI, *Chemical Engineering Research & Design.* 86, 416-421.

Wang, X., Hu, Y., Song, L., Xing, W., Lu, H., Lv, P., Jie, G., 2011. UV-curable waterborne polyurethane acrylate modified with octavinyl POSS for weatherable coating applications, *Journal of Polymer Research.* 18, 721-729.

Wang, Z.M., Gao, D.B., Yang, J.W., Chen, Y.L., 1999. Synthesis and characterization of UV-curable waterborne polyurethane-acrylate ionomers for coatings, *J Appl Polym Sci.* 73, 2869-2876.

Wei, Y., Cheng, F., Hou, G., 2007. Synthesis and properties of fatty acid esters of cellulose, *Journal of Scientific & Industrial Research.* 66, 1019-1024.

Wolfson, A., Litvak, G., Dlugy, C., Shotland, Y., Tavor, D., 2009. Employing crude glycerol from biodiesel production as an alternative green reaction medium, *Industrial Crops and Products.* 30, 78-81.

Xia, Y., Larock, R.C., 2011a. Castor-Oil-Based Waterborne Polyurethane Dispersions Cured with an Aziridine-Based Crosslinker, *Macromolecular Materials and Engineering.* 296, 703-709.

Xia, Y., Larock, R.C., 2011b. Preparation and Properties of Aqueous Castor Oil-based Polyurethane-Silica Nanocomposite Dispersions through a Sol-Gel Process, *Macromolecular Rapid Communications.* 32, 1331-1337.

Xia, Y., Larock, R.C., 2011c. Soybean Oil-Isosorbide-Based Waterborne Polyurethane-Urea Dispersions, *Chemsuschem.* 4, 386-391.

Xiu, S., Shahbazi, A., Shirley, V., Mims, M.R., Wallace, C.W., 2010. Effectiveness and mechanisms of crude glycerol on the biofuel production from swine manure through hydrothermal pyrolysis, *J. Anal. Appl. Pyrolysis.* 87, 194-198.

Xu, J., Zhao, X., Wang, W., Du, W., Liu, D., 2012. Microbial conversion of biodiesel byproduct glycerol to triacylglycerols by oleaginous yeast *Rhodosporidium toruloides*

and the individual effect of some impurities on lipid production, *Biochem. Eng. J.* 65, 30-36.

Xue, B., Wen, J., Xu, F., Sun, R., 2013. Polyols production by chemical modification of autocatalyzed ethanol-water lignin from *Betula alnoides*, *J Appl Polym Sci.* 129, 434-442.

Yamada, T., Ono, H., 1999. Rapid liquefaction of lignocellulosic waste by using ethylene carbonate, *Bioresour. Technol.* 70, 61-67.

Yamada, T., Ono, H., 2001. Characterization of the products resulting from ethylene glycol liquefaction of cellulose, *Journal of Wood Science.* 47, 458-464.

Yamada, T., Aratani, M., Kubo, S., Ono, H., 2007. Chemical analysis of the product in acid-catalyzed solvolysis of cellulose using polyethylene glycol and ethylene carbonate, *Journal of Wood Science.* 53, 487-493.

Yan, Y., Hu, M., Wang, Z., 2010. Kinetic study on the liquefaction of cornstalk in polyhydric alcohols, *Industrial Crops and Products.* 32, 349-352.

Yan, Y., Pang, H., Yang, X., Zhang, R., Liao, B., 2008. Preparation and characterization of water-blown polyurethane foams from liquefied cornstalk polyol, *J Appl Polym Sci.* 110, 1099-1111.

Yao, Y., Yoshioka, M., Shiraishi, N., 1993. Combined Liquefaction of Wood and Starch in a Polyethylene-Glycol Glycerin Blended Solvent, *Mokuzai Gakkaishi.* 39, 930-938.

Yao, Y.G., Yoshioka, M., Shiraishi, N., 1996. Water-absorbing polyurethane foams from liquefied starch, *J Appl Polym Sci.* 60, 1939-1949.

Yao, Y., Yoshioka, M., Shiraishi, N., 1995. Rigid Polyurethane Foams from Combined Liquefaction Mixtures of Wood and Starch, *Mokuzai Gakkaishi.* 41, 659-668.

Yu, F., Le, Z., Chen, P., Liu, Y., Lin, X., Ruan, R., 2008. Atmospheric pressure liquefaction of dried distillers grains (DDG) and making polyurethane foams from liquefied DDG, *Appl. Biochem. Biotechnol.* 148, 235-243.

Yu, F., Ruan, R., Lin, X., Liu, Y., Fu, R., Li, Y., Chen, P., Gao, Y., 2006. Reaction kinetics of stover liquefaction in recycled stover polyol, *Appl. Biochem. Biotechnol.* 130, 563-573.

Zhang, H., Ding, F., Luo, C., Xiong, L., Chen, X., 2012a. Liquefaction and characterization of acid hydrolysis residue of corncob in polyhydric alcohols, *Industrial Crops and Products.* 39, 47-51.

Zhang, H., Pang, H., Shi, J., Fu, T., Liao, B., 2012b. Investigation of Liquefied Wood Residues Based on Cellulose, Hemicellulose, and Lignin, *J Appl Polym Sci.* 123, 850-856.

Zhang, T., Zhou, Y., Liu, D., Petrus, L., 2007. Qualitative analysis of products formed during the acid catalyzed liquefaction of bagasse in ethylene glycol, *Bioresour. Technol.* 98, 1454-1459.

Zhao, Y., Yan, N., Feng, M., 2012. Polyurethane foams derived from liquefied mountain pine beetle-infested barks, *J Appl Polym Sci.* 123, 2849-2858.

Zhou, C., Beltramini, J.N., Fan, Y., Lu, G.Q., 2008. Chemoselective catalytic conversion of glycerol as a biorenewable source to valuable commodity chemicals, *Chem. Soc. Rev.* 37, 527-549.

Zlatanic, A., Lava, C., Zhang, W., Petrovic, Z.S., 2004. Effect of structure on properties of polyols and polyurethanes based on different vegetable oils, *Journal of Polymer Science Part B-Polymer Physics.* 42, 809-819.